NTNU

Norwegian University of
Science and Technology

Autonomous heading control in position mooring with thruster assist

Silje Aarvik Johannessen

Marine Technology
Submission date: October 2017
Supervisor: Roger Skjetne, IMT
Co-supervisor: Dong T. Nguyen, IMT
Jon Bjørnø, IMT
Hans-Martin Heyn, IMT

Norwegian University of Science and Technology
Department of Marine Technology

NTNU Trondheim
Norwegian University of Science and Technology
Department of Marine Technology

MSC THESIS DESCRIPTION SHEET

Name of the candidate:	Johannessen, Silje Aarvik
Field of study:	Marine control engineering
Thesis title (Norwegian):	Autonom retningsstyring i thruster-assistert forankring av fartøy
Thesis title (English):	Autonomous heading control in position mooring with thruster assist

Background

Stationkeeping systems that combine mooring lines with thrusters are highly relevant for offshore petroleum activities, including arctic offshore operations. The Norwegian offshore industry is experiencing an increased demand for integrated offshore operations both in open waters and in Arctic ice-covered waters. Challenges lie especially in operations under *extreme load conditions*. There has been much attention in the research community on stationkeeping operations, especially by Dynamic Positioning (DP) and Thruster-Assisted Position Mooring (TAPM) of turret-anchored offshore vessels. Within TAPM, the mean environmental loads shall be balanced by the mooring lines, while the thrusters are used for *automatic heading control* to keep the heading pointed towards the incoming waves or drifting sea-ice. In addition, the thrusters are used for extra *surge/sway damping* and to aid the mooring lines in case of extreme loads. Also, what is known as *setpoint chasing* is used to provide restoring loads around the equilibrium position given by the mean environmental loads.

TAPM thus require one nominal control strategy during the normal loading condition, and then possibly switch to another control strategy under abnormal loading conditions. In this thesis, the focus is on the normal condition, where we want to develop a guidance system and controller to automatically find and control the heading of a TAPM vessel in order to minimize the amount of thrust. The *extremum seeking (ES)* theory may be interesting as a method to automatically find the optimal heading. At the same time a basis guidance system design should be made to compare the results of the ES scheme with. A guidance system and controller to automatically find and control the optimal position of the vessel should also be made, using a relevant setpoint chasing method.

The model ship C/S Inocean Cat I Drillship, in short C/S Arctic Drillship (CSAD), is used for the simulation studies and experimental testing. The main focus will be based on the simulation studies.

Work description

1. Perform a background and literature review to provide information and relevant references on:
   - Stationkeeping marine operations by turret-moored structures with thruster assist.
   - Simulation models of turret-moored structures with azimuth thrusters, including wave, wind, and current loads.
   - TAPM control design models, incl. wave-frequency motion.
   - Typical TAPM control methods, with focus on automatic heading control.
   - Setpoint chasing control method.
   - Extremum seeking control method.
   - The MC-Lab, the CSAD model ship, and TAPM for CSAD.

   Write a list with abbreviations and definitions of terms, explaining relevant concepts related to the literature study and project assignment.

2. Establish a 6DOF simulation model for the CSAD model ship. The simulation model should be based on a FEM model for the mooring lines, and include loads from waves and current. Verify that the open-loop model has expected behaviors to various inputs. The model can be taken directly from other sources, based upon proper referencing, and adapted to your work.

3. Develop a controller based on setpoint chasing, with damping and restoring control in surge and sway to use in moderate weather conditions. Implement the control law in your simulator and test its performance.

4. Derive a guidance system for autonomous control of the heading (note that *autonomous* here refers to the ability of the TAPM control system to determine itself the "optimal" heading setpoint and control the vessel correspondingly):
   - Design and implement a heading guidance and control where the user specifies manually the setpoint heading (based on knowledge of the incoming waves) – to be used as a basis for testing and comparison.
   - Develop an autonomous guidance and control scheme based on ES.
   - If possible, propose and develop your alternative autonomous guidance method.

5. Perform a simulation study of all the controllers. Compare and contrast the results.

6. Implement the relevant guidance and control algorithms for CSAD, test in MC-Lab. Discuss the validity of the methods in a real eanvironment.

Tentative

7. Derive an autonomous heading guidance law based on the principles of weather optimal position control (WOPC). Compare and contrast the results to the tasks above.

Specifications

The scope of work may prove to be larger than initially anticipated. By the approval from the supervisor, described topics may be deleted or reduced in extent without consequences with regard to grading.

The candidate shall present personal contribution to the resolution of problems within the scope of work. Theories and conclusions should be based on mathematical derivations and logic reasoning identifying the various steps in the deduction.

The report shall be organized in a logical structure to give a clear exposition of background, results, assessments, and conclusions. The text should be brief and to the point, with a clear language. Rigorous mathematical deductions and illustrating figures are preferred over lengthy textual descriptions. The report shall have font size 11 pts. It shall be written in English (preferably US) and contain the following elements: Title page, abstract, acknowledgements, thesis specification, list of symbols and acronyms, table of contents, introduction with objective, background, and scope and delimitations, main body with problem formulations, derivations/developments and results, conclusions with recommendations for further work, references, and optional appendices. All figures, tables, and equations shall be numerated. The original contribution of the candidate and material taken from other sources shall be clearly identified. Work from other sources shall be properly acknowledged using quotations and a Harvard citation style (e.g. *natbib* Latex package). The work is expected to be conducted in an honest and ethical manner, without any sort of plagiarism and misconduct. Such practice is taken very seriously by the university and will have consequences. NTNU can use the results freely in research and teaching by proper referencing, unless otherwise agreed upon.

The thesis shall be submitted with a printed and electronic copy to the main supervisor, with the printed copy signed by the candidate, and otherwise according to NTNU procedures. The final revised version of this thesis description must be included. Computer code, pictures, videos, data series, and a PDF version of the report shall be enclosed electronically with all submitted versions.

Start date: 1 April, 2017 **Due date:** As specified by the administration.

Supervisor: Roger Skjetne
Co-advisor(s): Dong T. Nguyen, Jon Bjørnø, Hans-Martin Heyn

Santa Barbara,


Roger Skjetne
Digitally signed by Roger Skjetne
Date: 2017.08.28 13:47:03 -07'00'

Roger Skjetne, Supervisor

Preface

This master thesis was done as a part of the study program, Marine Technology, at NTNU in Trondheim, and was carried out during the spring and the summer of 2017. In March 2017 I delivered a project thesis involving a pre-study of the same topic. Some of the material from that has been further developed in this master thesis.

I started this master thesis by performing a literature review of the concepts Thruster-Assisted Position Mooring (TAPM), setpoint chasing and Extremum Seeking (ES). Subsequently, I modified an existing simulation model of the vessel C/S Inocean Cat I Drillship, by introducing mooring lines based on a Finite Element Method (FEM) as a replacement for the existing Catenary equation based mooring lines. Further, I developed a controller and different guidance systems which were tested both on the simulation model and on a model ship in the Marine Cybernetics Laboratory (MC Lab). Of the guidance systems I developed, two were autonomous for optimal heading, and they were based on the ES algorithm. ES has never before been tested for this purpose.

The assignment has been both challenging and very interesting to work on, but sometimes also frustrating. I feel I have gained substantial knowledge in this area during the work.

I met some challenges during my laboratory time. I figured out early that the model ship was taking on water, which made the testing more difficult. After a while the leakage became more severe, which prevented me from testing all my systems. I did also have my laboratory time during the summer, something which made it hard to find someone to sit in the laboratory with me while I was testing.

Trondheim, October 6, 2017

Silje Aarvik Johannessen

Acknowledgment

I have received valuable help during this master thesis, and I would like to acknowledge and thank these experienced people for their contributions.

I would first like to thank my supervisor, Professor Roger Skjetne, for the valuable guidance he provided. I am especially thankful that he was available on mail also during his vacation.

My co-advisors, Dong T. Nguyan, Jon Bjørnø and Hans-Martin Heyn for their knowledge, support, time and feedback. Thank you for the time you spent with me investigating the problematic areas, in order to help me finding better solutions. Especially thanks to Dong for several guidance meetings, for always being available on mail and for correcting my report. Thank you, Jon Bjørnø, for all the time and guidance you provided in the MC Lab.

I will also thank my fellow students for a great study period. Especially thanks to Mari Galta og Hanne Hornsletten for the time you spent with me in the MC Lab.

Finally, I would like to thank my family for their support, encouragement and for proofreading the report.

Abstract

The main topic of this thesis is Thruster-Assisted Position Mooring (TAPM), which is a positioning system for automatic thruster assistance of a moored structure. The system has been commercially available since the late 1980s, and is a cost-effective alternative for offshore oil production compared to permanent platforms.

A literature review on the topic is provided, and mathematical descriptions of an TAPM vessel and control systems are derived. A 6 Degree Of Freedom (DOF) simulation model of a 1:90 scaled model of an Arctic drillship with the name C/S Inocean Cat I Drillship, in short C/S Arctic Drillship (CSAD), has been established. This simulation model is based on existing models, where for instance the mooring model is based on the Finite Element Method (FEM). CSAD is further used during simulations of the different control systems in normal conditions.

Since an TAPM vessel is located in the same position over years, the choice regarding its desired position and heading are extremely important. By using the TAPM system optimal due to the environment, the amount of thrust required will be minimized, leading to a reduced fuel consumption, which in turn will reduce both the operational cost and emission.

Two new autonomous heading guidance systems to use in an TAPM operation are developed in this thesis. The main objective of these guidance systems is to determine the optimal heading setpoint. The theory Extremum Seeking (ES) has been investigated in an attempt to find the optimal heading, both fast and accurate. Two approaches of the theory, the sinusoidal perturbation based ES and the numerical optimization based ES, have been used in order to make two autonomous guidance systems for heading. The ES theory is known from other industries, but have until now not been tested for an TAPM application.

In order to obtain a complete optimal control system, the autonomous heading guidance systems have been combined with a guidance system based on setpoint chasing to generate the earth-fixed position for surge and sway. This is further tested on the simulation model CSAD.

From the simulation results, it can be concluded that both of the ES methods can be used in order to seek towards the optimal heading. However, the methods will need to be further investigated and optimized in order to be used efficiently for this application.

Sammendrag

Hovedtemaet i denne avhandlingen er thruster-assistert forankring (TAPM), som er ett posisjoneringssystem for automatisk thruster assistanse av en forankret struktur. Systemet har vært kommersielt tilgjengelig siden slutten av 1980-tallet, og er et kostnadseffektivt alternativ for offshore oljeproduksjon sammenlignet med permanente plattformer.

En gjennomgang av allerede kjent litteratur om emnet er gitt, samt matematiske utledninger av et TAPM fartøy og kontrollsystemer. En simulerings modell i en skala 1:90 av ett arktisk drillskip med navn C/S Inocean Cat I Drillship, i kort form C/S Arctic Drillship (CSAD), er etablert i 6 frihetsgrader (DOF). Simuleringsmodellen er satt sammen av allerede eksisterende modeller, hvor forankringsmodellen er basert på metoden Finite Element Method (FEM). CSAD, er videre brukt til testing av kontrollsystemer under normale forhold.

Siden et TAPM fartøy kan befinne seg i samme posisjon over flere år, vil valget av ønsket posisjon og ønsket retning av fartøyet (heading) være kritisk. Ved å utnytte posisjoneringssystemet til det fulle med hensyn på omgivelsene, er det mulig å finne optimale verdier for posisjon og heading slik at bruken av thrust vil bli minimert. Dette vil føre til en reduksjon i drivstofforbruk, som igjen vil redusere både driftskostnader og utslipp.

I denne avhandlingen er to nye autonome veiledningssystemer for heading utviklet, til bruk under TAPM operasjoner. Meningen med et autonomt veiledningssystemene for heading er å beregne denne optimale headingen til skipet, så kontrolleren vet hvor den skal posisjonere skipet. Teorien Extremum Seeking (ES) har blitt undersøkt i ett forsøk på å finne den optimale headingen både raskt og nøyaktig. To tilnærminger av ES teorien, sinusoidal perturbation based ES og numerical optimization based ES, er brukt til å lage de to nye autonome veiledningssystemer for heading. ES er kjent fra andre industrier, men har ikke før blitt testet for applikasjoner med TAPM.

For å oppnå ett komplett optimalt styringssystem, er det også utviklet veiledningssystem for å generere earth-fixed posisjon for surge og sway, basert på en metode som heter setpoint chasing. Dette er testet sammen med de to autonome veiledningssystemene for heading på simuleringsmodellen CSAD.

Fra simuleringene, kan det konkluderes med at de to ES teoriene kan brukes i søket mot den optimale verdien av heading. Metodene er fortsatt ikke helt optimale og vil derfor trenge videre forsking og optimalisering før det kan virke optimalt for dette formålet.

Contents

Master description sheet i
Preface iii
Acknowledgment v
Abstract vii
Sammendrag ix
List of figures xiv
List of tables xvii
Abbreviations xix
Symbols xxi
Terms and concepts xxiii

1 Introduction **1**
1.1 Background and motivation 1
1.2 Literature review 3
1.2.1 Stationkeeping 3
1.2.2 Seakeeping 3
1.2.3 Dynamic positioning 3
1.2.4 Thruster-assisted position mooring 4
1.2.5 Optimal heading 6
1.2.6 Weather optimal position control 6
1.2.7 Setpoint chasing 8
1.2.8 Extremum seeking 9
1.2.9 Statoil's Cat I Arctic Drillship 11
1.2.10 C/S Inocean Cat I Drillship model 12
1.2.11 MC-Lab 14
1.3 Objective and scope 17
1.3.1 Objective 17
1.3.2 Scope 17
1.4 Organization of the thesis 19

2 Mathematical modeling **21**
2.1 Kinematics . . . 21
2.2 Kinetics . . . 23
2.2.1 LF model . . . 23
2.2.2 WF model . . . 24
2.2.3 Mooring model . . . 24
2.3 TAPM control design model . . . 27
2.3.1 LF model . . . 27
2.3.2 Bias model . . . 29
2.3.3 WF model . . . 29
2.3.4 Measurement . . . 29

3 Simulation model of CSAD **31**
3.1 6 DOF simulation model of the CSAD . . . 31
3.1.1 Froude scaling . . . 32
3.2 Weather parameters . . . 32
3.3 System verification . . . 33

4 Controller and observer design **37**
4.1 Controller . . . 37
4.2 Observer . . . 39

5 Guidance system design **41**
5.1 Reference filter . . . 42
5.2 User specified guidance system . . . 43
5.2.1 Verification . . . 43
5.3 Setpoint chasing . . . 45
5.3.1 Verification . . . 46
5.4 Sinusoidal perturbation based extremum seeking . . . 48
5.4.1 Simplified 1 DOF system of yaw . . . 49
5.4.2 Verification of the guidance system in the simplified system . . . 52
5.5 Numerical optimization based extremum seeking . . . 55
5.5.1 Verification . . . 59

6 Experiment setup **61**
6.1 Mooring lines . . . 61
6.2 Waves . . . 63
6.3 Qualisys motion capture system . . . 64

7 Results **65**

7.1 Simulation 65
7.1.1 Scenario definitions 66
7.1.2 Scenario 1: simulation results 68
7.1.3 Scenario 2: simulation results 72
7.2 Experiment 76

8 Discussion **81**

9 Conclusion **85**
9.1 Further work 87

Bibliography **88**

A Attached zip-file **I**
A.1 Content I
A.2 Content of the folder: Experiment I
A.3 Content of the folder: Simulation II
A.4 Remarks regarding the programs IX

List of Figures

1.1 Principal figure of TAPM (Strand et al.; 1997). 4
1.2 Weather optimal positioning principle (Fossen and Strand; 2001). 7
1.3 Structure of a TAPM system including an optimal setpoint generator (adapted from Nguyen and Sørensen (2009)). 8
1.4 ES loop for a general plant (adapted from Ariyur and Krstić (2003)) 10
1.5 Cat I Arctic Drillship (Jorde; 2014) 11
1.6 The model of CSAD (Bjørnø; 2016) 12
1.7 Placement and constraints of the thrusters on CSAD (Bjørnø et al.; 2017) . 13
1.8 MC Lab (NTNU; 2017b) 14

2.1 Different reference frames used in TAPM. 21
2.2 Mooring line configuration (Aamo and Fossen; 2001). 24

3.1 Initial simulation position of the mooring lines. 33
3.2 The vessel position of a open loop system exposed by environmental forces with direction of 180 degree. 34
3.3 The vessel position of a open loop system exposed by environmental forces with direction of 200 degree. 35

4.1 Stiffness estimation. 39

5.1 Guidance system. 41
5.2 Verification of the user specified guidance system. 44
5.3 A block diagram of the setpoint generator. 45
5.4 Verification of the guidance system with setpoint chasing. 47
5.5 Sinusoidal perturbation based ES scheme. 48
5.6 Verification of a sinusoidal perturbation based ES controller tested on a simplified 1DOF system. 53
5.7 Verification of a sinusoidal perturbation based ES controller tested on a simplified 1DOF system with a simplified reference filter. 54
5.8 Numerical optimization based ES scheme for yaw. 55

5.9 The different scenarios for the discrete ES controller 57
5.10 Flow chart describing the ES numerical optimization based method 58
5.11 Verification of the numerical optimization based ES guidance system. . . . 59

6.1 Experimental setup of the mooring system. 62
6.2 Main components of the experimental mooring system. 62
6.3 Detection of the position and directions of CSAD with the use of Qualisys. 64

7.1 Guidance system number 1: User specified guidance system for heading for scenario 1. 68
7.2 Guidance system number 2: Sinusoidal perturbation based ES guidance system for heading for scenario 1. 69
7.3 Guidance system number 3: Numerical optimization based ES autonomous guidance system for heading for scenario 1. 70
7.4 Guidance system number 1: User specified guidance system for heading for scenario 2. 72
7.5 Guidance system number 2: Sinusoidal perturbation based ES guidance system for heading for scenario 2. 73
7.6 Guidance system number 3: Numerical optimization based ES autonomous guidance system for heading for scenario 2. 74
7.7 Experiment, $H_s = 0.0139m$: User specified guidance system in heading and setpoint chasing for the North and East position. 78
7.8 Experiment, $H_s = 0.0222m$: User specified guidance system in heading and setpoint chasing for the North and East position. 79
7.9 Experiment, $H_s = 0.0139m$: Rotation of basin frame. 80

A.1 Content of the folder User specified guidance system. II
A.2 Content of the folder SPES and SP. III
A.3 Content of the folder Simplified yaw ES. III
A.4 Content of the folder Setpoint chasing user. IV
A.5 Content of the folder Setpoint chasing. V
A.6 Content of the folder Open loop CSAD. VI
A.7 Content of the folder Numerical optimization guidance system. VII
A.8 Content of the folder NOES and SP. VIII

List of Tables

1.1 C/S Inocean Cat I Drillship dimensions 12
1.2 C/S Inocean Cat I Drillship model dimensions 13
1.3 Thruster parameter identification for CSAD model 13
1.4 Wave generator capacity 15

3.1 Characteristics of the mooring lines 31
3.2 Froude scaling. 32
3.3 Moderate sea state. 33
3.4 Weather parameters used in the simulations 34

6.1 Wave parameters used in the experiments. 63

Abbreviations

ABS Antilock Breaking Systems.

COT Centre Of Turret.

CSAD C/S Inocean Cat I Drillship, in short C/S Arctic Drillship.

DOF Degree Of Freedom.

DP Dynamic Positioning.

DP-vessel Dynamically Positioned vessel.

ES Extremum Seeking.

FEM Finite Element Method.

FPSO Floating Production Storage and Off-loading.

FZP Field Zero Point.

GNSS Global Navigation Satellite System.

IMO International Maritime Organization.

LF Low-Frequency.

MC Lab Marine Cybernetics Laboratory.

MODU Mobile Offshore Drilling Unit.

NTNU Norwegian University of Science and Technology.

ODE Ordinary Differential Equations.

PID-controller Proportional, Integral and Derivative controller.

PM Position Mooring.

QTM Qualisys Track Manager.

TAPM Thruster-Assisted Position Mooring.

TP Terminal Point.

VO Vessel Origin.

WF Wave-Frequency.

WOPC Weather Optimal Positioning Control.

Symbols

H_s Significant wave height.

Hz Hertz.

β_c Current direction.

β_{env} Mean environmental force direction.

β_w Mean wave direction.

ν_c Current velocity.

ω_p Peak wave frequency.

ψ^* Optimal heading.

ψ_d Desired heading.

kg kilogram.

m Meter.

mm millimeter.

s second.

Terms and concepts

- **Dynamic positioning system**
  A dynamic positioning system is a control system that automatically maintain a vessels position and heading by use of its own thrusters.

- **Equilibrium position**
  The equilibrium position of a TAPM system is defined as the position of the vessel without thruster assistance where the mean environmental loads are balanced by the mooring forces.

- **Extremum seeking**
  Extremum Seeking (ES) is a non model based method of adaptive control, and is used in situations where the reference trajectory or the setpoint are unknown. With help of the ES algorithm a setpoint is found in order to achieve an optimal value of the output. ES can also be used for tuning parameters of a feedback law.

- **Field zero point**
  The field zero point is defined as the equilibrium position of a moored vessel when there is no environmental loads acting on the vessel. The field zero point is defined as the origin of earth-fixed reference frame and is often located in the centre of the turret.

- **Finite Element Method**
  Finite Element Method (FEM) is a numerical mathematically method and is a widely used technique in structural engineering in order to describe the behavior and performance of structural components. In this report the mooring lines will be modeled based on FEM.

- **Heading**
  The heading of the vessel is the angle between the x-axis of the body-fixed reference frame and the true north axis of the earth-fixed reference frame, and is describing the orientation of the vessel.

- **Optimal heading**
  Optimal heading is the heading where the vessel is standing against the mean environmental loads.

- **Setpoint chasing**
  Setpoint chasing is an method used to automatically generate a new setpoint for a TAPM vessel in varying environmental conditions in order to find the optimal

equilibrium position in which the mooring loads and the environmental loads are in balance.

- **Stationkeeping**
  The term sationkeeping is used about a situation where maintaining a vessel's position fixed.

- **Thruster-assisted position mooring system**
  Thruster-Assisted Position Mooring (TAPM) system is a control system that uses a combination of mooring lines and dynamic positioning in order to maintain a vessels position. In TAPM there is defined a safety circle around the vessel. The vessel should operate inside this circle at all time in order to avoid the mooring lines to break.

- **Weather-vaning**
  Weather-vaning is a term describing that the vessel is orientated such that the moment due to mean current, wind and wave forces is zero and at the same time maintain fixed position and heading.

Chapter 1

Introduction

1.1 Background and motivation

After the Ekofisk discovery in 1969, the oil and gas industry quickly developed into the most dominant industry in Norway. Today, the trend is that the Norwegian offshore industry is experiencing an increased demand for integrated operations with use of marine vessels, both in open waters and in Arctic ice-covered waters. To perform offshore operations, it is required that the vessel has a stationkeeping system in order to maintain a fixed position with high accuracy even in rough environments. There are two main types of marine positioning systems used in the industry today, Dynamic Positioning (DP) systems used for free floating vessels and Thruster-Assisted Position Mooring (TAPM) systems used for anchored vessels (Sørensen et al.; 1999).

A TAPM system should, in addition to finding and holding the position and the heading of a vessel, also damp its motions. In order to find the position and the heading, the control system need to know the vessel's desired setpoints. Often these setpoints are specified manually by the user. Since offshore vessels like Floating Production Storage and Offloading (FPSO) can remain in the same location for years, it is extremely important to choose setpoints that are equal to the optimal values for both the heading and the position. At the optimal heading and position, the vessel will minimize the fuel consumption, which is good both in terms of economy and emission to the environment. With wrong setpoint, the thruster will fight against the mooring system, causing unnecessary high use of thrust and safety issues. Even a small offset in the optimal heading will result in a significantly larger use of thrust. Since it is difficult to decide the optimal setpoints manually, guidance systems for online autonomous control are developed using different setpoint determination algorithms.

This thesis will, through simulation and experiments, try out some new methods for online automatic determination of a more optimal setpoint for heading. These methods are known from other industries, but have until now not been used in TAPM applications.

1.2 Literature review

1.2.1 Stationkeeping

Acording to Fossen (2011) the term stationkeeping of a marine craft implies stabilization of the surge, sway and yaw motions. Meaning maintaining a vessel's position and heading fixed even in challenging weather.

1.2.2 Seakeeping

The term seakeeping on the other hand is, according to Fossen (2011), the study of motion of a craft when its heading (ψ) and speed (U) are constant while it is exposed too wave excitation. This also includes the case of zero speed.

1.2.3 Dynamic positioning

The International Maritime Organization (IMO) gives in their guideline, IMO (1994), the following definition of a Dynamically Positioned vessel (DP-vessel):

> *"Dynamically positioned vessel (DP-vessel) means a unit or a vessel which automatically maintains its position (fixed location or predetermined track) exclusevely by means of thruster force."*

Further, they are defining a Dynamic Positioning (DP) system as:

> *"Dynamic positioning system (DP system) means the complete installation necessary for dynaamically positioning a vessel comprising the following sub-systems:*
>
> - *power system,*
> - *thruster system, and*
> - *DP-control system."*

According to Sørensen (2013), the first DP system was developed in the 1960s. At this time the system was using single-input-single-outout PID-control algorithms in combination with lowpass and/or notch filter. Later, in the 1970s, more advanced methods for multivariable control were proposed.

1.2.4 Thruster-assisted position mooring

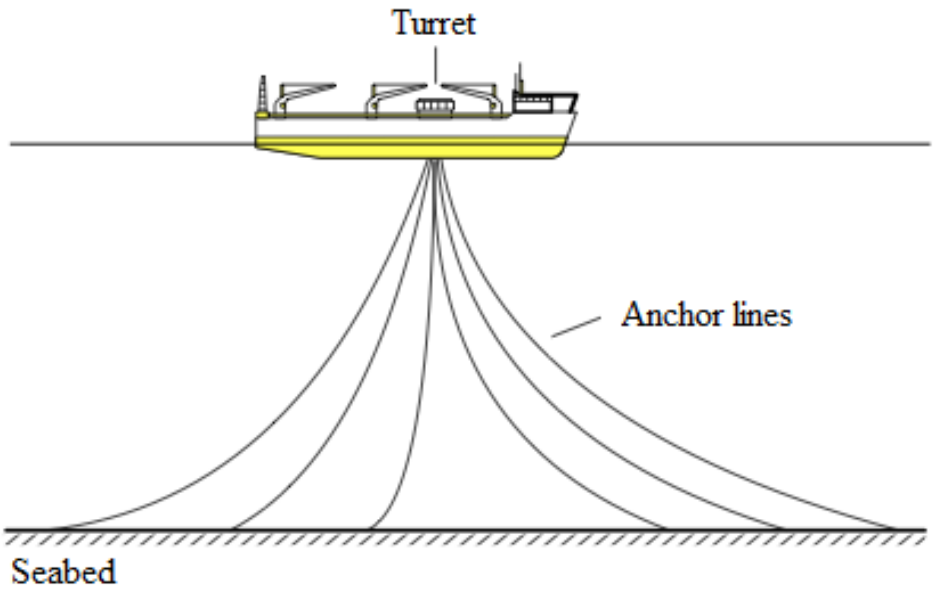

Figure 1.1: Principal figure of TAPM (Strand et al.; 1997).

Thruster-Assisted Position Mooring (TAPM) is a control system for automatic thruster assistance of a moored structure. A principal drawing of a TAPM system is shown in Figure 1.1. According to Aamo and Fossen (1999), this system has been commercially available since the late 1980s. TAPM is a cost-effective alternative to permanent platforms for offshore oil production. The system is in the industry also referred to as Position Mooring (PM) or Posmoor, which is a DNVGL notation (DNVGL; 2013).

Aamo and Fossen (1999) divides a TAPM system into two parts, a conventional mooring system and a DP system. As seen in Figure 1.1, the vessel is equipped with a turret positioned through the hull. The mooring lines are fixed both to the seabed and to the turret, which allows the vessel to freely rotate about the turret. Most of the stationkeeping in surge and sway is provided by the mooring system, while the thrusters are mainly used for damping the surge, sway, and yaw motion, and to keep the desired heading. In normal weather conditions, the fuel consumption is kept to a minimum, while in case of rough weather, the thrusters have to assist in the position keeping as well. The thrusters have to assist in order to avoid that the line tensions rising above the mooring lines safety limits, which could in worst case lead to line breakages.

According to Skjetne (2014), the literature proposes a safety circle around the vessel, with the Field Zero Point (FZP) as the centre. The FZP is the equilibrium position of the moored vessel when there is no environmental loads acting on the vessel. Inside this circle there is a minimal risk of line breakage, while outside there is a high risk of line

breakage. When the vessel is outside the safety circle, the thrusters should be used in order to bring the vessel back in and maintain a position inside the safety circle.

The mooring lines can be composed of chain, wirelines or synthetic material, and are often partitioned into several segments of different types and properties (Strand et al.; 1997).

Control strategies for TAPM

Over the years, several control strategies have been proposed for the TAPM system. The following are considered as the basic control modes.

- *Heading control*
  The main prupose of a heading controller is to keep the vessels heading angle at a desired value, such that the vessel's heading is towards the mean environmental load, which will minimize the vessel's fuel consumption. Both Strand et al. (1998) and Sørensen et al. (1999) proposed a Proportional, Integral and Derivative controller (PID-controller). Later, Fossen and Strand (2001) proposed a more advanced heading controller called Weather Optimal Positioning Control (WOPC), where the optimal heading is automatically estimated. WOPC will be further described later in the literature review.

- *Surge-sway damping control*
  The main purpose of a surge-sway damping controller is to reduce possible large oscillations in surge and sway, and thereby reduce the stress on the mooring system. A damping controller like this was proposed by Strand et al. (1998) and Sørensen et al. (1999).

- *Roll-pitch damping control*
  When applying the conventional horizontal-plane control strategy, certain marine constructions with small water plane area can experience undesired roll and pitch motions caused by the thruster usage in the combination with the mooring system. To reduce this motion, Sørensen and Peter Strand (2000), proposed a roll-pitch damping controller.

- *Line break detection and compensation*
  Line breakage of one or several mooring lines can occur. A line break detection algorithm is used in order to detect a line break and automatic feedforward thrust to compensate for this, in order to prevent another line break. This controller was proposed by Strand et al. (1998).

1.2.5 Optimal heading

The term optimal heading (ψ^*) will in this thesis concern the angle where the vessel's fuel consumption is held to a minimum. According to Fossen and Strand (2001), for a vessel with a port/starboard symmetry to obtain ψ^*, the mean environmental forces due to wind, waves and ocean currents have to act through the centerline of the vessel. The vessel will at this heading also obtain a sway force and a yaw moment equal to zero. It is important to use the optimal heading in order to save fuel, both in terms of economy and emissions. Using the optimal heading, the vessels has the least offset from the FZP.

ψ^* can be calculated from (1.1), where β_{env} is the angle of the mean environmental forces and π are subtracted in order for the vessel to stand against the mean environmental forces.

$$\psi^* = \beta_{env} - \pi \tag{1.1}$$

1.2.6 Weather optimal position control

Normally, vessels and free-floating rigs with TAPM systems or DP systems are designed for stationkeeping by specifying a desired constant position and desired constant heading angle. The desired heading (ψ_d) should be chosen equal ψ^*, but unfortunately it is impossible to measure or compute the direction of the mean environmental force, which will make the choice impossible. The mean wind direction on the other hand can easily be measured, and according to Fossen and Strand (2001), ψ_d is usually decided only depending on that. However, in rough weather this will result in large off-sets from the true mean direction of the total environmental force. Even a small off-set from ψ^* will result in a large use of thrust.

Since the optimal heading is calculated with respect to the weather, it is often referred to as the weather optimal heading. Several approaches in the field of WOPC is made over the years.

According to Fossen (2011), one popular method to compute the weather optimal heading is to monitor the resulting thrust force in the x and y directions. The method involves turning the bow of the ship in one direction until the thruster force in sway approaches to zero. It is appealing, but has a catch. There is no sensor that can measure the resulting thruster forces directly. Instead the angular speed and pitch of the propellers can be measured, and then the thrust in each direction have to be computed based on a model of the thruster characteristic. This can, unfortunately, result in pretty rough estimates.

Another method used to find the optimal heading, is the one proposed by Pinkster and Nienhuis (1986). The principle of this method is to control the x and y position using a feedback PID-controller, in addition to feedback from the yaw velocity. The method has shown to be applicable for large tankers, but has some catches as well. The method requires that the rotation point of the vessel is located a certain distance forward of the centre of gravity, and it also puts restriction on the number and the configuration of the thrusters installed.

A new concept for WOPC of ships and free-floating rigs were developed by Fossen and Strand (2001), using polar coordinates and nonlinear backstepping. The control objective of this method is for the vessel heading to automatically adjust to the mean environmental forces in order to obtain the optimal heading without using any environmental sensors.

This WOPC theory tells that a vessel can be exponentially stabilized on a circle arc with a constant radius by letting the bow of the ship point toward the origin of the circle. At the same time, the vessel can maintain a fixed position, by designing a translatory circle center control law. Further, the circle centre is translated online such that the Cartesian position is constant, while the bow of the ship is automatically turned up against the mean environmental force to obtain weather-vaning.

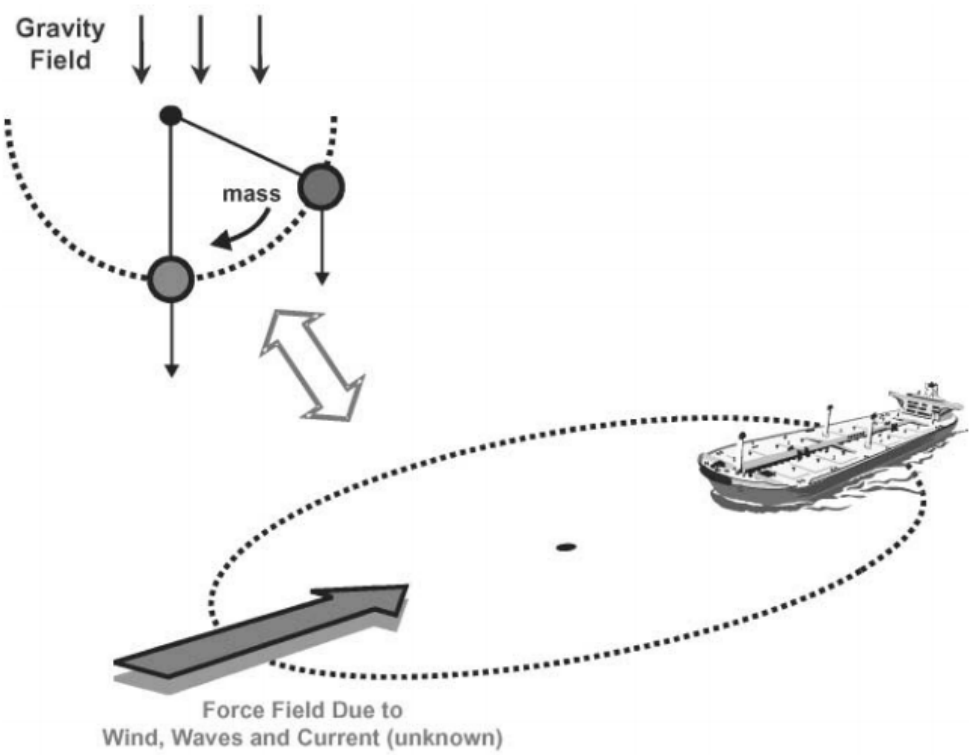

Figure 1.2: Weather optimal positioning principle (Fossen and Strand; 2001).

The approach of the WOPC is motivated by a pendulum in a gravity field, see Figure 1.2. For the pendulum, the gravity is the unmeasured and unknown force field, and will in WOPC be interpreted as the mean environmental force. Moreover, the idea is that the circular motion of the controlled ship will copy the dynamics of a pendulum in the gravity field.

1.2.7 Setpoint chasing

Setpoint chasing is, according to Nguyen and Sørensen (2007, 2009), a method used to find and control a TAPM-vessel to its equilibrium position. When a TAPM-vessel stays in its equilibrium position, the utilization of the mooring system is maximized and the thrust is minimized. This will improve the vessel's performance. The control law used in setpoint chasing is the PID-control, where the setpoint can be found by different methods and is forwarded to the controller as the desired position.

In setpoint chasing, it is normal to distinguish between moderate environmental conditions and extreme environmental conditions. The setpoint found in moderate environmental conditions is the equilibrium position of the vessel, while, due to risk of line breakage in the extreme environmental conditions, the setpoint is chosen to be a position closer to the FZP than the equilibrium position.

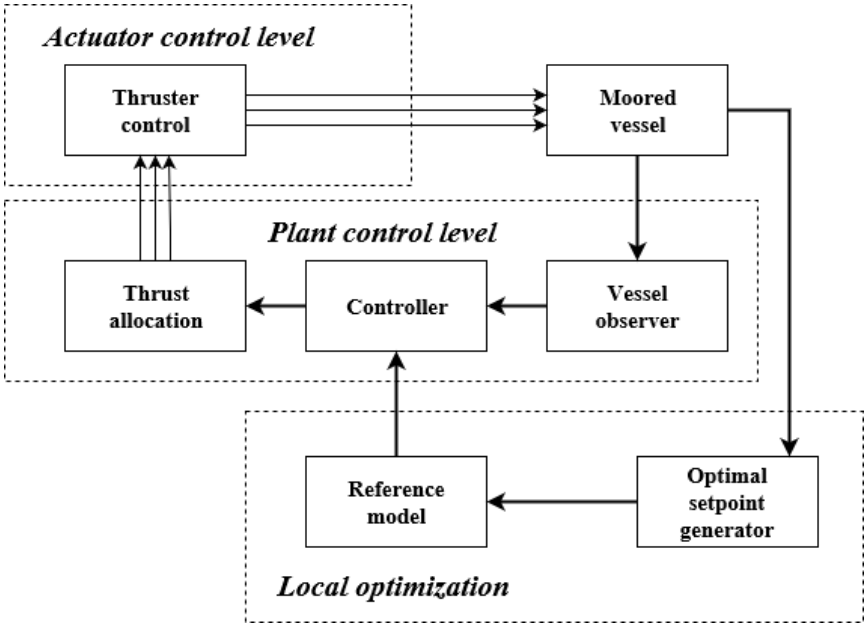

Figure 1.3: Structure of a TAPM system including an optimal setpoint generator (adapted from Nguyen and Sørensen (2009)).

A structure of a TAPM system including an optimal setpoint generator can be seen in

Figure 1.3. This is a real-time marine control system, and can be divided into three levels; actuator control level, plant control level and local optimization level. The local optimization level can also be called a guidance system. In this manner the guidance system is autonomous. The guidance system provides the plant control system with setpoints to follow online.

Different methods have been proposed for setpoint chasing, there among FEM-based (Sørensen et al.; 2001), reliability-based (Berntsen et al.; 2006; Leira et al.; 2008) and setpoint chasing by lowpass filter (Nguyen and Sørensen; 2007, 2009).

1.2.8 Extremum seeking

Extremum Seeking (ES) is, according to Ariyur and Krstić (2003), a non-model-based method of adaptive control. It is used in situations where the reference trajectory or the setpoint for a system are unknown. ES can also be used for online tuning of the parameters of a PID-controller (Killingsworth and Krstic; 2006).

According to Nesic (2011), ES is an approach for online optimization for a system with steady-state behaviour. The ES algorithm can seek an extreme of some steady-state function without knowing the model.

The principle of ES can, according to Zhang and Ordóñez (2012), be divided into two function layers. First, the system have to seek an extremum of an output function. Secondly, be able to control the system and drive the output function to that extremum.

According to Nesic (2011) the first paper on the topic of ES can be addressed back to 1922. After that, the topic was, according to Ariyur and Krstić (2003), a popular control application in the 1940s-1960s, and had in the 1990s a comeback as a research topic and a tool for industrial real-time optimization problems.

The ES method can, according to Nesic (2011), be classified in different manners. Some choose to distinguish between a deterministic versus a stochastic part of the theory, but others between continuous-time or real-time versus the discrete-time cases. In this thesis the last approach of the ES theory is used. Both real-time ES and discrete-time ES make use of different ES schemes in order to solve the problem, of which the real-time method of sinusoidal perturbation has been the most popular (Ariyur and Krstić; 2003).

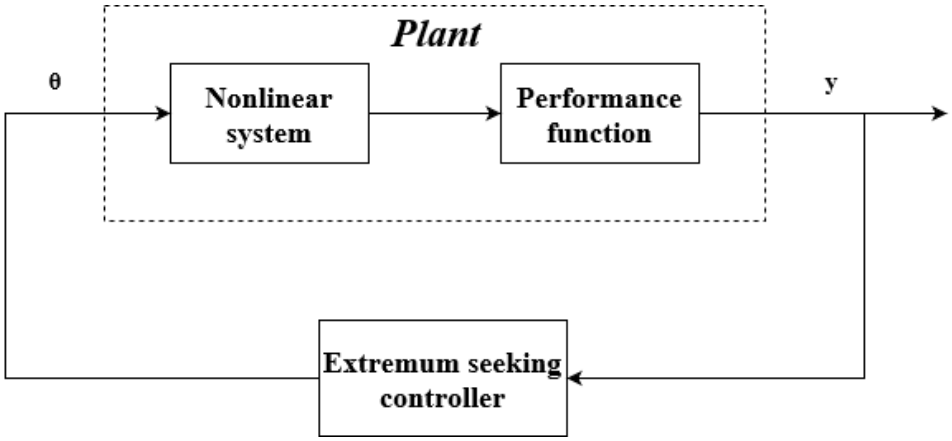

Figure 1.4: ES loop for a general plant (adapted from Ariyur and Krstić (2003))

Figure 1.4 shows a block diagram of a general ES scheme. Using ES theory, the plant of the system includes both a nonlinear system and a performance function, where the output of the plant, y, is the performance function. The performance function can also be called an objective function or a cost-function, and makes the ES problem into an optimization problem, see (1.2). An optimization problem finds the minimum or the maximum of a variable given certain constrains.

$$\min/\max J(.) \quad \text{subject to } \dot{x} = f(x, u) \tag{1.2}$$

According to Zhang and Ordóñez (2012), the performance function is generally a function of the state and is unknown or poorly known in the ES design. The lack of knowledge implies that the design of the ES controller is only based on the measurement of the performance function. ES control can sometimes also be called dynamic optimization, due to the fact that the arguments of the performance function to be optimized are constrained by a dynamic system.

With help of an ES algorithm, it is possible to tune a setpoint for the system based on the measurement of the performance function in order to achieve an optimal value of the output. In other words, the objective and the goal of ES control is to operate at a setpoint that represents the optimal value of a function being optimized in the control loop.

According to Ariyur and Krstić (2003), ES control is applicable in situations where there is a nonlinearity in the control problem, and the nonlinearity has a local minimum or a maximum. The nonlinearity may be in the plant or in the performance function.

Today, ES has been applied to various control problems. In the book, *Real-Time Optimization by Extremum-Seeking Control*, written by Ariyur and Krstić (2003), some examples

of different usage of the ES control theory can be seen. There are examples of formation flight, bioreactors, compressors, and Antilock Breaking Systems (ABS). In the example of the ABS, which is a safety system used in vehicles, the ES controller is used in order to seek the maximum of the friction force coefficient between the wheel and the ground, in order to minimize the stopping time of a vehicle.

According to Breu and Fossen (2010), ES control can also be used to determine the setpoint for the wave encounter frequency in order to avoide the condition of parametric roll, which is a dangerous phenomenon for ships caused by time-varying restoring forces.

1.2.9 Statoil's Cat I Arctic Drillship

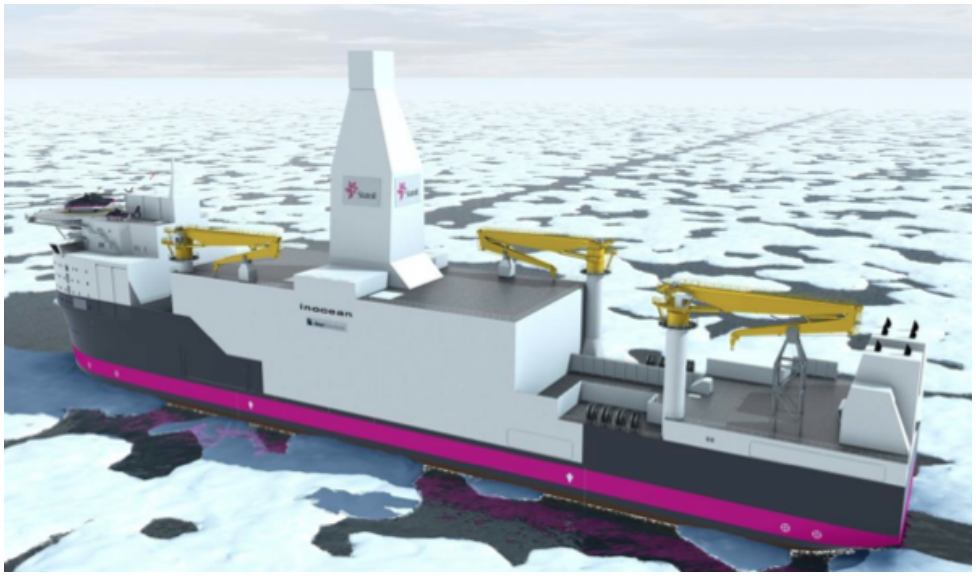

Figure 1.5: Cat I Arctic Drillship (Jorde; 2014)

In 2013, Inocean won, according to Jorde (2014), a contract from Statoil to design an Arctic drillship. The result of this is the Cat I Arctic Drillship, which is a DP and turret moored Mobile Offshore Drilling Unit (MODU), shown in Figure 1.5. The vessel is equipped with six thrusters and a turret system with a maximum of 12 mooring lines. The dimensions of the ship can be seen in Table 1.1.

Inocean (2013), describes their drillship in the following manner:

> *"A fully winterized drillship designed for unsupported shallow and deep water harsh environment operation and for shallow water arctic operation with ice management support. Turret moored on shallow depth, well center midship for maximum operability. Arranged with maximum focus on HSE with respect to*

operation and maintenance. Minimized fuel consumption and environmental footprint. Dual hull shape with bow form optimized for open water operation and aft ship designed for ice operation."

Table 1.1: C/S Inocean Cat I Drillship dimensions

Description	**Data**
Length over all (L_{oa})	232 [m]
Breadth (B)	40 [m]
Depth moulded (D)	19 [m]
Draft design (T)	12 [m]

1.2.10 C/S Inocean Cat I Drillship model

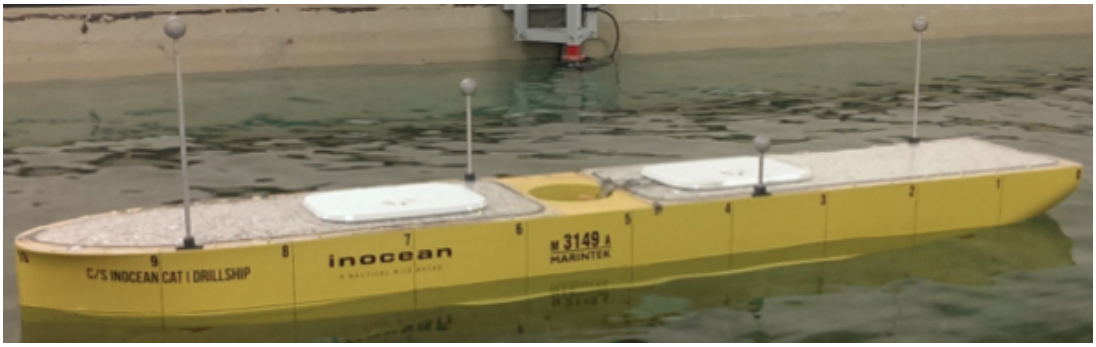

Figure 1.6: The model of CSAD (Bjørnø; 2016)

The same drawing of the hull of Statoil's Cat I Arctic Drillship, has been used by Sintef Ocean to build a model ship with 1:90 scaling of the same hull. The purpose of this vessel is to provide the Norwegian University of Science and Technology (NTNU) with a new model vessel for the cybership fleet in the Marine Cybernetics Laboratory (MC Lab). This cybership will be used to conduct research in the field of TAPM. More about the MC Lab will be covered in the next section of this thesis.

The model ship is named C/S Inocean Cat I Drillship, in short C/S Arctic Drillship (CSAD), and can be seen in Figure 1.6. The hull of CSAD is, according to Bjørnø et al. (2017), constructed in carbon fiber, with brackets for the thrusters and with a deck out of acrylic fiber covering all of the bottom deck. The deck is made planer, instead of a lowered mid-ship section. The main dimensions of the vessel in model scale are given in Table 1.2.

Table 1.2: C/S Inocean Cat I Drillship model dimensions

Description	**Data**
Length over all (L_{oa})	2.578 [m]
Breadth (B)	0.440 [m]
Depth moulded (D)	0.211 [m]
Draft design (T)	0.133 [m]

According to Bjørnø et al. (2017), the thruster system for CSAD is placed corresponding to the original hull. There are in total six azimuth thrusters installed, and the placement of each of them can be seen in Figure 1.7. The red zones on the figure indicates thruster-thruster interaction and is a forbidden thruster configuration. Thruster parameter identification for CSAD can be seen in Table 1.3.

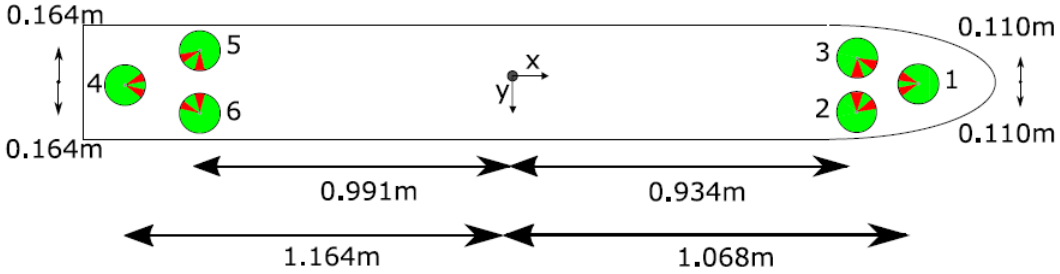

Figure 1.7: Placement and constraints of the thrusters on CSAD (Bjørnø et al.; 2017)

Table 1.3: Thruster parameter identification for CSAD model

Description	**Data**
Max shaft speed	94.9 [RPS]
Power	0.868 [W]
Propeller diameter	0.030 [m]
Steering speed	114 [deg/s]
Max torque	0.0015 [Nm]
Max thrust	1.50 [N]

CSAD is, according to Bjørnø et al. (2017), equipped with an inboard real-time embedded controller, the CompactRIO-9024 (cRIO) with different modules from National Instruments to control the system. Moreover, the model vessel is powered from six 12 volt 12 Ah lead batteries, and fitted with four silver spheres in order to obtain the position data in 6 Degree Of Freedom (DOF). The turret system installed takes a maximum

of 8 mooring lines. According to Bjørnø (2016), cRIO runs real-time control systems programmed either in LabVIEW or Simulink code through the software NI VeriStand.

More information about CSAD can be found in Bjørnø (2016) and Frederich (2016).

1.2.11 MC-Lab

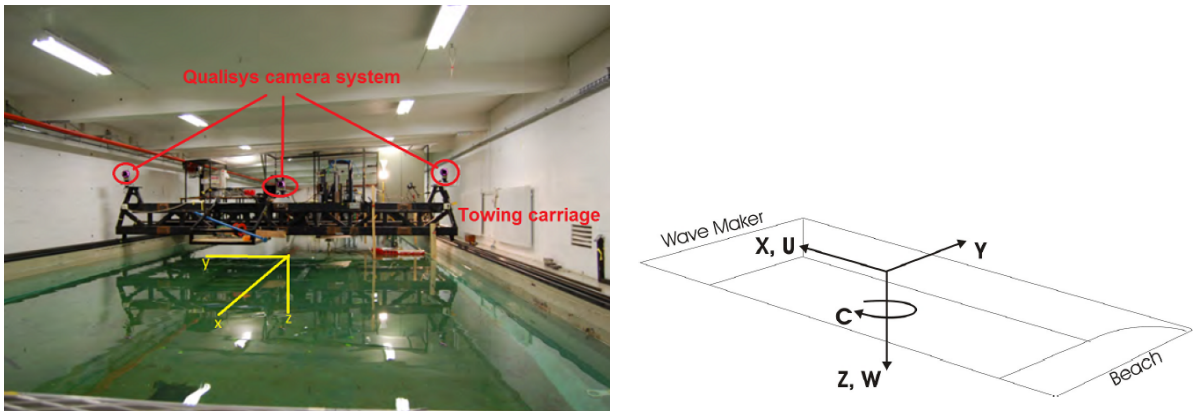

(a) Marine Cybernetics Laboratory (b) Coordinate system of the MC Lab

Figure 1.8: MC Lab (NTNU; 2017b)

The Marine Cybernetics Laboratory (MC Lab) is a small wave basin, with tank dimension of L x B x D = 40 m x 6,45 m x 1,5 m, and is located at Tyholt in Trondheim. The laboratory is operated by the Department of Marine Technology at NTNU, and is mainly used by Master students and PhD-candidates (NTNU; 2017a).

The MC Lab has a fleet of model vessels, see NTNU (2017b) for information about them, and the lab is especially suitable for testing marine motion control systems. The lab is also suitable for hydrodynamic tests, mainly do to an advanced towing carriage. In addition to the towing carriage, the laboratory also consists of the following fixed equipment; Qualisys motion capture system, wave generator and a video-camera.

The MC Lab can be seen in Figure 1.8a, while the definition of the coordinate system in the laboratory can be seen in Figure 1.8b. Due to safety and the risk of drowning, it is required, when using the basin, that at least two persons are present in the laboratory.

Towing carriage

The towing carriage is used in hydrodynamic testes, including to estimate a vessels damping term. According to NTNU (2017a), the towing carriage has the capability for precise

movement of the models in 6 DOF.

The carriage can be operated in a computer controlled mode or manually from the consol on the carriage. For more information about the setup, see NTNU (2017b).

Qualisys motion capture system

Qualisys motion capture system is a system that provides, with millimeter precision, a 6 DOF data tracking of a body in the MC Lab. It works in real-time and is configured to 50 Hz.

The positioning system consists, according to NTNU (2017b), of three Oqus high speed infrared cameras. The cameras are registering infrared reflectors, silver spheres, which are placed on the body of the vessel. One computer in the MC Lab is dedicated to run the software, Qualisys Track Manager (QTM). This computer receives camera data, which is transmitted using peer-to-peer networking. The QTM software performs triangulation and broadcasts the vessel position over the wireless network, in order for it to be available for the control system. For more information, see NTNU (2017b).

The MC Lab is equipped with this system both over and under the water surface, in order to emulate a full scale Global Navigation Satellite System (GNSS).

Wave generator

A single wave making machine with a width of 6 meter, is used to make waves in the basin. The machine is, according to NTNU (2017b), controlled by a dedicated computer and can produce both regular and irregular waves. The available wave spectra are the following; first order Stoke, JONSWAP, Pierson-Moskowitz, Bretschneider, ISSC and ITTC. See Table 1.4, for the capacity of the generator.

Table 1.4: Wave generator capacity

	Height [m]	**Period T** [s]
Regular waves	$H < 0.25$	$0.3 - 3.0$
Irregular waves	$H_s < 0.15$	$0.6 - 1.5$

Video-camera

Two high-resolution cameras, one on each side of the laboratory, is installed for recording activities in the basin. The cameras are remotely operated from a dedicated computer. For more information see NTNU (2017b).

1.3 Objective and scope

1.3.1 Objective

The objective of this thesis is to propose an optimal heading algorithm that can be used in the design of an autonomous guidance system for a TAPM vessel. It is decided to look into the non-model-based method of adaptive control, ES, to see if this control algorithm can be used efficiently to find the optimal heading of a vessel. ES has never before been tested for this purpose. The main contribution from the work will be two different ES control schemes, a sinusoidal perturbation based scheme and a numerical optimization based scheme, which can be used to find the optimal value for the heading.

In addition, this master thesis contributes with an updated simulation model of the TAPM vessel, CSAD, where the existing Catenary equation based mooring lines were replaced by mooring lines based on the Finite Element Method (FEM). Further, the thesis also contributes with a collection of literature reviews in the field of TAPM.

All programs are developed using MATLAB and Simulink, and are attached in a zip-file. The content of the attached file is further explained in Appendix A.

1.3.2 Scope

The scope of this master thesis are listed in the following.

1. Perform a background and literature review of relevant topics, especially on TAPM, CSAD and the MC Lab, in order to provide the necessary information on the subject.
2. Study the control methods setpoint chasing and extremum seeking.
3. Derive a mathematically description of a TAPM vessel and a TAPM control design model.
4. Establish a 6 DOF simulation model for CSAD model ship. The simulation model should include loads from waves and currents, and the mooring model should be based on FEM.
5. Derive a controller based on the theory of setpoint chasing.
6. Derive a guidance system where the user specifies manually the heading setpoint. This will be used as a basis for testing and caparison.

7. Derive a autonomous guidance method system based on the sinusoidal perturbation based ES scheme. Show its performance on a simplified system. If the results are good, then try to get it to work on the full system.
8. As the alternative autonomous guidance method, a discrete ES scheme are chosen.
9. Test the controllers on the simulation model. Test some of them during experimental work.

Boundaries and limitations

Because of the difficulties to perform good results from experimental work, the main focus will be on results from the simulations. In addition, a leakage in the model vessel, CSAD, prevented some of the systems from being tested in the MC Lab.

When it comes to the sinusoidal perturbation based ES controller, because of its complexity, the focus will be to show its performance on a simplified system before it is tested on the 6 DOF model.

1.4 Organization of the thesis

The thesis is built up around control strategies for optimal control of a vessel equipped with a TAPM system, where the focus is on finding the optimal heading. The model ship CSAD is used for simulation studies and experimental testing.

Chapter 1 introduces the thesis to the reader, and provides the relevant background. A literature review is provided on the following topics; stationkeeping, seakeeping, DP, TAPM with different control strategies, optimal heading, WOPC, setpoint chasing, ES, the model ship CSAD and the MC Lab. Chapter 1 also provides the objective and scope of the thesis.

Chapter 2 presents a full 6 DOF description of a mathematically model of a TAPM surface vessel. It also covers a description of a 3 DOF mathematically model of TAPM control design model.

Chapter 3 presents a 6 DOF simulation model of CSAD including a FEM model for the mooring lines.

Chapter 4 gives descriptions of a controller and an observer.

Chapter 5 gives descriptions of different guidance systems for heading, both user specified and autonomous guidance systems. Description of two different ES control schemes used for heading, the sinusoidal perturbation based scheme and the numerical optimization based scheme. In addition, the setpoint chasing is derived for surge and sway.

Chapter 6 describes the experimental setup for CSAD in the MC Lab.

Chapter 7 gives the results using the different controllers both on simulations and on experimental work.

Chapter 8 presents the discussion of the results. Some issues according to the experimental work is also discussed.

Chapter 9 concludes the master thesis and summarizes the main contributions. Suggestions for further work is also presented.

Appendix presents the MATLAB codes and the Simulink models used in the thesis.

Chapter 2

Mathematical modeling

2.1 Kinematics

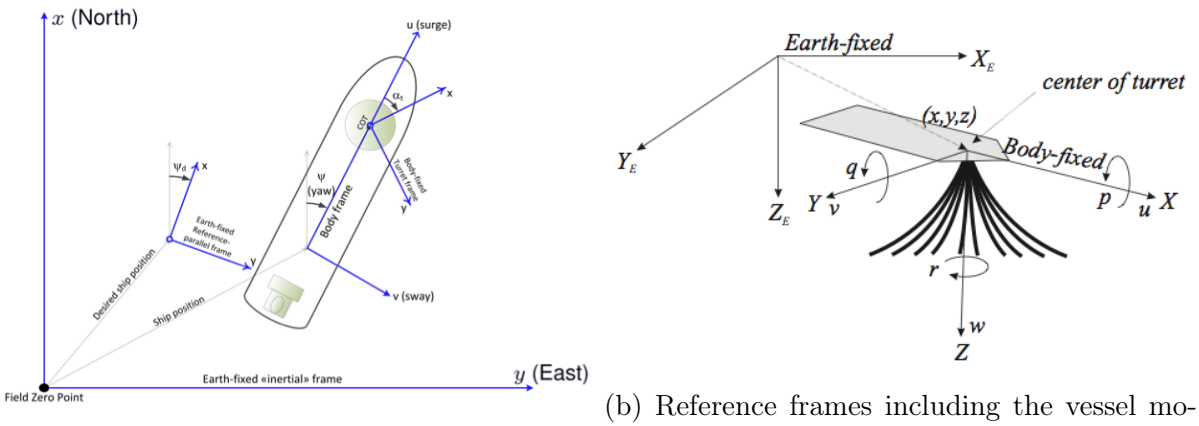

(a) Reference frames (Skjetne; 2014).

(b) Reference frames including the vessel motion parameters (Aamo and Fossen; 2001).

Figure 2.1: Different reference frames used in TAPM.

According to Skjetne (2014), there are four different reference frames used in TAPM, as seen in figure 2.1a.

- **Earth-fixed reference frame**
  The Earth-fixed reference frame is denoted as the $\{E\}$-frame, where the x-axis points towards true North (N), y-axis towards East (E) and z-axis downwards (D) normal to the Earth's surface. The origin is defined as the Field Zero Point (FZP) and is located in the Centre Of Turret (COT) when no environmental loads act on the vessel. For the experiments of the model ship in the MC-Lab, the Earth-fixed reference frame will be represented by a Basin-fixed reference frame.

- **Body-fixed reference frame**
  The Body-fixed reference frame is denoted as the $\{B\}$-frame and is fixed to the vessel. For convenience, the origin, Vessel Origin (VO), is a fixed point in the hull, typically ($L_{pp}/2$, $B/2$, z_{WL}) (Skjetne; 2014). The axis follows the right-hand convention with the x-axis as the longitudinal axis directed from aft to fore and the z-axis as the normal axis pointing downwards. The position and the orientation of the craft are described relative to the $\{E\}$-frame.

- **Vessel-parallel reference frame**
  The Vessel-parallel reference frame is denoted as the $\{D\}$-frame and is fixed in the $\{E\}$-frame. The frame is rotated towards the desired heading,ψ_d and with origin at the desired position (x_d, y_d).

- **Turret-fixed reference frame**
  The Turret-fixed reference frame is denoted as the $\{T\}$-frame and is fixed to the turret with origin at the COT. The frame is rotated relative to the body x-axis, with an angle α_t according to turret rotation.

A simplification can be made to the problem, when deciding that both the $\{T\}$-frame and the $\{B\}$-frame coincides, with origin at the COT, see Figure 2.1b. Only three reference frames are used in TAPM according to Strand et al. (1997) and Nguyen and Sørensen (2009). It is further assumed that the COT is located at the centre line of the vessel.

Generally the vessel's motion is described in 6 Degree Of Freedom (DOF), see Figure 2.1b. According to Fossen (2011), the 6 DOF is described relative to the $\{B\}$-frame, where surge (u), sway (v), and heave (w) represent the translational velocity along the X, Y, and Z-axis, respectively, and roll (p), pitch (q), and yaw (r) represent the rotation rate about the X, Y, and Z-axis, respectively.

The Body-fixed reference frame gives, according to (Fossen; 2011), the position and the orientation of the vessel described relative to the Earth-fixed reference frame. The relation between the two frames are given by (2.1), which is referred to as the 6 DOF kinematic equation.

$$\begin{aligned} \dot{\boldsymbol{\eta}} &= \mathbf{J}(\boldsymbol{\eta})\boldsymbol{\nu} \\ \boldsymbol{\eta} = [\boldsymbol{\eta}_1\, \boldsymbol{\eta}_2]^\top, &\quad \boldsymbol{\nu} = [\boldsymbol{\nu}_1\, \boldsymbol{\nu}_2]^T \end{aligned} \tag{2.1}$$

Where $\boldsymbol{\eta}_1 = [X_E, Y_E, Z_E]^T$ are the position in the Earth-fixed frame, $\boldsymbol{\eta}_2 = [\phi, \theta, \psi]^T$ are the Euler angles, $\boldsymbol{\nu}_1 = [u, v, w]^T$ are the linear velocities, and $\boldsymbol{\nu}_2 = [p, q, r]^T$ are the angular velocities. $\mathbf{J}(\boldsymbol{\eta})$ is given by (2.2), where $\mathbf{J}_{11}(\boldsymbol{\eta})$ is given by (2.3), $\mathbf{J}_{22}(\boldsymbol{\eta})$ is given by (2.4) and s=sin, c=cos and t=tan.

$$\mathbf{J}(\boldsymbol{\eta}) = \begin{bmatrix} \mathbf{J}_{11}(\boldsymbol{\eta}) & \mathbf{0} \\ \mathbf{0} & \mathbf{J}_{22}(\boldsymbol{\eta}) \end{bmatrix} \tag{2.2}$$

$$\mathbf{J}_{11}(\boldsymbol{\eta}) = \begin{bmatrix} c\psi c\theta & -s\phi + c\theta + c\phi s\theta s\phi & s\psi s\phi + c\psi c\phi s\theta \\ s\psi c\theta & c\psi c\phi + s\phi s\theta s\psi & -c\psi s\phi + s\theta s\psi s\phi \\ -s\theta & c\theta s\phi & c\theta c\phi \end{bmatrix} \tag{2.3}$$

$$\mathbf{J}_{22}(\boldsymbol{\eta}) = \begin{bmatrix} 1 & s\phi t\theta & c\phi t\theta \\ 0 & c\phi & -s\phi \\ 0 & \frac{s\phi}{c\theta} & \frac{c\phi}{c\theta} \end{bmatrix} \tag{2.4}$$

2.2 Kinetics

In mathematical modeling of the dynamics of a marine vessel it is common to divide the overall model into two sub-models, a Low-Frequency (LF) model and a Wave-Frequency (WF) model. The two models are combined through superposition. The WF motions are assumed to be caused by first-order wave loads, while the LF motions are assumed nonlinear and caused by second-order mean and slowly varying wave loads, current loads, wind loads, mooring, and thrust forces. A detailed explanation of the full 6 DOF model can be found in both Sørensen (2013) and Fossen (2011).

2.2.1 LF model

$$\mathbf{M}_{RB}\dot{\boldsymbol{\nu}} + \mathbf{M}_A\dot{\boldsymbol{\nu}} + \mathbf{C}_{RB}(\boldsymbol{\nu})\boldsymbol{\nu} + \mathbf{C}_A(\boldsymbol{\nu}_r)\boldsymbol{\nu}_r + \mathbf{D}(\boldsymbol{\nu}_r)\boldsymbol{\nu}_r + \mathbf{G}(\boldsymbol{\eta}) = \boldsymbol{\tau}_{env} + \boldsymbol{\tau}_{moor} + \boldsymbol{\tau}_c \tag{2.5}$$

The LF model is, according to Sørensen (2013), given by equation (2.5), where $\mathbf{M}_{RB}$ and $\mathbf{M}_A$ are the inertia matrix and the added mass respectively, $\mathbf{C}_{RB}(\boldsymbol{\nu})$ and $\mathbf{C}_A(\boldsymbol{\nu}_r)$ are the Coriolis and centripetal terms and the added mass respectively, $\mathbf{D}(\boldsymbol{\nu}_r)$ is the damping matrix and $\mathbf{G}(\boldsymbol{\eta})$ is the generalized restoring force caused by the buoyancy and gravitation. $\boldsymbol{\nu}_r$ is the relative velocity between the velocity of the ship and the velocity of the water current. The right-hand side of the equation represents the generalized external forces, where $\boldsymbol{\tau}_c$ is the control force provided by the thrusters, $\boldsymbol{\tau}_{env} = \boldsymbol{\tau}_{wave2} + \boldsymbol{\tau}_{wind}$ are the environmental loads due to wind loads and second-order wave drift loads and $\boldsymbol{\tau}_{moor}$ are the mooring forces. The mooring forces will be discussed later in this chapter.

2.2.2 WF model

$$\mathbf{M}(\omega)\ddot{\boldsymbol{\eta}}_{Rw} + \mathbf{D}_p(\omega)\dot{\boldsymbol{\eta}}_{Rw} + \mathbf{G}\boldsymbol{\eta}_{Rw} = \boldsymbol{\tau}_{wave1} \tag{2.6}$$

$$\dot{\boldsymbol{\eta}}_w = \mathbf{J}(\bar{\boldsymbol{\eta}}_2)\dot{\boldsymbol{\eta}}_{Rw} \tag{2.7}$$

In stationkeeping operations, small motions about the desired position can be assumed and the coupled equations of the WF model in 6 DOF can be assumed to be linear, see (2.6) and (2.7), where $\boldsymbol{\tau}_{wave1}$ is the first order wave excitation vector. $\mathbf{M}(\omega)$ is the system inertia matrix containing frequency dependent added mass coefficients and the vessel's mass and moment of inertia, $\mathbf{D}_p(\omega)$ is the wave radiation damping matrix and $\mathbf{G}$ is the linearized restoring coefficient matrix that only affects heave, roll and pitch. $\boldsymbol{\eta}_{Rw}$ is the WF motion vector in the $\{D\}$-frame, $\boldsymbol{\eta}_w$ is the WF motion vector in the $\{E\}$-frame and $\bar{\boldsymbol{\eta}}_2 = [0\ 0\ \psi_d]^T$. For a detailed explanation of the model see Faltinsen (1990) and Sørensen (2013).

2.2.3 Mooring model

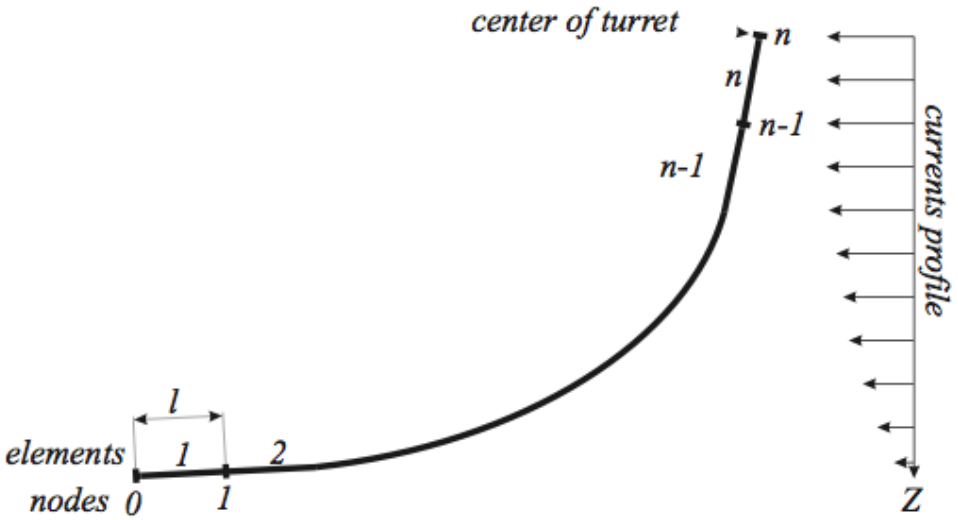

Figure 2.2: Mooring line configuration (Aamo and Fossen; 2001).

For TAPM, a multi-cable mooring system is needed. The mooring lines are connected to the vessel directly or through a turret. In this thesis, a turret is used. Each line enters the turret through a Terminal Point (TP), which is the point where the mooring forces act on the vessel. According to Triantafyllou (1990), the mooring lines are subjected to three types of excitations: Large amplitude LF motions, medium amplitude WF motion and small amplitude vibrations. A horizontal-plane spread mooring model can, according

to Nguyen and Sørensen (2009), be described according to (2.8), where $\mathbf{g}_{mo}$ and $\mathbf{d}_{mo}$ are the earth-fixed restoring force and damping due to the mooring system. The nonlinear mooring line parameters are found by the Finite Element Method (FEM), according to Aamo and Fossen (2001). See figure 2.2 for a visualisation of the problem.

$$\boldsymbol{\tau}_{moor} = -\mathbf{J}^{-1}(\boldsymbol{\eta}_2)\mathbf{g}_{mo}(\boldsymbol{\eta}) - \mathbf{d}_{mo}(\boldsymbol{\nu}_r) \tag{2.8}$$

In the approach of FEM, the hydrodynamic loads on the cables are modelled according to *Morison's equation*, see Faltinsen (1990) for a detailed explanation. All the mooring cables are pretensioned in order to avoid the occurrence of zero tension. Furthermore, the mooring cables bending and torsional stiffness are assumed to be neglected. To simplify the problem, the added mass of each cable is neglected and it is assumed that each cable is supported by fixed end-points.

A multi-cable mooring system consists of m-cables, where each cable is uniformly partitioned into n segments, and the nodal points are enumerated from 0 to n. The position vector in Earth-fixed coordinates is denoted $\mathbf{r}_k^j \in \mathcal{R}^3$ for the k^{th} nodal point of the j^{th} cable. The relative velocity is denoted $\mathbf{v}_k^j = \dot{\mathbf{r}}_k^j - \mathbf{v}_c(\mathbf{r}_k^j)$, where $\mathbf{v}_c(\mathbf{r}_k^j)$ is the ambient fluid velocity at the node.

In Aamo and Fossen (2001), two boundary conditions are given in order solve the problem.

1. The first nodal point, $\mathbf{r}_0^j$, is fixed for $j = 1, 2, ..., m$.
2. The last nodal point, $\mathbf{r}_n^j$, is connected to a fixed point on the vessel, $\mathbf{p}^j$. This implies that $\mathbf{p}^j$ for $j = 1, 2, ..., m$ are constant vectors given in the body-fixed frame.

This leads to two set of Ordinary Differential Equations (ODE), where (2.9) is valid for $k = 1, 2, ..., n-1$, and (2.10) is valid for the last nodal point. The terms in (2.9) are defined in (2.11) and the terms in (2.10) are defined in (2.12).

$$\mathbf{M}_k^j \dot{\mathbf{v}}_k^j + \mathbf{D}_k^j \mathbf{v}_k^j + \mathbf{k}_k^j + \mathbf{g}_k^j = \mathbf{0}, \quad k = 1, 2, ..., n-1, \quad j = 1, 2, ..., m \tag{2.9}$$

$$\mathbf{M}_n^j \dot{\mathbf{v}}_n^j + \mathbf{D}_n^j \mathbf{v}_n^j + \mathbf{k}_n^j + \mathbf{g}_n^j = \mathbf{0}, \quad j = 1, 2, ..., m \tag{2.10}$$

$$
\begin{aligned}
\mathbf{M}_k^j &= [\rho_0 l_j + \frac{C_1^j}{2}(\varepsilon_k^j + \varepsilon_{k+1}^j)]\mathbf{I}_{3x3} - \frac{C_1^j}{2}(\varepsilon_k^j \mathbf{P}_k^j + \varepsilon_{k+1}^j \mathbf{P}_{k+1}^j) \\
\mathbf{D}_k^j &= \frac{C_2^j}{2}[|\mathbf{v}_k^j \cdot \mathbf{l}_k^j|\mathbf{P}_k^j + |\mathbf{v}_k^j \cdot \mathbf{l}_{k+1}^j|\mathbf{P}_{k+1}^j] \\
&\quad + \frac{C_3^j}{2}[\varepsilon_k^j |(\mathbf{I}_{3x3} - \mathbf{P}_k^j)\mathbf{v}_k^j|(\mathbf{I}_{3x3} - \mathbf{P}_k^j) + \varepsilon_{k+1}^j |(\mathbf{I}_{3x3} - \mathbf{P}_{k+1}^j)\mathbf{v}_k^j|(\mathbf{I}_{3x3} - \mathbf{P}_{k+1}^j)] \\
\mathbf{k}_k^j &= \frac{E_j A_{0j}}{l_j}[\frac{\varepsilon_k^j - l_j}{\varepsilon_k^j}\mathbf{l}_k^j - \frac{\varepsilon_{k+1}^j - l_j}{\varepsilon_{k+1}^j}\mathbf{l}_{k+1}^j] \\
\mathbf{g}_k^j &= -l_j \rho_0^j \frac{\rho_c^j - \rho_w}{\rho_c^j}[0\ 0\ g]^T
\end{aligned}
\tag{2.11}
$$

$$
\begin{aligned}
\mathbf{M}_n^j &= (\rho_0 l_j + C_1^j \varepsilon_n^j)\mathbf{I}_{3x3} - C_1^j \varepsilon_n^j \mathbf{P}_n^j \\
\mathbf{D}_n^j &= C_2^j |\mathbf{v}_n^j \cdot \mathbf{l}_n^j|\mathbf{P}_n^j + C_3^j \varepsilon_n^j |(\mathbf{I}_{3x3} - \mathbf{P}_n^j)\mathbf{v}_n^j|(\mathbf{I}_{3x3} - \mathbf{P}_n^j) \\
\mathbf{k}_n^j &= \frac{E_j A_{0j}}{l_j}\frac{\varepsilon_n^j - l_j}{\varepsilon_n^j}\mathbf{l}_n^j \\
\mathbf{g}_n^j &= -\frac{1}{2} l_j \rho_0^j \frac{\rho_c^j - \rho_w}{\rho_c^j}[0\ 0\ g]^T
\end{aligned}
\tag{2.12}
$$

Where,

$$
\begin{aligned}
\mathbf{l}_k &= \mathbf{r}_k - \mathbf{r}_{k-1}, \quad \in \mathcal{R}^3 \\
e_k &= \frac{|\mathbf{l}_k|}{l_j} - 1, \quad \in \mathcal{R} \\
\varepsilon_k &= |\mathbf{l}_k|, \quad \in \mathcal{R}
\end{aligned}
\tag{2.13}
$$

$$
\mathbf{P}_k^j \triangleq \frac{\mathbf{l}_k^j \mathbf{l}_k^{jT}}{\varepsilon_k^{j2}} \tag{2.14}
$$

The constants are defined as (2.15), where C_{MN}^j, C_{DT}^j, C_{DN}^j are the hydrodynamic mass, the tangential drag and the normal drag coefficients for the j^{th} cable, respectively. l_j is the length of each element in the j^{th} cable.

$$
C_1^j = C_{MN}^j \frac{\pi d_j^2}{4}\rho_w, \quad C_2^j = \frac{1}{2}C_{DT}^j d_j \rho_w, \quad C_3^j = \frac{1}{2}C_{DN}^j d_j \rho_w \tag{2.15}
$$

The position and velocity of the last nodal points are given as follow,

$$
\mathbf{r}_n^j = \eta_1 + \mathbf{J}_1(\eta_2)\mathbf{p}^j, \quad j = 1, 2, ..., m \tag{2.16}
$$

$$
\mathbf{v}_n^j = \mathbf{J}_1(\eta_2)\nu_1 + \frac{d}{dt}(\mathbf{J}_1(\eta_2))\mathbf{p}^j, \quad j = 1, 2, ..., m \tag{2.17}
$$

According to Aamo and Fossen (2001), when coupling the mooring cables to the vessel, it is safe to ignore the inertia, drag, hydrostatic and gravity effects of the last nodal

point. This means that $\mathbf{M}_n^j$, $\mathbf{D}_n^j$ and $\mathbf{g}_n^j$ in (2.10) can be neglected since the effect of these terms will be small compared to the mass, damping and restoring forces of the vessel. The damping component in (2.8) is then neglected, and the mooring forces acting on the vessel from all mooring lines will then be given by (2.18).

$$\boldsymbol{\tau}_{moor} \triangleq \begin{bmatrix} -\tau_{moor}^1 \\ -\tau_{moor}^2 \end{bmatrix} = \begin{bmatrix} -\mathbf{J}_1(\eta_2)^T \sum_{j=1}^{m} \mathbf{k}_n^j \\ -\sum_{j=1}^{m} (\mathbf{J}_1(\eta_2)^T \mathbf{k}_n^j) \times \mathbf{p}^j \end{bmatrix} \tag{2.18}$$

2.3 TAPM control design model

A control design model is a simplified model of a real and complex system, and this should only include the main physical characteristics of the dynamic system. The control design model of a system should behave similarly to the real system.

2.3.1 LF model

According to Sørensen (2013), when deriving a control design model of a surface vessel, it can be assumed that only the motions in the horizontal plan, which are surge, sway and yaw, are of interest. This assumption introduce the 3 DOF kinematic equation (2.19), where $\mathbf{R}(\psi)$ is expressed by (2.20), $\boldsymbol{\nu} = [u\ v\ r]^T$ and $\boldsymbol{\eta} = [X_E\ Y_E\ \psi]^T$.

$$\dot{\boldsymbol{\eta}} = \mathbf{R}(\psi)\boldsymbol{\nu} \tag{2.19}$$

$$\mathbf{R}(\psi) = \begin{bmatrix} c\psi & -s\psi & 0 \\ s\psi & c\psi & 0 \\ 0 & 0 & 1 \end{bmatrix} \tag{2.20}$$

When assuming that the vessel is used in TAPM, the LF model described by equation (2.5) can be simplified. It can be assumed that the velocities are small. Hence, the Coriolis and centripetal terms can be neglected, and the linear damping can be assumed much larger than the nonlinear damping, which gives a damping matrix equal to the linear damping, $\mathbf{D} = \mathbf{D}_L$.

In addition, a bias term, $\mathbf{b} \in \mathcal{R}^3$, is inserted in the equation. The bias model accounts for external slowly-varying forces and moments due to second-order wave loads, ocean

currents and wind, and also errors in the modeling.

According to Nguyen and Sørensen (2007), the damping part of the mooring is assumed to be neglected. According to Aamo and Fossen (2001), this can be done because the damping of the mooring is small compared to the damping of the vessel. When assuming $\mathbf{p} = [0\ 0\ 0]^T$ and that the mooring model applies in 3 DOF, (2.18) can be rewritten to (2.21). The mooring forces have to be generalized in order to fit the 3 DOF control design model.

$$\boldsymbol{\tau}_{moor} = -\mathbf{R}(\psi)^T \begin{bmatrix} \mathbf{I}_{2x2} & 0 \\ 0 & 0 \end{bmatrix} \sum_{j=1}^{m} \mathbf{k}_n^j = -\mathbf{R}(\psi)^T \bar{\mathbf{g}}_{m0} \tag{2.21}$$

It is further assumed that the anchor line length is fixed and that the influence of the current field along the mooring lines are neglected. According to Fang et al. (2013), the generalized mooring forces at a working point, $\boldsymbol{\eta} = \boldsymbol{\eta}_0$, can be approximated by taking 1st-order Taylor expansion of (2.21), as seen in equation (2.22).

$$\bar{\mathbf{g}}_{m0}(\boldsymbol{\eta}) = \bar{\mathbf{g}}_{m0}(\boldsymbol{\eta}_0) + \mathbf{G}_{m0}(\boldsymbol{\eta} - \boldsymbol{\eta}_0) + O(2) \tag{2.22}$$

Where,

$$\mathbf{G}_{m0} = \left. \frac{\partial \bar{\mathbf{g}}_{m0}}{\partial \boldsymbol{\eta}} \right|_{\boldsymbol{\eta}=\boldsymbol{\eta}_0} \tag{2.23}$$

When $\boldsymbol{\eta}_0 = 0$, the following expression of the mooring force is found.

$$\boldsymbol{\tau}_{moor} = -\mathbf{R}^T(\psi)\mathbf{G}_{m0}\boldsymbol{\eta} \tag{2.24}$$

Since FEM is a numerical method, it can be difficult to find a good estimate of (2.23), therefore a second method has to be used instead. According to Gjessing (2015), an estimate of a linearized $\mathbf{G}_{m0}$ can be found by simulating the mooring model with an input of different positions. The restoring force at each position should be measured after a given time, in order for the system to get settled at the given position. The position vector should be chosen based on how far the ship can move, which depends on the length of the mooring lines and its elasticity. After the restoring force is measured for each position, the values have to be plotted against each other. Linear regression should be applied to find an approximation of G_{m0}. The slope of this graph will be the linearized restoring force in both surge and sway.

When all the simplifications are accounted for, the new LF model is, according to Sørensen

(2013), given by equation (2.25).

$$\mathbf{M}\dot{\boldsymbol{\nu}} + \mathbf{D}\boldsymbol{\nu} + \mathbf{R}^T(\psi)\bar{\mathbf{g}}_{m0}(0) + \mathbf{R}^T(\psi)\mathbf{G}_{m0}\boldsymbol{\eta} = \boldsymbol{\tau}_c + \mathbf{R}^T(\psi)\mathbf{b} \tag{2.25}$$

Where $\mathbf{M} \in \mathcal{R}^{3x3}$ is the mass matrix including added mass and $\boldsymbol{\tau}_c \in \mathcal{R}^3$ is the control input vector.

2.3.2 Bias model

According to Sørensen (2013), the first order *Markov* model is the most frequently used to model the bias, see equation (2.26). Where $\mathbf{w}_b \in \mathcal{R}^3$ is the zero-mean Gaussian white noise vector, $\mathbf{T}_b \in \mathcal{R}^{3x3}$ is a diagonal matrix of the bias time constant, and $\mathbf{E}_b \in \mathcal{R}^{3x3}$ is a diagonal matrix scaling the amplitude of $\mathbf{w}_b$.

$$\dot{\mathbf{b}} = -\mathbf{T}_b^{-1}\mathbf{b} + \mathbf{E}_b\mathbf{w}_b \tag{2.26}$$

2.3.3 WF model

The WF model is obtained, according to Sørensen (2013), by assuming (2.6) to be a second-order linear model driven by a zero-mean Gaussian white noise vector, $\mathbf{w}_w \in \mathcal{R}^3$, as seen below.

$$\dot{\boldsymbol{\xi}}_w = \mathbf{A}_w\boldsymbol{\xi}_w + \mathbf{E}_w\mathbf{w}_w \tag{2.27}$$

Where $\boldsymbol{\xi}_w$ is the state of the WF model, $\mathbf{E}_w \in \mathcal{R}^{6x3}$ is the disturbance matrix and $\mathbf{A}_w \in \mathcal{R}^{6x6}$ is the system matrix according to (2.28). Here $\boldsymbol{\Omega} \in \mathcal{R}^{3x3}$ is a diagonal matrix containing the dominating frequencies of the vessel subjected to first-order wave loads and $\boldsymbol{\Lambda} \in \mathcal{R}^{3x3}$ is a diagonal matrix of the damping ratios. The dominating period is often in a interval of 5-20 seconds and the damping ratio is often in an interval of 0.1-0.5.

$$\mathbf{A}_w = \begin{bmatrix} \mathbf{0}_{3x3} & \mathbf{I}_{3x3} \\ -\boldsymbol{\Omega}^2 & -2\boldsymbol{\Lambda}\boldsymbol{\Omega} \end{bmatrix} \tag{2.28}$$

2.3.4 Measurement

The measurement equation is given by equation (2.29), where $\mathbf{v} \in \mathcal{R}^3$ is a zero-mean Gaussian measurement noise vector and $\mathbf{C}_w = [\mathbf{0}_{3x3}\ \mathbf{I}_{3x3}]$ is a measurement matrix (Sørensen;

2013).

$$\mathbf{y} = \boldsymbol{\eta} + \mathbf{C}_w \boldsymbol{\xi}_w + \mathbf{v} \tag{2.29}$$

Chapter 3

Simulation model of CSAD

3.1 6 DOF simulation model of the CSAD

For the vessel model, a 6 DOF Simulink model of CSAD made by Bjørnø (2016) is used. This vessel model included a mooring model based on the Catenary equation, which herein has been replaced by a Simulink model based on FEM, taken from Ren (2015). Some modifications are made to the mooring model to be able to fit the vessel model. The model can use up to 8 mooring lines. The mathematics behind the full 6 DOF model of CSAD is conducted according to Chapter 2.

According to Aamo and Fossen (2001), a simplification can be made to the system by assuming that all the mooring lines are connected to the centre of the turret, which is the centre of the body-fixed reference frame. Assuming this, the last nodal point, $\mathbf{r}_n$, of all mooring lines are connected to the same fixed point on the vessel, $\mathbf{p} = [0\ 0\ 0]^T$. According to (2.16), this assumption indicates that $\mathbf{r}_n$ is equal to the position of the vessel, $\boldsymbol{\eta}_1$.

Table 3.1: Characteristics of the mooring lines

Description	**Data**
Length	2250 [m]
Diameter	0.08 [m]
Elastic modulus	45.757 [GPa]

The parameters used for the mooring model are taken from an example in Aamo and Fossen (2001), see Table 3.1. The parameters are in full scale and because of that it is necessary to scale it down according to the CSAD model scale of 1:90. The scaling is

done using Froude scaling, which is further explained in the following subsection.

In a control system, the control forces provided by the motion controller and the control forces provided by the thrusters are not necessarily the same. Therefore, a thrust allocation algorithm is needed in order to distribute the generalized forces from the motion controller to each of the thrusters on the vessel and thereby finding the commanded thrust and angles, which are needed to calculate the the control force provided by the thrusters in each DOFs. The thrust allocation system used in this thesis is made by Frederich (2016).

3.1.1 Froude scaling

In order to perform experiments with model ships, the real physical conditions have to be mapped to a model scale. To do this, the Froude similitude law can be applied to give realistic values between a full scale ship and a model scale ship. According to this law it is considered that the gravity is the dominating force acting on the hull. A geometrical similarity requirement, $\lambda = \frac{L_F}{L_M}$, is needed in order to calculate the physical parameters in Table 3.2. The subscript F stands for a full scale ship and the subscript M stands for model ship. For further explanation of Froude Scaling, see Steen (2011).

Table 3.2: Froude scaling.

Physical Parameter	**Relationship between Full-scale and Model-scale**
Length [m]	$L_F = \lambda L_M$
Mass [kg]	$m_F = \frac{\rho_F}{\rho_M}\lambda^3 m_M$
Force [N]	$F_F = \frac{\rho_F}{\rho_M}\lambda^3 F_M$
Moment [Nm]	$M_F = \frac{\rho_F}{\rho_M}\lambda^4 M_M$
Pressure [Pa]	$p_F = \frac{\rho_F}{\rho_M}\lambda p_M$
Acceleration $[m/s^2]$	$a_F = a_M$
Time [s]	$t_F = \sqrt{\lambda} t_M$

3.2 Weather parameters

According to Price and Bishop (1974), waves can be divided into different sea states depending on frequencies and wave heights. Based on this, they have classified ten different sea states in the northern North Atlantic, from calm to phenomenal. For this thesis, the focus is on normal weather conditions, and the specifications from the moderate sea state

are therefore used. The moderate sea state in the northern North Atlantic can, according to Price and Bishop (1974), be classified by Table 3.3. The parameters are in full scale, and in order to be used with the model ship the waves need to be scaled to the model scale of 1:90 according to the Froude scaling in Table 3.2.

Table 3.3: Moderate sea state.

Parameter	**Value**
Significant wave height (H_s)	$1.25 - 2.5$ [m]
Peak wave frequency (ω_p)	$0.79 - 0.68$ [rad/s]

The web-site, OSCAR (2014), shows the velocity of the surface current in the ocean around the world. A value for the surface current (ν_c) equal 0.2 $[m/s]$ is used, which is taken from the ocean around Norway. ν_c is also scaled according to Table 3.2.

3.3 System verification

The simulations are done with only four mooring lines. The initial positions of the mooring lines in model scale are shown in Figure 3.1. The weather parameters used can be seen in Table 3.4.

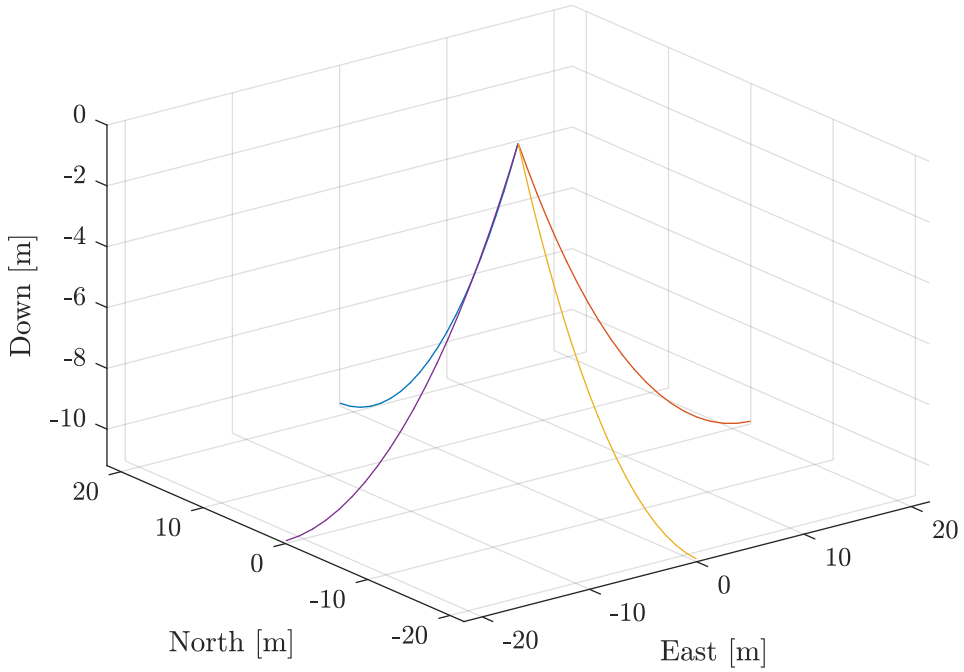

Figure 3.1: Initial simulation position of the mooring lines.

Table 3.4: Weather parameters used in the simulations

Parameter	**Full scale**	**Model scale**
Significant wave height (H_s)	2 [m]	0.0222 [m]
Peak wave frequency (ω_p)	0.724 [rad/s]	6.869 [rad/s]
Current velocity (ν_c)	0.2 [m/s]	0.0211 [m/s]

To verify the simulation model, the open loop system is tested with no thrust. Since the moored vessel is exposed to waves and current, it will move depending on mean wave direction (β_w) and the current direction (β_c). The start position of the vessel is, $\eta = [0\ 0\ 0\ 0\ 0\ 0]$.

For the first test, both the direction of the waves and current are equal 180 degree, $\beta_w = \beta_c = 180$ degree. In this simulation the waves and current are pointing against the vessel, called head sea, and can be seen in Figure 3.2. In Figure 3.2a it can be seen that the vessel is drifting $-0.4\ m$ backwards, before it is stabilizing because the mooring lines are holding it back. As seen in Figure 3.2b, both the east position and the heading are approximately zero.

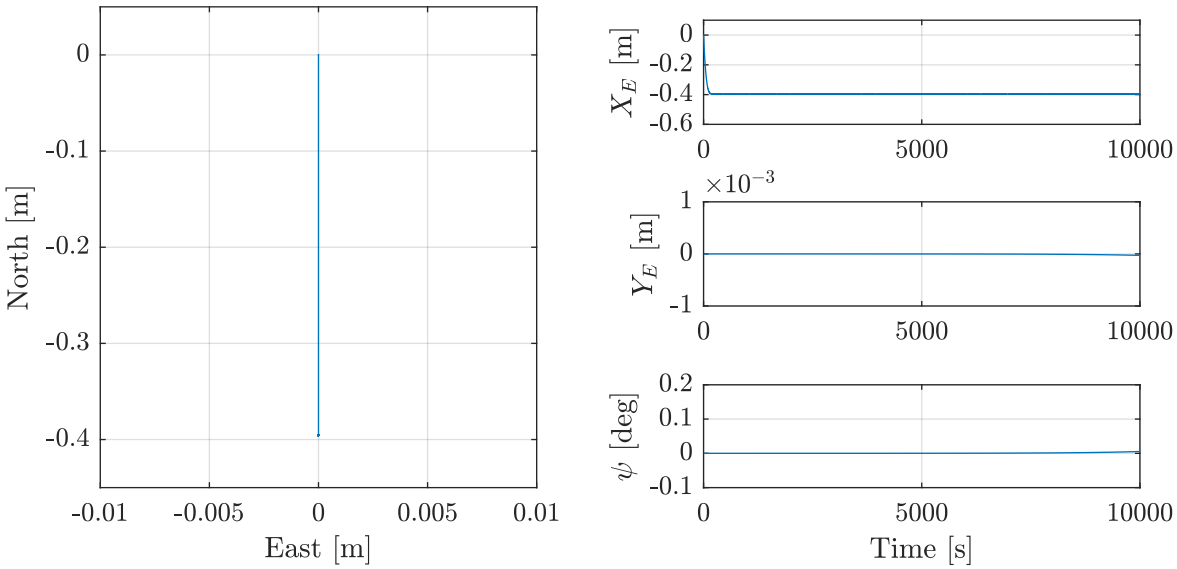

(a) North and east.

(b) Position and heading over time.

Figure 3.2: The vessel position of a open loop system exposed by environmental forces with direction of 180 degree.

In the second test, both the direction of the waves and current are equal 200 degrees, $\beta_w = \beta_c = 200$ degrees. For this simulation the waves and current will point against the

starboard part of the bow of the vessel, called bow sea, and can be seen in Figure 3.3. In Figure 3.3a it can be seen that the vessel is drifting backwards and to the port side, before it is stabilizing. As seen in Figure 3.3b, the north position is stabilizing at approximately $-0.05\ m$, the east position at $-0.7\ m$ and the heading at 20 degrees. From this it can be seen that the vessel has turned so the waves and current are pointing against the bow, as during the first test.

From this, it can be concluded that the simulation model works.

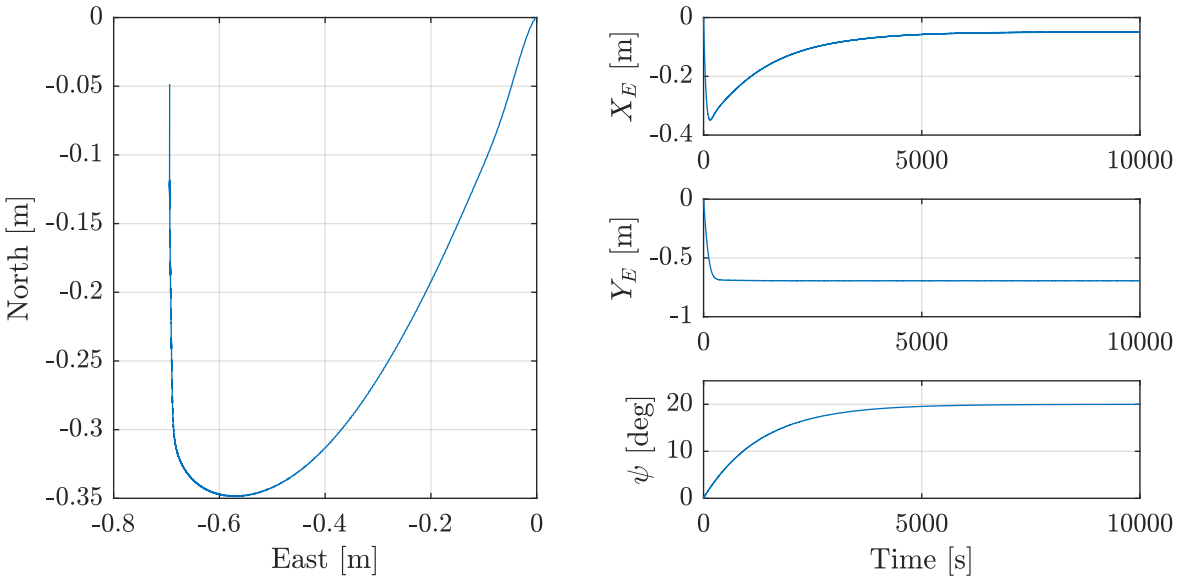

(a) North and east.

(b) Position and heading over time.

Figure 3.3: The vessel position of a open loop system exposed by environmental forces with direction of 200 degree.

Chapter 4

Controller and observer design

4.1 Controller

The objective of a controller is to bring the vessel to its desired position and then keep it there. A widely used controller is the PID-controller, which will be used in this thesis.

According to Nguyen and Sørensen (2009), a nonlinear output PID-controller is expressed mathematically by (4.1), where $\dot{\boldsymbol{\xi}} = \boldsymbol{\eta} - \boldsymbol{\eta}_d$, $\mathbf{K}_{p,i,d}$ are the controller gains, which have to be bigger than zero according to (4.2), and where $\mathbf{H}_{p,i,d}$ are the projection matrices. The projection matrices can be used to enable and disable the proportional, integral and derivative part of the control force in surge, sway and yaw.

$$\boldsymbol{\tau}_{PID} = -\mathbf{H}_i\mathbf{K}_i\mathbf{R}(\psi)^T\boldsymbol{\xi} - \mathbf{H}_p\mathbf{K}_p\mathbf{R}(\psi)^T(\boldsymbol{\eta} - \boldsymbol{\eta}_d) - \mathbf{H}_d\mathbf{K}_d(\boldsymbol{\nu} - \boldsymbol{\nu}_d) \tag{4.1}$$

$$\mathbf{K}_p > 0 \quad , \quad \mathbf{K}_d > 0 \quad , \quad \mathbf{K}_i > 0 \tag{4.2}$$

The most difficult part in controller design, is to decide suitable controller gains, $\mathbf{K}_{p,i,d}$, in order to make the closed loop system stable. The method of pole placement of a mass-damper-spring system can be used by assuming that the DOFs are decoupled. The motions of a vessel contains coupled DOFs, and because of that this method is not exact, but gives good approximations of the controller gains, and can be further tuned if desired.

In the following a suggestion of how to compute the controller gains is given according to Fossen (2011). The derivation is for surge, but should be done in the same way also for sway and yaw.

Assume the simplified system in (4.3), where $G_{m0}x$ describes the mooring force. The

system is applied by the simplified control law, (4.4).

$$M\ddot{x} + D\dot{x} + G_{mo}x = \tau_c \tag{4.3}$$

$$\tau_c = -K_p x - K_d \dot{x} \tag{4.4}$$

By substituting (4.4) into (4.3), the simplified system can be expressed by the closed-loop system, (4.5). An equivalent system to (4.5) can be expressed by (4.6).

$$\ddot{x} + \frac{D + K_d}{M}\dot{x} + \frac{G_{mo} + K_p}{M}x = 0 \tag{4.5}$$

$$\ddot{x} + 2\zeta\omega_n\dot{x} + \omega_n^2 x = 0 \tag{4.6}$$

From the two equivalent systems, two relations can be found in order to calculate K_p and K_d, (4.7) and (4.8) respectively. In order to use the calculation the relative damping ratio, ζ, and the naturally frequency, ω_n, have to be specified. ζ should be defined in the interval between zero and one, $0 < \zeta < 1$, and ω_n should be defined knowing that the natural period T_n of the controller should be lower than the natural period of the system.

$$K_p = \omega_n^2 M - G_{mo} \tag{4.7}$$

$$K_d = 2\zeta\omega_n M - D \tag{4.8}$$

By making the system more complex through adding disturbance like environmental loads, an integral action should be added to the controller to compensate for such disturbance. By applying the knowledge of the two relations in (4.9), the integral gain can be found according to (4.10).

$$\frac{1}{T_i} \approx \frac{\omega_n}{10} \quad , \quad T_i = \frac{K_p}{K_i} \tag{4.9}$$

$$K_i = \frac{K_p}{T_i} \tag{4.10}$$

In order to find the controller gains based on the equations above, the linearized restoring force matrix, $\mathbf{G}_{mo}$, is needed. $\mathbf{G}_{mo}$ is found according to the second method proposed in Chapter 2.3.1. The restoring force in surge given by the mooring system is measured at given displacements in X_E. The values are plotted against each other, and linear regression is applied, see the result in Figure 4.1. The slope of this graph is the linearized restoring force in both surge and sway and is found in the matrix (4.11).

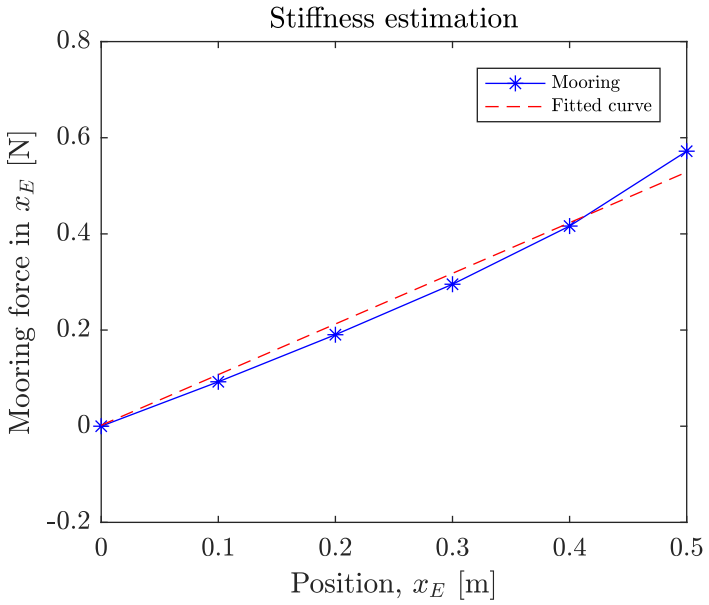

Figure 4.1: Stiffness estimation.

$$\mathbf{G}_{m0} = \begin{bmatrix} G_x & 0 & 0 \\ 0 & G_y & 0 \\ 0 & 0 & G_\psi \end{bmatrix} = \begin{bmatrix} 1.053 & 0 & 0 \\ 0 & 1.053 & 0 \\ 0 & 0 & 0 \end{bmatrix} \tag{4.11}$$

A PID-controller is a feedback controller, and when including this in the open loop system in Chapter 3, the system becomes a closed loop. From now on when referring to a closed loop system this means a system including the feedback controller.

4.2 Observer

A measured signal in a control system often consists of noise, which will have a negative impact on the performance of the controller. Because of that an observer is needed in order to provide estimates of the states. The main purposes of an observer for a positioning system are reconstruction of non-measured data, dead reckoning and wave filtering (Sørensen; 2013). According to Fossen (2011), there exists different types of observers, of which the Luenberger observer, the Kalman filter and the nonlinear passive observer are the most common.

In this master thesis, the design of an observer is not a part of the assignment. However, since the measurements from the practical experiments in the MC Lab will contain noise it is decided to use the nonlinear passive observer design by Bjørnø (2016). In the simulation

model this type of noise is eliminated by turning of the 1^{st} order wave loads, and therefore an observer is not needed in the simulations.

The nonlinear passive observer used during in the MC Lab experiments, is based on Fossen and Strand (1999). The main motivation for this observer was to reduce the tuning parameters found in the Kalman filter design.

The nonlinear passive observer model can be seen in equations (4.12) - (4.16), and is found by copying the dynamics of the control design model from Chapter 2.3.

$$\dot{\hat{\boldsymbol{\xi}}} = \mathbf{A}_w \hat{\boldsymbol{\xi}} + \mathbf{K}_1(\boldsymbol{\omega}_0)\tilde{\mathbf{y}} \tag{4.12}$$

$$\dot{\hat{\boldsymbol{\eta}}} = \mathbf{R}(\psi)\hat{\boldsymbol{\nu}} + \mathbf{K}_2\tilde{\mathbf{y}} \tag{4.13}$$

$$\dot{\hat{\mathbf{b}}} = -\mathbf{T}_b\hat{\mathbf{b}} + \mathbf{K}_3\tilde{\mathbf{y}} \tag{4.14}$$

$$\mathbf{M}\dot{\hat{\boldsymbol{\nu}}} = -\mathbf{D}\hat{\boldsymbol{\nu}} + \mathbf{R}^T(\psi)\hat{\mathbf{b}} - \mathbf{R}^T(\psi)\mathbf{G}_{m0}\hat{\boldsymbol{\eta}} + \boldsymbol{\tau}_c + \mathbf{R}^T(\psi)\mathbf{K}_4\tilde{\mathbf{y}} \tag{4.15}$$

$$\mathbf{y} = \hat{\boldsymbol{\eta}} + \mathbf{C}_w\hat{\boldsymbol{\xi}} \tag{4.16}$$

In this model, $\tilde{\mathbf{y}} = \mathbf{y} - \hat{\mathbf{y}}$ is the estimation error, and $\mathbf{K}_1(\boldsymbol{\omega}_0) \in \mathcal{R}^{6x3}$ and $\mathbf{K}_{2,3,4} \in \mathcal{R}^{3x3}$ are the observer gain matrices. $\mathbf{K}_1(\boldsymbol{\omega}_0)$ is a function of the wave spectra peak frequencies in surge, sway and yaw. The observer is further explained in Fossen and Strand (1999) and Fossen (2011).

Chapter 5

Guidance system design

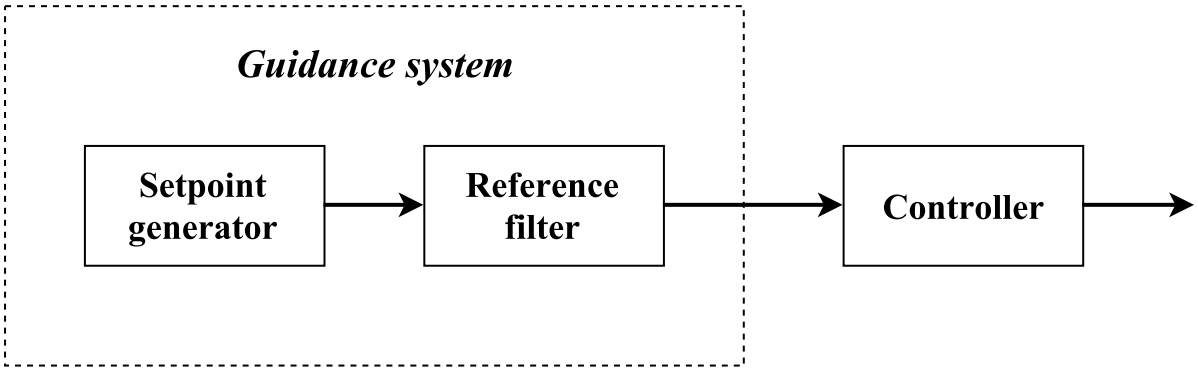

Figure 5.1: Guidance system.

All control systems include a guidance system. A guidance system is used to calculate or decide the desired position and heading given to a controller. The guidance system consists of a setpoint generator and a reference filter, see Figure 5.1. The setpoints are defined by a setpoint generator, and filtered in the reference filter making a smooth transfer between the current position and heading of the vessel to the setpoint.

In this thesis the following two types of guidance systems will be used, a user specified guidance system for manual setting of the setpoint values for North, East and heading, and an autonomous guidance systems for online setting of the values using several different designs for the setpoint generator. The different methods will also be combined, meaning for instance that a user specified guidance system for heading can be used together with an autonomous guidance system for surge and sway.

A known autonomous guidance system design called setpoint chasing will be used in order to generate the optimal desired earth-fixed position for surge and sway. In addition,

two new designs for autonomous guidance systems for heading will be derived based on the ES theory, which in turn is based on either sinusoidal perturbation or numerical optimization. These methods are known from other industries, but have until now not been used in TAPM applications. It is desirable to check if ES can be an efficient way to find the optimal heading during an operation both in terms of economy and emission. The different methods will be further explained and verified during simulations later in this chapter.

5.1 Reference filter

A controller will not handle well rapid changes in the position and heading. For this reason a reference filter is needed in order to provide a more optimal performance. According to Nguyen and Sørensen (2009), a reference filter is necessary in a control system to provide a smooth change between the vessel's position and a new desired position and heading given by the setpoint generator. This is especially important in autonomous guidance systems because the setpoints will change often.

Different reference filters do exist. According to Nguyen and Sørensen (2009), a suitable reference model can be described mathematically by (5.1) - (5.3).

$$\dot{\boldsymbol{\eta}}_d = \mathbf{v}_d^e \tag{5.1}$$

$$\dot{\mathbf{v}}_d^e = -\boldsymbol{\Gamma}\boldsymbol{\eta}_d - \boldsymbol{\Omega}\boldsymbol{\nu}_d^e + \boldsymbol{\Gamma}\mathbf{x}_{ref} \tag{5.2}$$

$$\dot{\mathbf{x}}_{ref} = -\mathbf{A}_f\mathbf{x}_{ref} + \mathbf{A}_f\boldsymbol{\eta}_r \tag{5.3}$$

Where $\mathbf{v}_d^e \in \mathcal{R}^3$ and $\boldsymbol{\eta}_d \in \mathcal{R}^3$ define the desired velocity and position trajectories in earth-fixed reference frame, respectively. $\mathbf{A}_f$ represent the first-order diagonal and nonnegative setpoint filter gain matrix and is given by (5.4), and $\boldsymbol{\eta}_r \in \mathcal{R}^3$ defines the setpoints in earth-fixed coordinates defined by the setpoint generator. The vector $\mathbf{x}_{ref} \in \mathcal{R}^3$ are the filtered reference coordinates to be used in the controller.

The reference filter consists of the following design parameters (5.5), a nonnegative damping matrix $\boldsymbol{\Omega} \in \mathcal{R}^{3x3}$, and a diagonal stiffness matrix $\boldsymbol{\Gamma} \in \mathcal{R}^{3x3}$. See Sørensen (2013) for further explanation of the reference model.

$$\mathbf{A}_f = \begin{bmatrix} \frac{1}{t_1} & 0 & 0 \\ 0 & \frac{1}{t_2} & 0 \\ 0 & 0 & \frac{1}{t_3} \end{bmatrix} \tag{5.4}$$

$$\mathbf{\Omega} = \begin{bmatrix} 2\zeta_1\omega_1 & 0 & 0 \\ 0 & 2\zeta_2\omega_2 & 0 \\ 0 & 0 & 2\zeta_3\omega_3 \end{bmatrix} \quad , \quad \mathbf{\Gamma} = \begin{bmatrix} \omega_1^2 & 0 & 0 \\ 0 & \omega_2^2 & 0 \\ 0 & 0 & \omega_3^2 \end{bmatrix} \tag{5.5}$$

5.2 User specified guidance system

The most commonly used guidance system is the one where the user specifies the values. With reference to Figure 5.1, this means that the setpoint generator is represented by a human. The user can either define one desired setpoint for the position and the heading, or a trajectory of different setpoints for the vessel to follow. The main disadvantage of this user-specified guidance system is that it is difficult to make the system perform optimal, since the user might not choose the optimal values where the vessel minimized its thrust utilization.

5.2.1 Verification

In this section, a verification of the closed loop system including the user specified guidance system is shown. The vessel has the following start position, $\eta = [0\ 0\ 0]^T$, and is exposed by waves and current with a direction of 200 degrees, $\beta_w = \beta_c = 200$ degrees. The desired position and desired heading is given as, $\boldsymbol{\eta}_d = [X_{Ed} \quad Y_{Ed} \quad \psi_d]^T = [-0.1 \quad 0.1 \quad -(20 * \pi/180)]^T$.

As seen in Figure 5.2a, the position and heading of the vessel converge to the desired values after approximately 300 s. As can be seen in Figure 5.2b this is not the optimal values since the vessel still needs some amount of thrust to maintain its position and heading. By this it can be concluded that the user specified guidance system works, but is not optimal for these user given values. This also illustrates the challenge with this method.

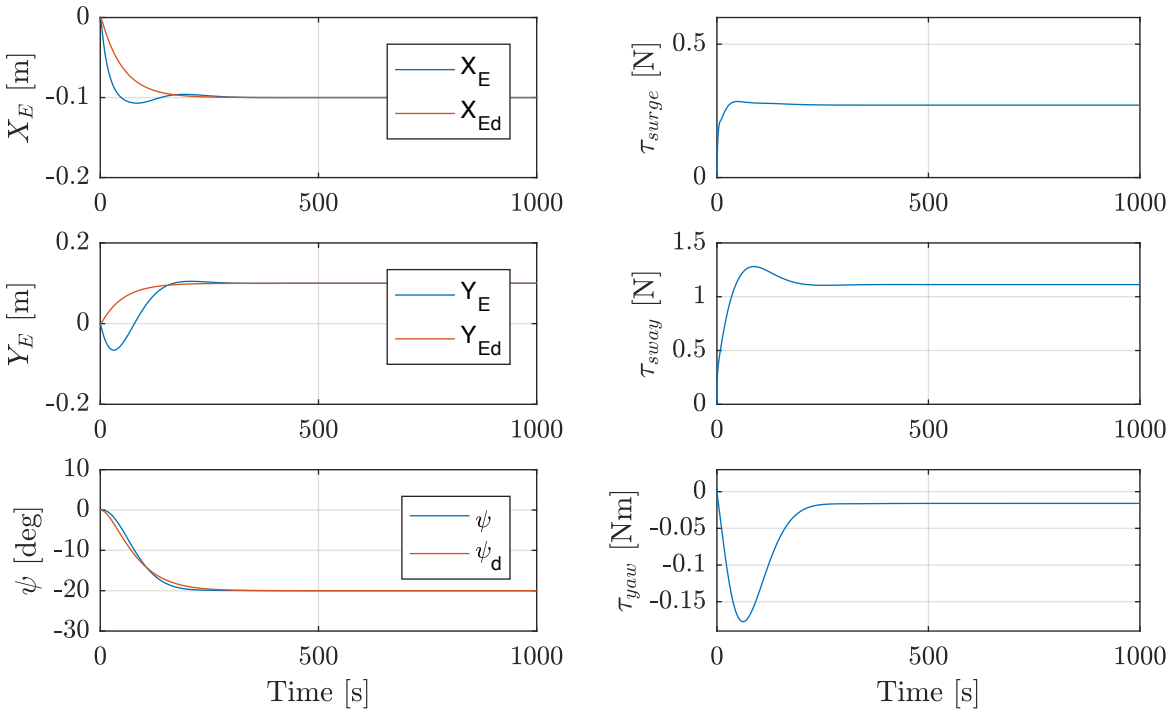

(a) Position. (b) Thrust used.

Figure 5.2: Verification of the user specified guidance system.

5.3 Setpoint chasing

The principle of setpoint chasing is used to make an autonomous guidance system in surge and sway. It is decided to use the setpoint chasing method of lowpass filtering as the setpoint generator for the case of moderate environmental conditions.

According to Sørensen (2013), in a lowpass filter, only the part of the signal with low frequencies will be recognized, while the part with high frequencies will be rejected. A lowpass filter uses a defined cutoff frequency to define which part of the signal to carry on. In this manner unwanted noise in a measurement can be removed.

The purpose of this setpoint generator will be to calculate online, the optimal values of the North and East coordinates. According to Nguyen and Sørensen (2009), the optimal values, the desired setpoint for surge and sway are defined as, $\boldsymbol{\eta}_r = [x_r \ , \ y_r]^T$, and is the position where the mean environmental loads acting on the vessel are balanced by the mooring forces. To achieve this, it is assumed that $\boldsymbol{\eta}_r$ is the lowpass signal of the LF position of surge and sway, $\boldsymbol{\eta}_{xy} = [x_{LF} \ , \ y_{LF}]^T$, and can be found by (5.6). Where $\boldsymbol{\Lambda} \in \mathcal{R}^{2x2}$ is the first-order diagonal and nonnegative filter gain matrix, given by (5.7), where $\frac{1}{T_{si}}\ Hz$ is the cutoff frequencies. A block diagram of this setpoint generator can be seen in Figure 5.3.

$$\dot{\boldsymbol{\eta}}_r = -\boldsymbol{\Lambda}\boldsymbol{\eta} r + \boldsymbol{\Lambda}\boldsymbol{\eta}_{xy} \tag{5.6}$$

$$\boldsymbol{\Lambda} = \begin{bmatrix} \frac{1}{T_{s1}} & 0 \\ 0 & \frac{1}{T_{s2}} \end{bmatrix} \tag{5.7}$$

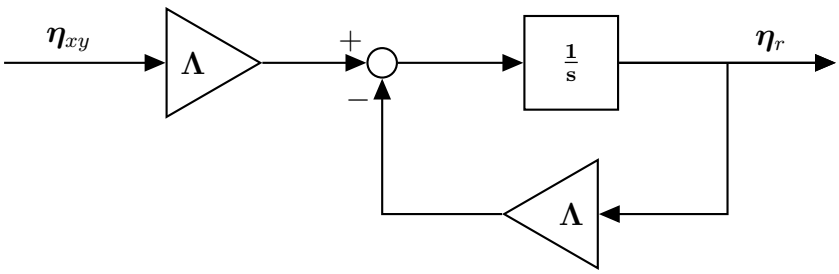

Figure 5.3: A block diagram of the setpoint generator.

The setpoint given by a guidance system using the setpoint chasing algorithm, when the vessel is exposed to moderate environmental loads, is controlled with use of a proportional and damping controller. This means that the integral part in the PID-controller designed

in (4.1) will be disabled in surge and sway, and can be corrected directly through the projection matrix $\mathbf{H}_i$. In order to control the heading at the same time, all the parts in the controller is needed for yaw. In this way, the mooring system will compensate the mean environmental loads in surge and sway, and the thruster assistance will counteract the remaining dynamic environmental loads, which makes the system more optimal over time.

According to Nguyen and Sørensen (2009), the restoring part of the controller provides additional stiffness to the system besides the mooring stiffness. This can change the natural frequency of the TAPM-vessel to a frequency away from the bandwidth of the LF wave loads and then prevent resonance.

5.3.1 Verification

This section verifies that the autonomous guidance system, using setpoint chasing, works optimally for surge and sway. This is tested in the closed loop system where the desired heading is still set manually by the user, $\psi_d = 20$ degrees. The vessel has the following start position, $\eta = [0\ 0\ 0]^T$, and is exposed by waves and current with a direction of 200 degrees, $\beta_w = \beta_c = 200$ degrees.

As seen in Figure 5.4a, surge and sway follow the desired position well and converges to the optimal position after approximately 300 s. At the optimal position the thruster force in surge and sway is zero as seen in Figure 5.4b. By this it can be concluded that the setpoint chasing algorithm works well.

However, in a full autonomous guidance system where also the heading is set automatically, the optimal position will vary depending on the setting for the heading.

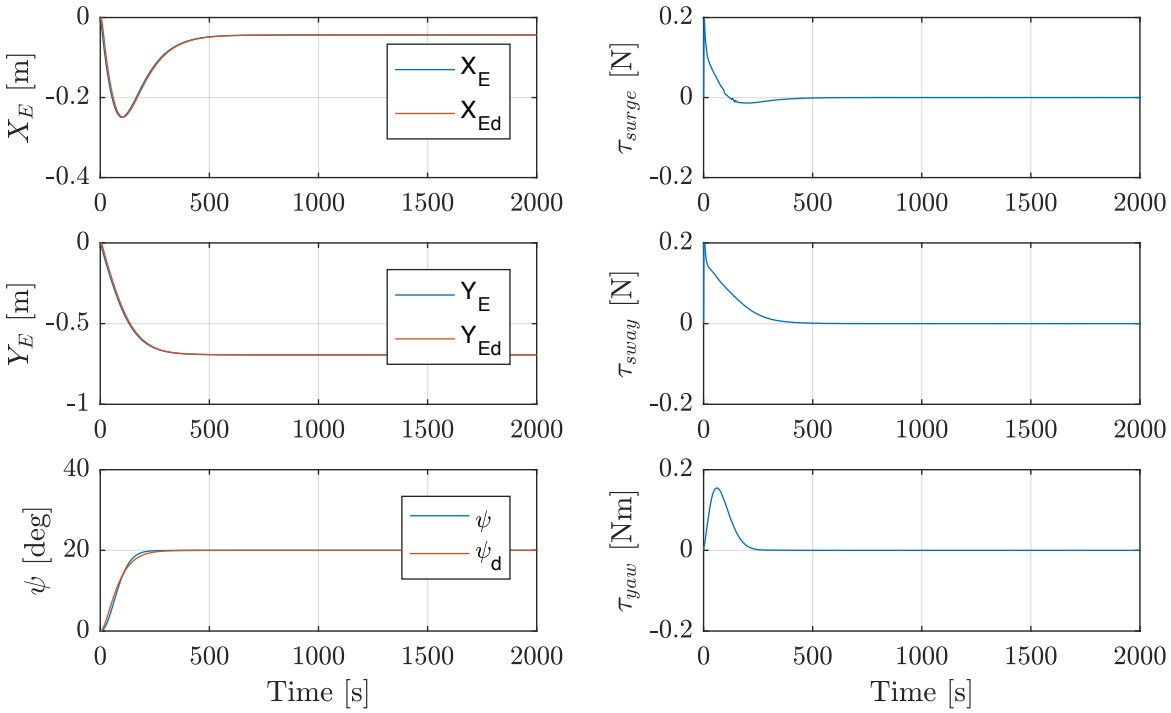

(a) Position. (b) Thrust used.

Figure 5.4: Verification of the guidance system with setpoint chasing.

5.4 Sinusoidal perturbation based extremum seeking

In the following, a real-time autonomous guidance system for heading is constructed based on the ES methodology presented in Ariyur and Krstić (2003). This methodology uses an ES scheme called sinusoidal perturbation based ES, and can be seen in Figure 5.5. The scheme consists of a plant and a dynamic feedback loop. The plant includes a system with an inner feedback controller and a performance function, where the output of the plant is a measurement of the performance function, y. The dynamic feedback loop, which represents everything inside the dotted block in the figure, is called an ES loop or an ES controller. The purpose of the ES controller will be to seek an extremum of the measurement y without any further knowledge of the plant. The extremum can be either a maximum or a minimum.

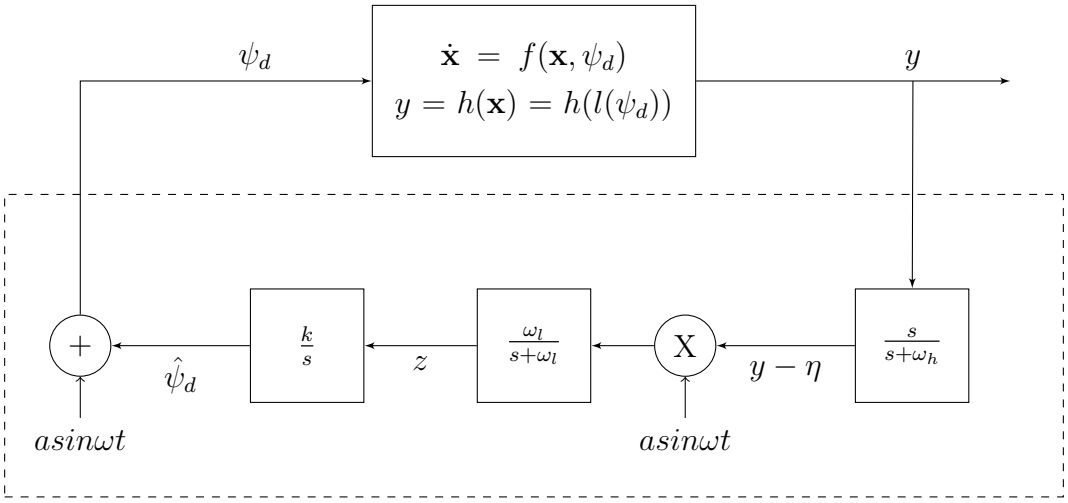

Figure 5.5: Sinusoidal perturbation based ES scheme.

In this autonomous guidance system for heading, the ES controller will be used to online estimate a value of ψ_d during a seek for the optimal heading (ψ^*). Here, ψ^* is decided to be the value where y is maximized.

What characterizes this ES scheme from other schemes is, according to Ariyur and Krstić (2003), that this ES controller uses probing signals $asin(\omega t)$ to include slow perturbations to the estimates of ψ_d in order to converge to ψ^*.

According to Ariyur and Krstić (2003), in a general problem, a nonlinearity with an extremum will arise as a reference-to-output equilibrium map of a general nonlinear system. Where the system is assumed to be stable at each of these equilibria by the inner feedback controller.

In order to describe this ES scheme, it is decided to look into a simplified 1 DOF system of the yaw motion of the vessel.

5.4.1 Simplified 1 DOF system of yaw

A simplified model of the vessels yaw motion is represented by (5.8). Where $u = -K_p(\psi - \psi_d) - K_i\xi - K_d r$, is the feedback controller with the intention of controlling the system to the ψ_d.

$$\begin{aligned} \dot{\xi} &= \psi - \psi_d \\ \dot{\psi} &= r \\ I\dot{r} &= -dr + u + W(\alpha) \end{aligned} \tag{5.8}$$

$W(\alpha)$ represents the environmental moment acting on the simplified yaw model, and is decided to be defined as the nonlinear function (5.9), where α is the angle of attack. It is decided that $W(\alpha)$ only is valid in the interval, $-\frac{\pi}{2} \leq \alpha \leq \frac{\pi}{2}$. α can also be expressed as $\alpha = \beta_w - \pi - \psi$, where β_w is the mean direction of the environmental loads.

By assuming that the optimal value of the angle of attack is, $\alpha^* = 0$, and that the direction of the environmental loads are constant, the optimal heading can be found by $\psi^* = \beta_w - \pi$. By rewriting, a new expression of α can be found as, $\alpha = \psi^* + \pi - \pi - \psi = \psi^* - \psi$. In order to obtain, $\alpha^* = 0$, it can be seen that $\psi^* = \psi$ have to be true.

$$W(\alpha) = Msin(\alpha) = Msin(\psi^* - \psi) = W(\psi^* - \psi) \tag{5.9}$$

M represents the maximum moment that can act on the vessel model. The sign of M can be decided depending on which definition of the environmental load that is desirable. A positive M gives a stabilizing moment also known as weather-vaning, while a negative M gives a destabilizing moment.

By inserting the controller into (5.8), a closed loop system can be written as (5.10).

$$\begin{aligned} \dot{\xi} &= \psi - \psi_d \\ \dot{\psi} &= r \\ \dot{r} &= -\frac{K_p}{I}(\psi - \psi_d) - \frac{K_i}{I}\xi - \frac{K_d + d}{I}r + \frac{W(\psi^* - \psi)}{I} \end{aligned} \tag{5.10}$$

To make the simplified model of yaw to a problem suitable for ES, according to the ES scheme described in Figure 5.5, the closed loop system (5.10) can be considered as the inner closed loop system which together with a performance function can be considered as the plant. This will from now on be described as the closed loop nonlinear system (5.11), where $x = [\xi \quad \psi \quad r]$ is the state, ψ_d is the input generated from the ES controller and y is the output of the plant. Both f and h are smooth functions.

$$\begin{aligned} \dot{\mathbf{x}} &= f(\mathbf{x}, \psi_d) \\ y &= h(\mathbf{x}) \end{aligned} \tag{5.11}$$

According to Ariyur and Krstić (2003), assumption 1-3 below can be made for this closed-loop system.

Assumption 1 *There exists a smooth function l:* $\mathcal{R} \to \mathcal{R}^n$ *such that* $f(\boldsymbol{x}, \psi_d) = 0$ *if and only if* $\boldsymbol{x} = l(\psi_d)$.

Assumption 2 *For each* $\psi_d \in \mathcal{R}$*, the equilibrium* $\boldsymbol{x} = l(\psi_d)$ *of the system is locally exponentially stable.*

Assumption 3 *There exists* $\psi^* \in \mathcal{R}$ *such that* $(h \circ l)'(\psi^*) = 0$ *and* $(h \circ l)''(\psi^*) < 0$.

By applying assumption 1 to the system, $f(\mathbf{x}, \psi_d) = 0$ is true only if $\mathbf{x} = l(\psi_d)$. This assumption gives the relations in (5.12).

$$\begin{aligned} x_1 &= \xi = l_1(\psi_d) = \frac{1}{K_i} W(\psi^* - \psi) \\ x_2 &= \psi = l_2(\psi_d) = \psi_d \\ x_3 &= r = l_3(\psi_d) = 0 \end{aligned} \tag{5.12}$$

Knowing the above, and assuming that ψ_d is a constant, the inner system can be rewritten depending on the error according to (5.13). This gives (5.14), and it can be seen that when $\mathbf{e} = 0$ the system is in its equilibrium.

$$\mathbf{e} = \mathbf{x} - l(\psi_d) \tag{5.13}$$

$$\begin{aligned} \dot{e}_1 &= e_2 \\ \dot{e}_2 &= e_3 \\ \dot{e}_3 &= -K_i e_1 - K_p e_2 - (K_d + d) e_3 + W(\psi^* - e_2 - \psi_d) - W(\psi^* - \psi_d) \end{aligned} \tag{5.14}$$

For assumption 2 to be valid, the controller gains, K_p, K_i and K_d, have to be tuned

such that the system is Hurwitz when $W = 0$. If this is true, the system is stable when $\mathbf{x} = l(\psi_d)$, and it can be assumed that the controller will exponentially stabilize any of the equilibria that the ES controller may produce of ψ_d.

Assumption 3 is particularly central to the ES problem. According to Ariyur and Krstić (2003), the objective of the ES controller is to develop a feedback mechanism which maximizes a steady-state value of the plant output, y, without knowledge of ψ^*, or the functions h and l. This means that the ES controller only has available measurement of y. From this assumption, it can be assumed that the output equilibrium map $y = h(l(\psi_d))$ has a maximum when $\psi_d = \psi^*$. This example deals with the seek of a maximum. A problem with the seek of a minimum would be treated in the same way, but will use -y instead of y.

Now, a performance function needs to be designed. In this manner a function can be chosen freely as long as the function is smooth and has its maximum at $\psi_d = \psi^*$.

The inner controller for the yaw model was earlier defined as, $u = g(\mathbf{x}, \psi_d)$, and will in steady-state condition equals, $u_{ss} = g(l(\psi_d), \psi_d) = -W(\psi^* - \psi)$. Given a constant ψ_d, it will be the integral part that describes how much thrust the vessel uses in the steady-state condition.

Based on the restrictions above, and by the knowledge that the thrust is zero when $\psi_d = \psi^*$, a valid performance function can be chosen as (5.15). $c > 0$ is used in order to increase the convergence. At the equilibrium, where $x_1 = \xi_{ss} = l_1(\psi_d)$, the performance function can be given according to (5.16).

$$y = h(x) = -c * (K_i \xi)^2 \tag{5.15}$$

$$y = h(l(\psi_d)) = -c(W(\psi^* - \psi))^2 \tag{5.16}$$

According to Ariyur and Krstić (2003), some design parameters are needed in the ES controller, see Figure 5.5, and are selected as (5.17). Where ω and δ are small positive constants, and ω'_H, ω'_L and K' are O(1) positive constants. Both a, the amplitude of the perturbation signals, and k, the adaption gain, need to be small. In addition, the cutoff frequencies of the filters, ω_h and ω_l, need to be lower than the frequency of the perturbation signals ω.

$$\begin{aligned} \omega_h &= \omega\omega_H = \omega\delta\omega'_H = O(\omega\delta) \\ \omega_l &= \omega\omega_L = \omega\delta\omega'_L = O(\omega\delta) \\ k &= \omega K = \omega\delta K' = O(\omega\delta) \end{aligned} \tag{5.17}$$

According to Ariyur and Krstić (2003), the overall feedback system in Figure 5.5 operates in three different time scales as following.

- *"fastest - the plant with the stabilizing controller,*
- *medium - the periodic perturbation,*
- *slow - the filters in the ES scheme."*

Including the ES controller, the overall system can be summarized as (5.18) and (5.19).

$$\dot{\mathbf{x}} = f(\mathbf{x}, \hat{\psi}_d + asin\omega t) \tag{5.18}$$

$$\begin{aligned} \dot{\hat{\psi}}_d &= kz \\ \dot{z} &= -\omega_l z + \omega_l(y - \eta)asin\omega t \\ \dot{\eta} &= -\omega_h \eta + \omega_h y \end{aligned} \tag{5.19}$$

By introduce some new coordinates and a new time scale $\tau = \omega t$, the system in (5.18) and (5.19), can, according to Ariyur and Krstić (2003), be rewritten to (5.21) and (5.22).

$$\begin{aligned} \tilde{\psi}_d &= \hat{\psi}_d - \psi^* \\ \tilde{\eta} &= \eta - h(l(\psi^*)) \end{aligned} \tag{5.20}$$

$$\omega \frac{d\mathbf{x}}{d\tau} = f(\mathbf{x}, \psi^* + \tilde{\psi}_d + asin\tau) \tag{5.21}$$

$$\frac{d}{d\tau}\begin{bmatrix} \tilde{\psi}_d \\ z \\ \tilde{\eta} \end{bmatrix} = \delta \begin{bmatrix} K'z \\ -\omega'_L z + \omega'_L(h(x) - h \circ l(\psi^*) - \tilde{\eta})asin\tau \\ -\omega'_H \tilde{\eta} + \omega'_H(h(x) - h \circ l(\psi^*)) \end{bmatrix} \tag{5.22}$$

5.4.2 Verification of the guidance system in the simplified system

As described above, the sinusoidal perturbation based ES controller works as an autonomous guidance system and provides the controller with online estimates for the desired heading. The guidance system is verified through a simulation with the simplified 1 DOF system of the yaw motion. In order to perform the simulation, a value of the maximum moment, M, of the environmental load needs to be defined. The wave model in the full 6 DOF system gives a stabilizing moment in yaw, and to make this verification more realistic it is decided to define it in the same manner. The mean environmental loads used in this simulation is defined as $Msin(\psi^* - \psi) = 0.05sin(20 - \psi)$. If the ES

controller works as expected, it will now seek for $\psi^* = 20$ degrees.

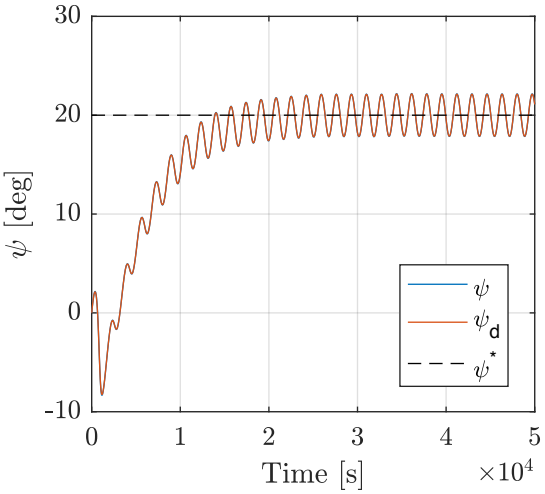

(a) Heading.

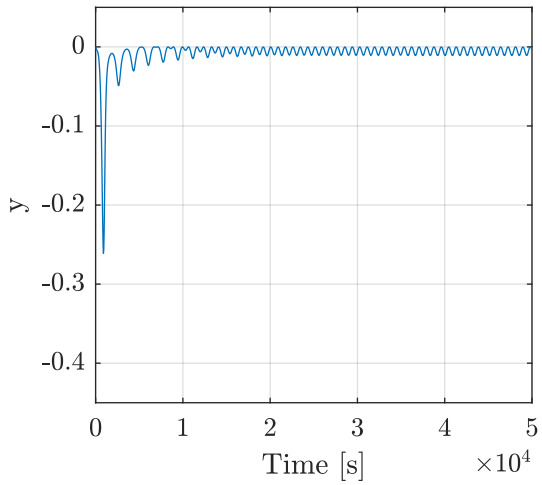

(b) Measurements of the performance function.

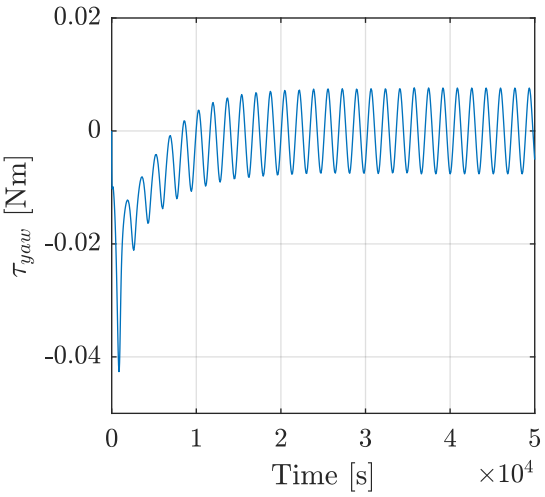

(c) Thrust used.

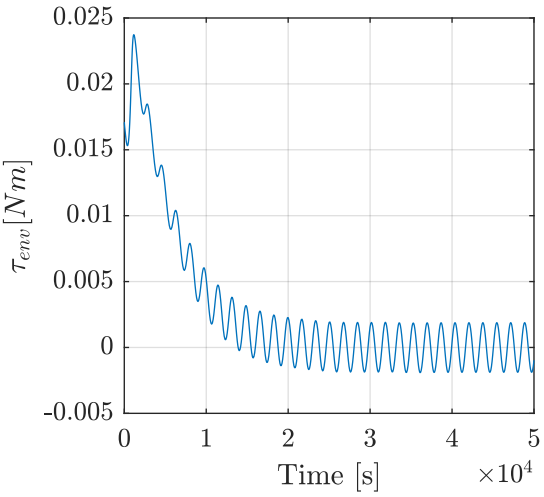

(d) Environmental loads.

Figure 5.6: Verification of a sinusoidal perturbation based ES controller tested on a simplified 1DOF system.

Figure 5.6b shows the measurement of the performance function over time, y. y decreases as the vessel's heading, see Figure 5.6a, approaches $\psi^* = 20$ degrees. As seen in Figure 5.6a, the ES controller finds ψ^* after awhile, but because of the perturbation signal, the ψ_d will oscillate around ψ^* which again will cause oscillations in the vessels heading. At the same time, when the heading is oscillating around ψ^*, the thrust moment from the controller, see Figure 5.6c, will oscillates around zero and the environmental moment, see Figure 5.6d will also oscillates around zero.

By inserting a simplified reference filter in order to filter the estimate of ψ_d generated by the ES controller, the performance is improved as seen in Figure 5.7. This will make the

oscillations in ψ_d smaller which again will give a smaller oscillation in the control moment. In addition, the convergence towards ψ^* is faster. From this it can be concluded that the sinusoidal perturbation based ES controller works as expected in finding ψ^*.

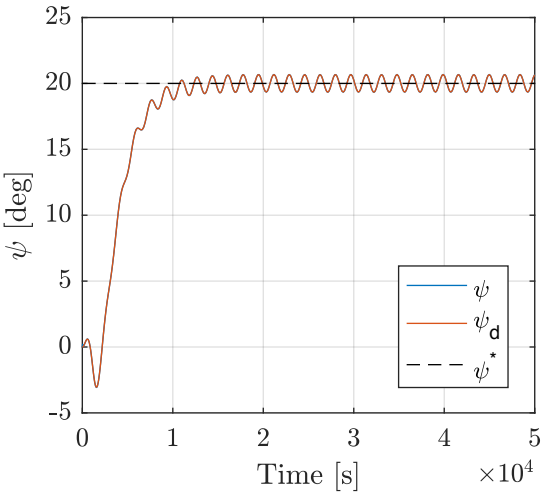

(a) Heading.

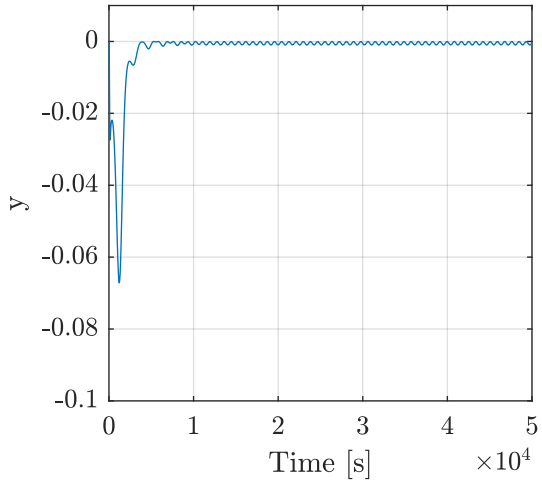

(b) Measurements of the performance function.

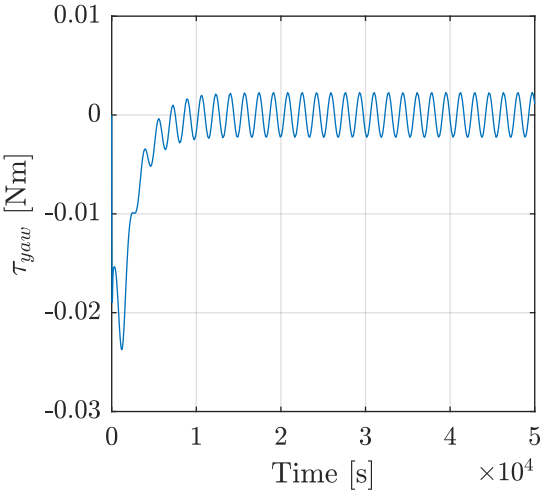

(c) Thrust used.

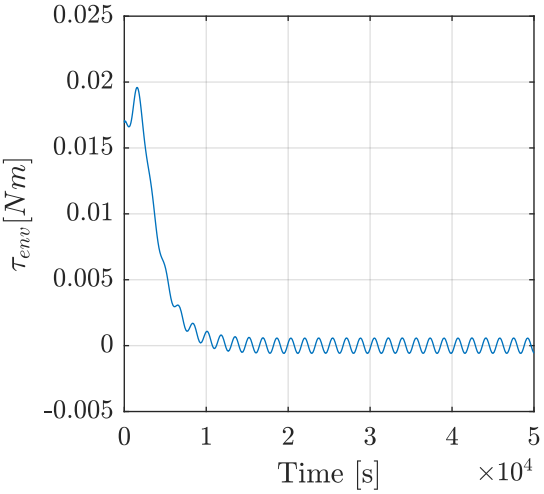

(d) Environmental loads.

Figure 5.7: Verification of a sinusoidal perturbation based ES controller tested on a simplified 1DOF system with a simplified reference filter.

5.5 Numerical optimization based extremum seeking

In the following, the extremum seeking control is considered as a type of constrained optimization problem, where the numerical optimization based ES scheme is derived in order to find the optimal heading of a TAPM vessel exposed to environmental loads.

According to Zhang and Ordóñez (2012), for this scheme, a numerical optimization algorithm is combined with a state regulator. As stated in Chapter 1.2.8, the system plant, in the view of ES, includes both a nonlinear system and a performance function, where the output of the plant is the performance function to be optimized. In the numerical optimization based ES scheme, the performance function is optimized through a numerical optimization algorithm, which is in the discrete-time. The output generated by the numerical optimization algorithm is sent to the state regulator. The purpose of the state regulator is to ensure that the state of the nonlinear system travels along the setpoints generated by the numerical optimization algorithm. Eventually, the output of the state regulator will converge to a minimum or a maximum of the performance function, depending on the definition. This will result in that the output generated by the numerical optimization algorithm has reached its optimal value.

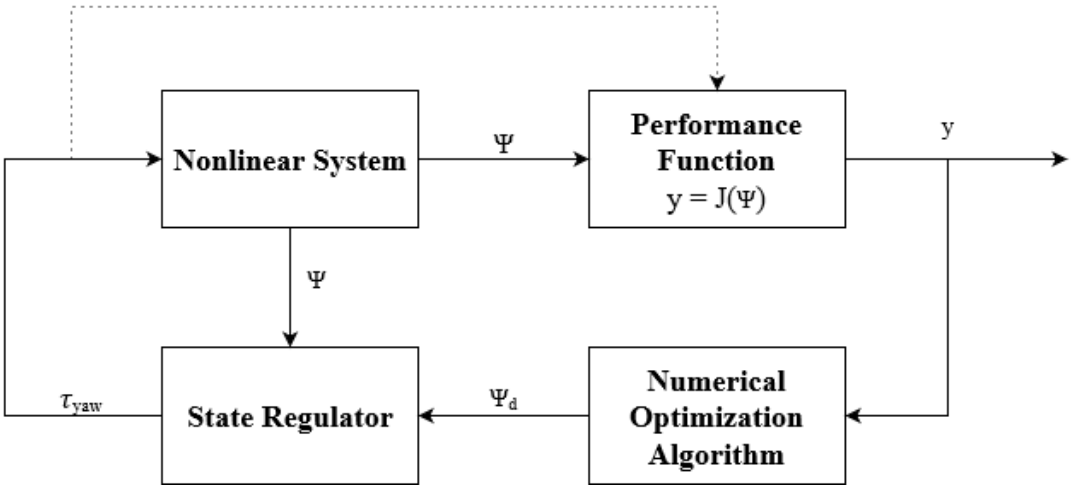

Figure 5.8: Numerical optimization based ES scheme for yaw.

Figure 5.8 shows a numerical optimization based ES scheme for yaw, suitable for the situation searching for an optimal heading. Instead of making a new discrete-time controller, it is decided to use the real-time PID-controller for yaw, given by (4.1), as the state regulator in this scheme. To be able to use this, the discrete-time signal generated by the numerical optimization algorithm is converted to a continuous signal.

It is decided to seek the minimum of the performance function, and the ES control problem

can therefore be stated as (5.23), where $\dot{\psi} = r$, according to (2.20).

$$\min J(\psi) \quad \text{subject to } \dot{\psi} = f(\psi, \tau_{yaw}) \tag{5.23}$$

According to Zhang and Ordóñez (2012), the goal of this ES controller will be to design a controller based on the measurement of the performance function, y, and the measurement of the state, ψ, to regulate ψ to an unknown minimizer, ψ^*, of an unknown performance function. This method is not limited to any particular optimization algorithm, and an arbitrary, but suitable, optimization algorithm is chosen in the following.

The state regulator drives the vessel to ψ_d after approximately 300 s, because of that it is decided that the numerical optimization algorithm should define a new estimate of ψ_d every 400 s. This means after the system shows steady-state behaviour for awhile.

Knowing that the control moment in yaw is equal to zero when the vessel is operating at the optimal heading, ψ^*, a suitable performance function can be chosen as (5.24), by searching its minimum. Since the numerical optimization algorithm is operating in the discrete-time, it is decided to send samples of, y, every 0.01 seconds during 400 seconds. An average of the samples during the last 100 seconds, meaning the average of the performance function when the system is showing steady-state behaviour is used further in the calculation of the optimal value, ψ^*. The doted line in Figure 5.8, represents a direct measurement of τ_{yaw} instead of calculating it over again.

$$\begin{aligned} y = J(\psi) &= \frac{1}{2}\tau_{yaw}^2 \\ &= \frac{1}{2}(-K_p(\psi - \psi_d) - K_i \int_0^t (\psi(T) - \psi_d(T))\ dT - K_d(r - r_d))^2 \end{aligned} \tag{5.24}$$

For the numerical optimization algorithm, a line searching method is used. The first step in this method is to decide a step length, $\Delta\psi$, and an initialization value of ψ_{d0} at the time t = 0. The second step will be to wait 400 s while the average from the samples during the last 100 s of the performance function, $\bar{J}(\psi_{d0})$, is calculated, as mentioned above. In the third step, the desired heading is changed, $\psi_d = \psi_{d0} + \Delta\psi$. During the fourth step, another 400 s of waiting time is applied and a new $\bar{J}(\psi_d)$ is calculated. In the fifth step, the direction of the search, a, is found using (5.25). In the sixth step, based on the sign of a, the next ψ_d is calculated, before the forth step is repeated. In order to calculate a using (5.25), the values from the last calculation have to be saved each time.

Based on the function of a, five different scenarios can occur. Four of the scenarios are described in Figure 5.9, where $\bar{J}(\psi_d) = J_{new}$, $\bar{J}(\psi_{d-1}) = J_{old}$. The desired heading used in the calculation of J_{new} is called ψ_{old} and the desired heading used to calculate J_{old} is

called ψ_{oldold}. The fifth scenario happens when $a \approx 0$, where ψ_d remains the same. At the time ψ_d remains unchanged, ψ^* is found, and the performance function is minimized. A flow chart of the steps are shown in Figure 5.10.

$$a = \frac{\bar{J}(\psi_d) - \bar{J}(\psi_{d-1})}{\psi_d - \psi_{d-1}} = \frac{J_{new} - J_{old}}{\psi_{old} - \psi_{oldold}} \tag{5.25}$$

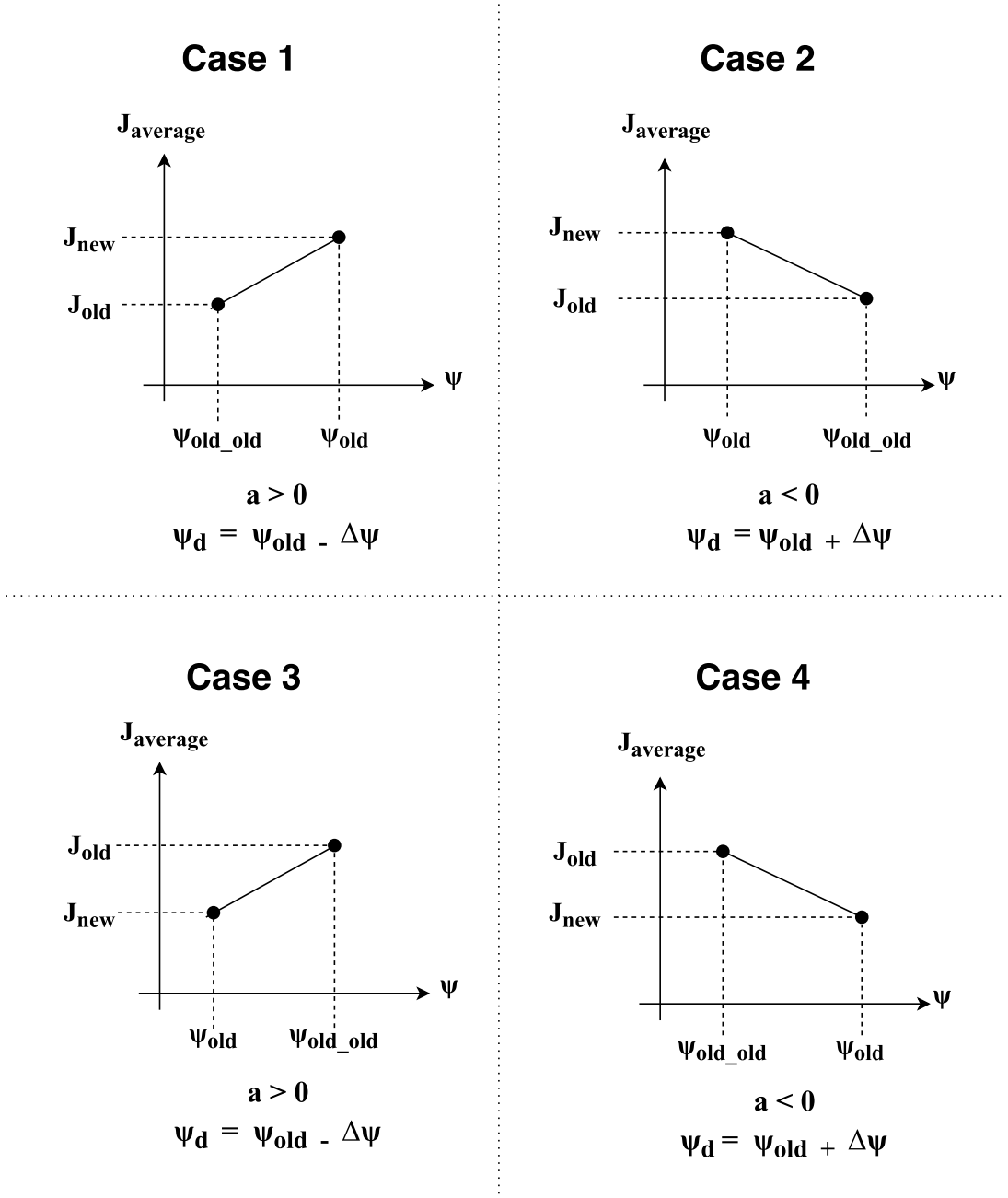

Figure 5.9: The different scenarios for the discrete ES controller

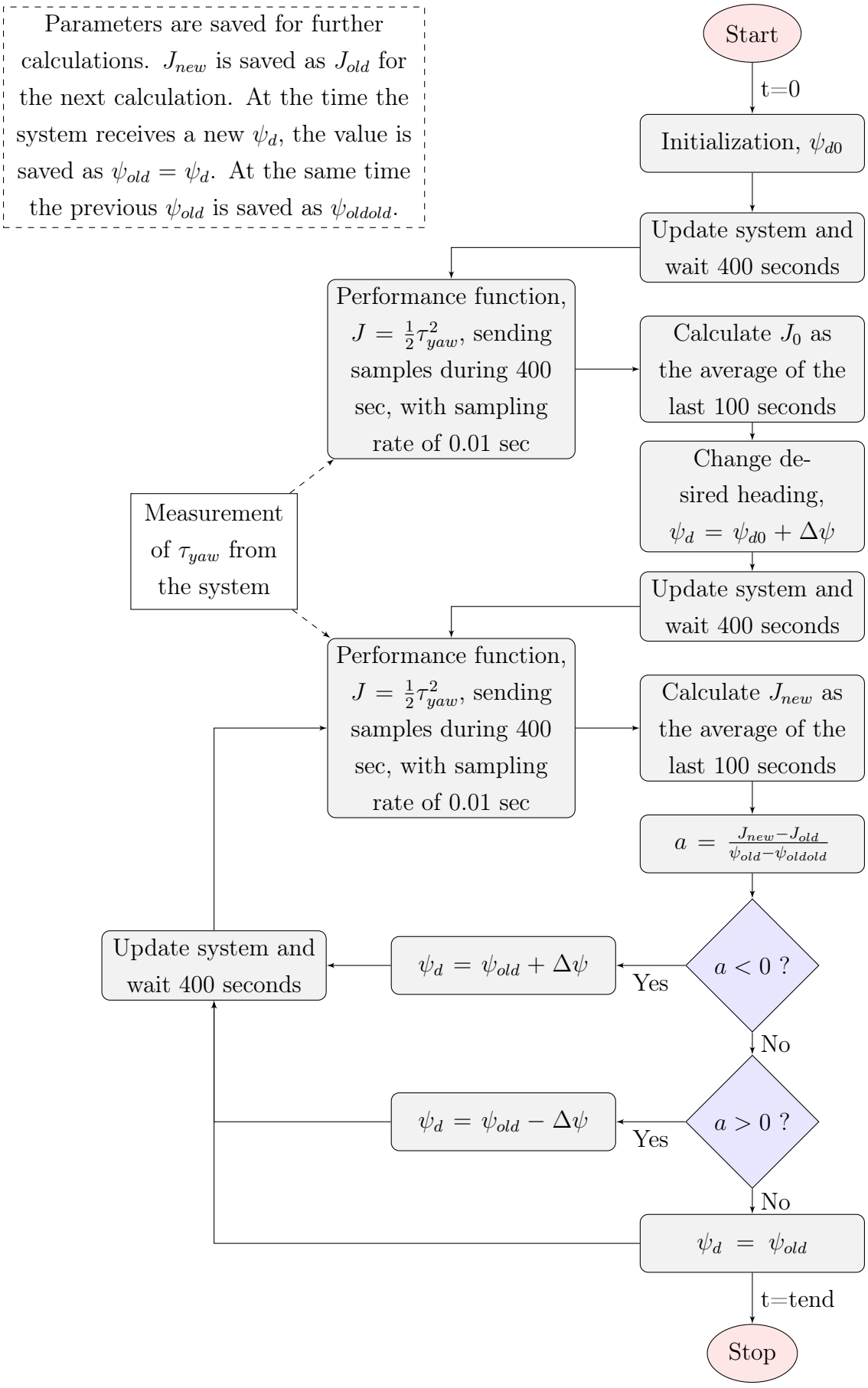

Figure 5.10: Flow chart describing the ES numerical optimization based method

5.5.1 Verification

As described above, the numerical optimization based ES controller works as an autonomous guidance system and provides the controller with online estimates for the desired heading. The guidance system is verified through a simulation with the 6 DOF simulation model. The controllers in surge and sway are switched off during this test. The vessel has the following start position, $\eta = [0\ 0\ 0]^T$, and is exposed to waves and current with a direction of 200 degrees, $\beta_w = \beta_c = 200$ degrees. For the simulation, the initialization value of the numerical optimization algorithm is $\psi_{d0} = 0$, and the step length is decided to be $\Delta\psi = 2$ degrees.

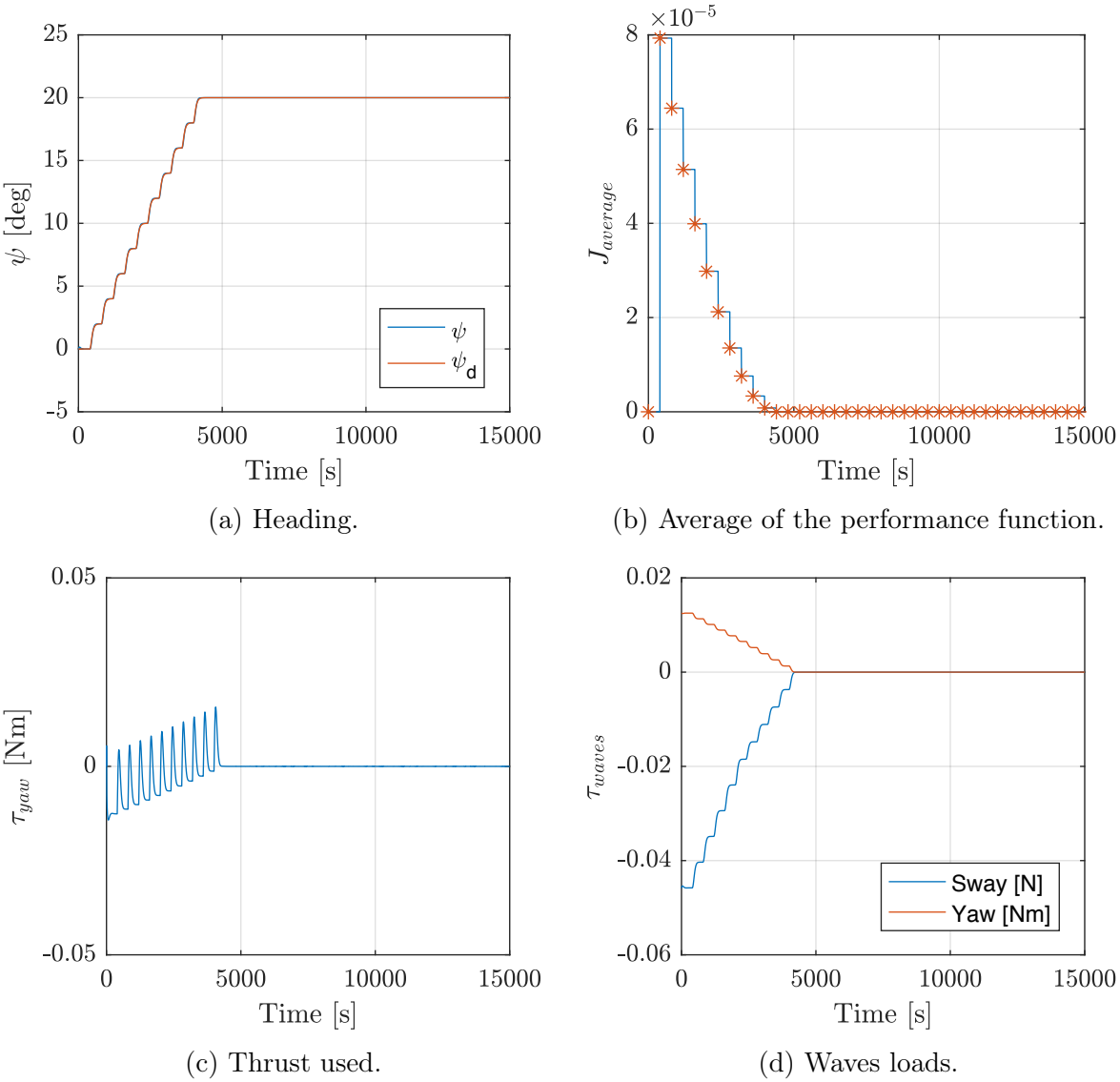

(a) Heading.

(b) Average of the performance function.

(c) Thrust used.

(d) Waves loads.

Figure 5.11: Verification of the numerical optimization based ES guidance system.

As seen in Figure 5.11a and 5.11b, the average of the performance function will decrease

as ψ goes towards ψ^*. At the same time the controller will give zero thrust in yaw, and the waves give zero force and zero moment in sway and yaw, as seen in Figure 5.11c and 5.11d respectively. Based on this it can be concluded that the numerical optimization based ES guidance system finds the right value of ψ^*.

Chapter 6

Experiment setup

To do experiments with CSAD in the MC Lab, three different computers are needed. One to control the vessel, one to control the waves and one for the Qualisys motion capture system.

The controller gains used in the simulations will not work for the experiments, and have to be re-tuned. The cRIO drives at 100 Hz, and because of that it is important that the solver method used in the Simulink model is set to a fixed step equal to 0.01 seconds.

6.1 Mooring lines

For the experimental work, it is difficult to replicate the mooring system from the simulation in order to give the same forces. In stead, 4 mooring lines were made according to Bjørnø (2016), which gives a good indication of the mooring forces.

Each mooring line is made of a polyester silk line. This silk line sinks in water, has a diameter of 2 mm and can withstand 74 kg. Two swivels and one spring are attached at each end of the line. Springs are used in order to obtain a restoring force and the swivels are used to prevent the line from twisting. One end of the line is attached to a 10 kg weight, which works as an anchor. A line made of propylene is bound around the slick weight to provide a means to fix tie the mooring line to the weight. This line floats in water, and has a diameter of 4 mm and can withstand 120 kg. It is made a loop at the end of the floating line which in combination with the buoyancy makes it easier to get hold of the anchor with a hook if its location needs to be adjusted. In order to approximate the curve of a real mooring line, two lead balls are fixed to the silk line close to the anchor. See Figure 6.1a for a illustration of one of the mooring lines.

The turret is equipped with four swivels, to make it easy to attach and detach the mooring lines. The underside of the turret can be seen in Figure 6.1b.

The experimental setup in the MC Lab can be seen in Figure 6.2, showing the model ship, CSAD, equipped with the 4 mooring lines. At this setup, the anchors are placed in a configuration so the mooring lines give some slack, which gives the vessel the possibility to move with a diameter of approximately 0.6 m about its origin.

(a) One of the mooring lines. (b) Turret upside down.

Figure 6.1: Experimental setup of the mooring system.

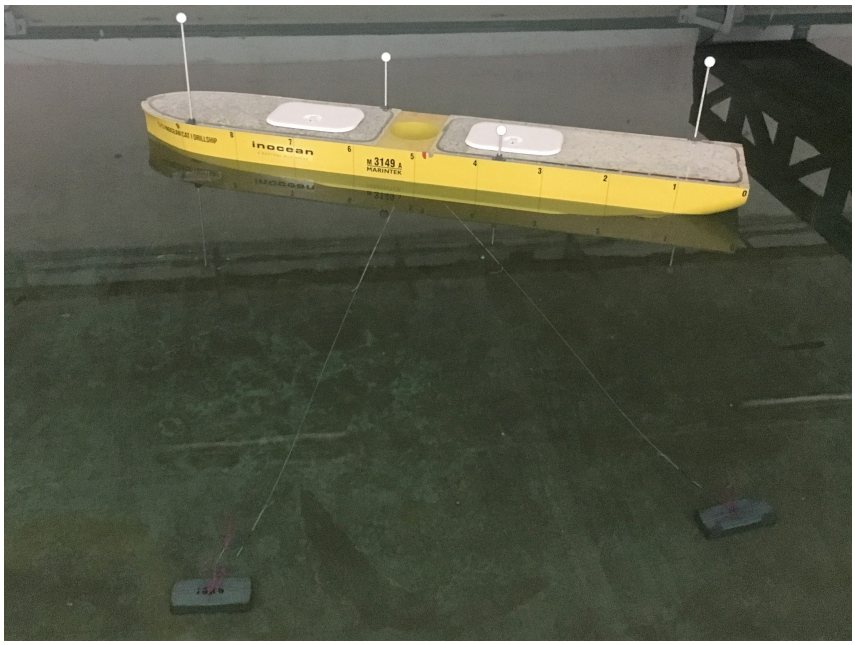

Figure 6.2: Main components of the experimental mooring system.

6.2 Waves

During the experiments, irregular waves with the ITTC wave spectrum are used. Two cases from the moderate sea state were tried, and the parameters can be found in Table 6.1.

Table 6.1: Wave parameters used in the experiments.

Full scale			**Model scale**		
$\mathbf{H}_s$ [m]	$\boldsymbol{\omega}_p$ $[rad/sec]$	$\mathbf{T}_s$ [sec]	$\mathbf{H}_s$ [m]	$\boldsymbol{\omega}_p$ $[rad/sec]$	$\mathbf{T}_s$ [sec]
1.25	0.79	7.9534	0.0139	7.495	0.8383
2	0.724	8.6784	0.0222	6.869	0.9147

In the MC Lab, waves are coming from the same direction at all times. In order to create a more comprehensive and realistic scenario, it is decided to make a controller that emulates a rotation of the basin frame, so that it appears as if the waves are coming from other directions as well. In this manner it will be more challenging for the guidance system to find the optimal heading during the experiments.

Since it is impossible to actually turn the basin frame itself, a regular proportional basin controller only for yaw is made, in order to instead turn the ship to a new heading. In this way the waves are hitting the ship from a different angle, which would be the same effect as by rotating the basin. When the ship is stable at this heading, this controller is turned off and replaced with the normal 3 DOF controller. Because the 3 DOF controller is reading its input from Qualisys, the heading measurement given from Qualisys needs to be adjusted at each reading by subtracting the same radian value as applied by the basin controller when changing the heading of the vessel.

6.3 Qualisys motion capture system

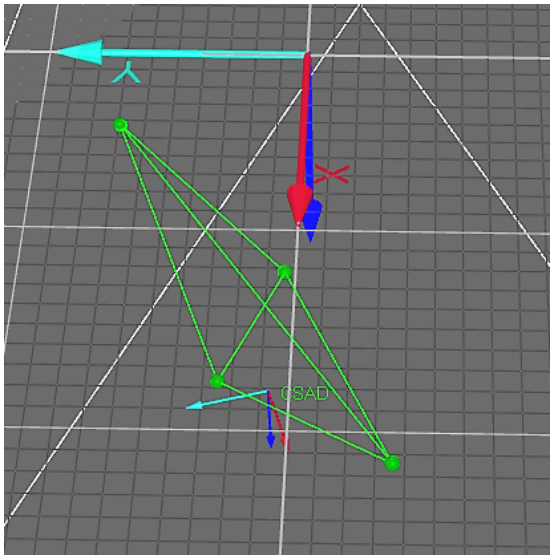

Figure 6.3: Detection of the position and directions of CSAD with the use of Qualisys.

The QTM software shows the position and the direction of CSAD according to Figure 6.3.

The definition of the FZP tells that the origin of the earth-fixed reference frame is located in the centre of the turret when no environmental loads act on the vessel. In the MC Lab, the earth-fixed reference frame is replaced by a basin-fixed reference frame.

As seen in Figure 6.3 of the setup, the origin of the basin-fixed reference frame is not in the COT. Because of that, the position, in both x and y, should be read from Qualisys when the heading is zero before starting any experiments. To get the results right, this can be corrected for during the plotting of the results, something which on the plot will move the vessel so that the origin of the basin-frame is in the COT.

Chapter 7

Results

7.1 Simulation

The following three different guidance systems for heading will be simulated in this thesis:

1. A user specified guidance system for heading, as described in Chapter 5.2.
2. An autonomous guidance system for heading based on sinusoidal perturbation based ES, as described in Chapter 5.4.
3. An autonomous guidance system for heading based on numerical optimization based ES, as described in Chapter 5.5.

All of these heading guidance systems will be combined with a guidance system for the North and East position based on setpoint chasing, as described in Chapter 5.3.

There are two remarks regarding the simulations. The first one is applicable for all the systems, while the second remark is only applicable for the autonomous guidance system for heading based on sinusoidal perturbation based ES.

The first remark is that the observer is not included in this simulations, since it is not a part of the thesis. The observer is neglected by turning off the 1^{st} order wave loads in the Simulink model.

The second remark is regarding the sinusoidal perturbation based ES guidance system for heading. This guidance system will be used to find the heading when simulating the full 6 DOF model, and the ES controller used in the simplified verification in Chapter 5.4, have been tuned further to fit this model. However, due to the complexity of the guidance system combined with the thruster allocation and the FEM model, the simulation turns

to be demanding with respect to both execution time and computer memory capacity. Because of that, it is decided to simplify the model when using the sinusoidal perturbation based ES guidance system for heading. For the simulations, the commanded thrust from the thruster allocation block, and the forces and moment from the controller, are similar, it is therefore decided to only use the controller. For a TAPM operation, the displacements of the vessel are small, hence, the mooring forces can be assumed linear, and therefore the linearized restoring force matrix outlined in Chapter 4.1 will replace the FEM model. These simplifications will result in some deviations from the real world, but the simulations are still regarded as a good approximation.

The main focus during the simulations are to test the validity of the three different guidance systems described above in order to determine how fast and how accurate they manage to find ψ^*. Each guidance system is tested for two scenarios as defined in Chapter 7.1.1. Scenario 1 is conducted in order to check the validity of the guidance systems seeking a ψ^* larger than the initial heading of the vessel, ψ_0, while scenario 2 is conducted to check the validity of seeking a ψ^* lower than ψ_0.

Chapter 7.1.2 presents the results using the three guidance systems, 1, 2 and 3 respectively, on scenario 1, while in Chapter 7.1.3 the similar is performed on scenario 2.

7.1.1 Scenario definitions

Scenario 1:

- Vessel start position, $\boldsymbol{\eta}_0 = [0\ 0\ 0]^T$.
- The vessel is exposed to waves and current with a direction of 200 degrees, $\beta_w = \beta_c = 200$ degrees.
- Weather parameters as described in Table 3.4.
- The initialization values of the reference filter and both of the ES controllers are set equal to the start position of the vessel.
- Based on the direction of the environmental loads, it is reasonable to assume that the $\psi^* = 20$ degrees. Because of that, the desired heading used in the user specified guidance system is set equal to $\psi_d = 20$ degrees.
- The step length used in the numerical optimization algorithm is decided to be $\Delta\psi = 2$ degrees.

Scenario 2:

- Vessel start position, $\boldsymbol{\eta}_0 = [0\ 0\ (20 * \pi/180)]^T$.
- The vessel is exposed to waves and current with a direction of 180 degrees, $\beta_w = \beta_c = 180$ degrees.
- Weather parameters as described in Table 3.4.
- The initialization values of the reference filter and both of the ES controllers are set equal to the start position of the vessel.
- Based on the direction of the environmental loads, it is reasonable to assume that the $\psi^* = 0$ degrees. Because of that, the desired heading used in the user specified guidance system is set equal to $\psi_d = 0$ degrees.
- The step length used in the numerical optimization algorithm is decided to be $\Delta\psi = 2$ degrees.

7.1.2 Scenario 1: simulation results

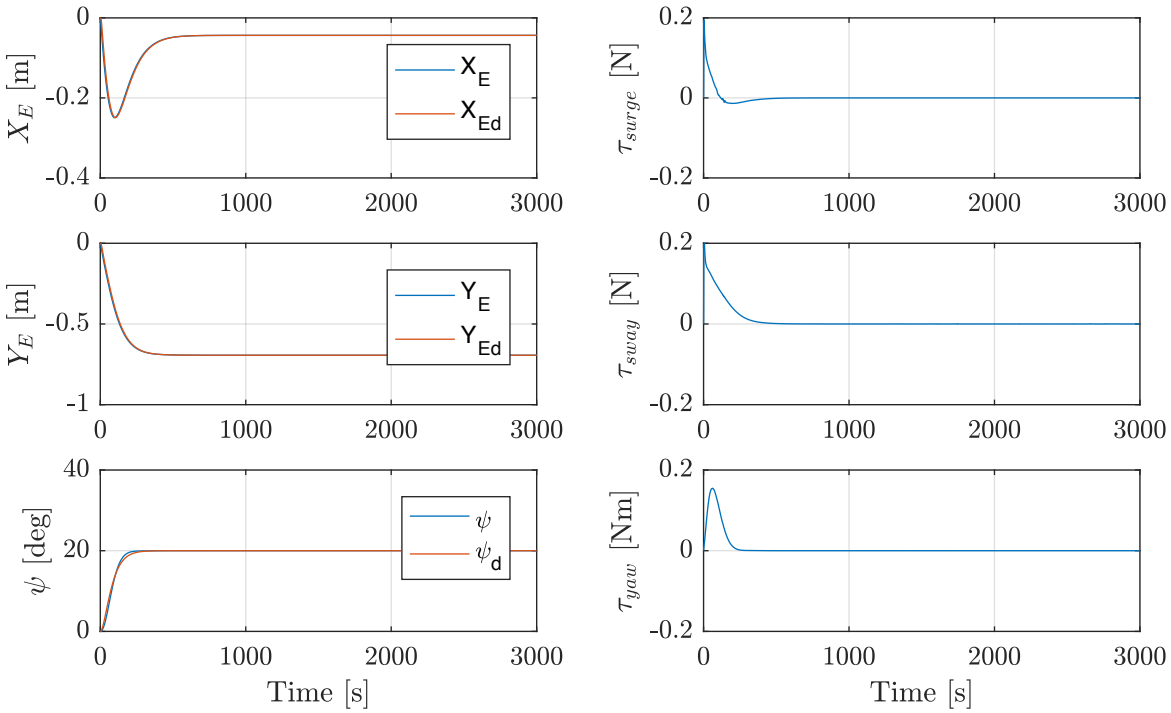

(a) Position over time.

(b) Thrust used over time.

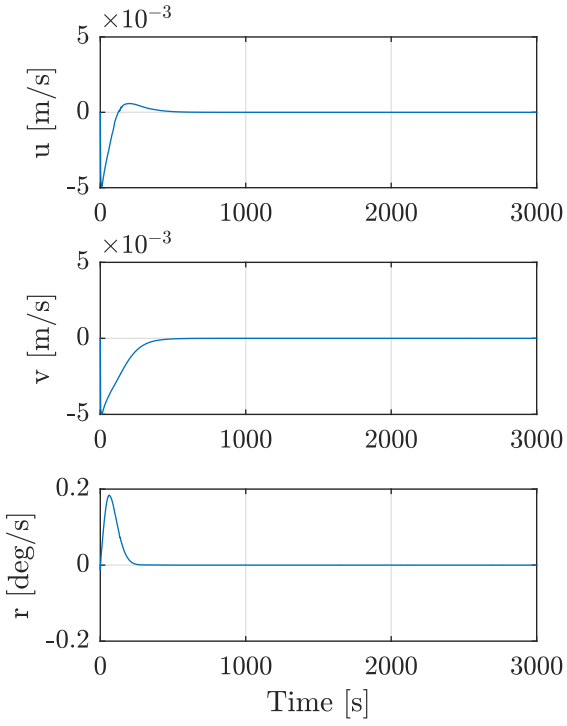

(c) Velocity over time.

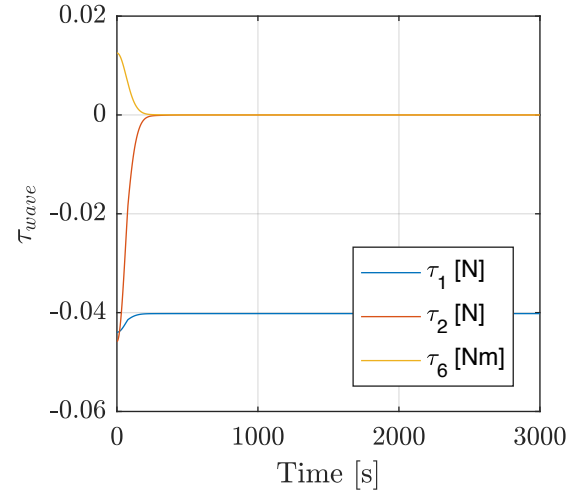

(d) Wave loads over time.

Figure 7.1: Guidance system number 1: User specified guidance system for heading for scenario 1.

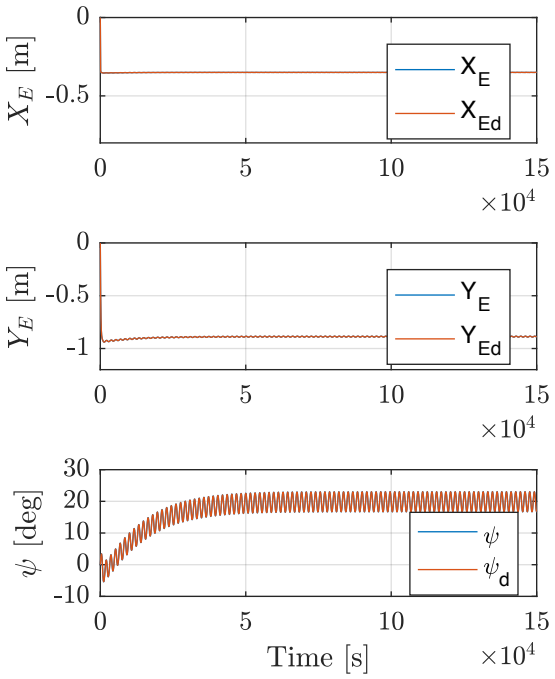

(a) Position over time.

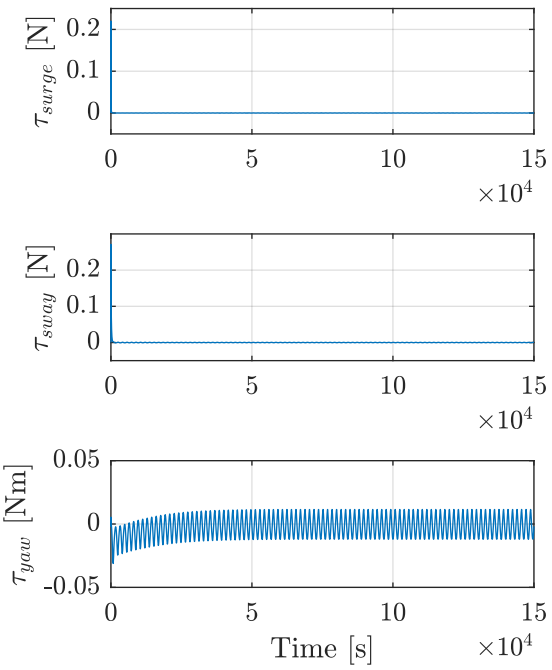

(b) Thrust used over time.

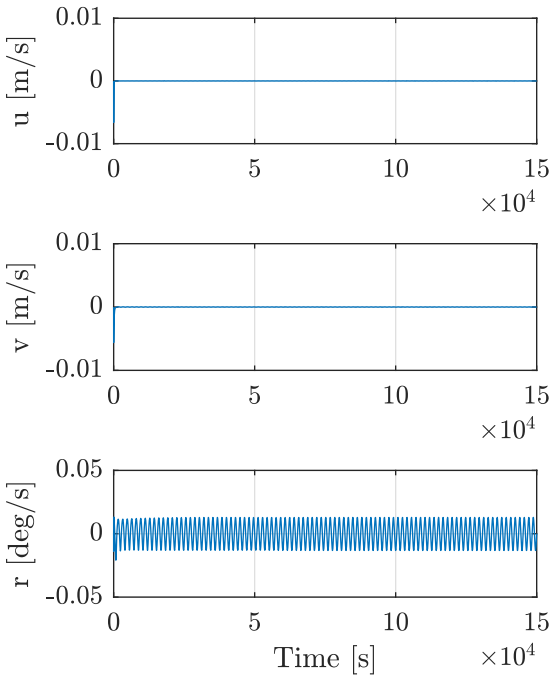

(c) Velocity over time.

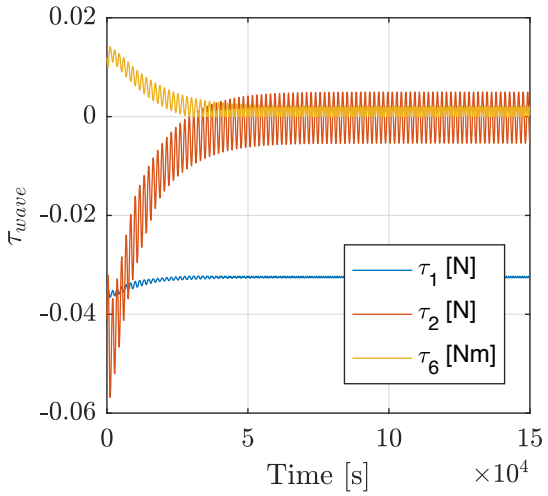

(d) Wave loads over time.

Figure 7.2: Guidance system number 2: Sinusoidal perturbation based ES guidance system for heading for scenario 1.

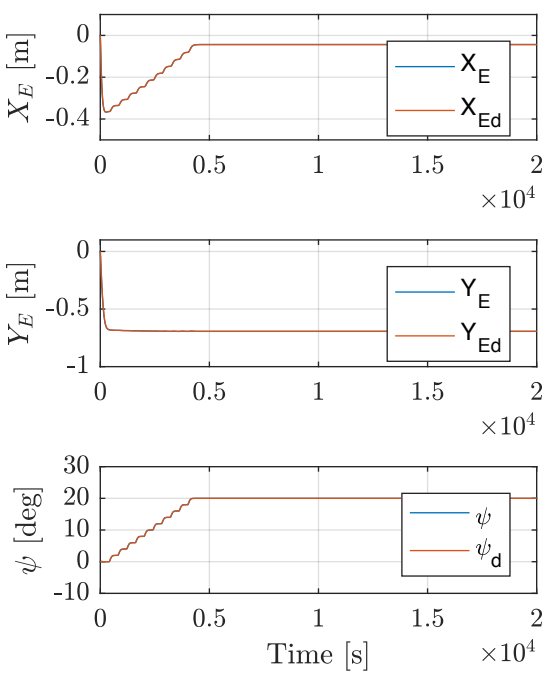

(a) Position over time.

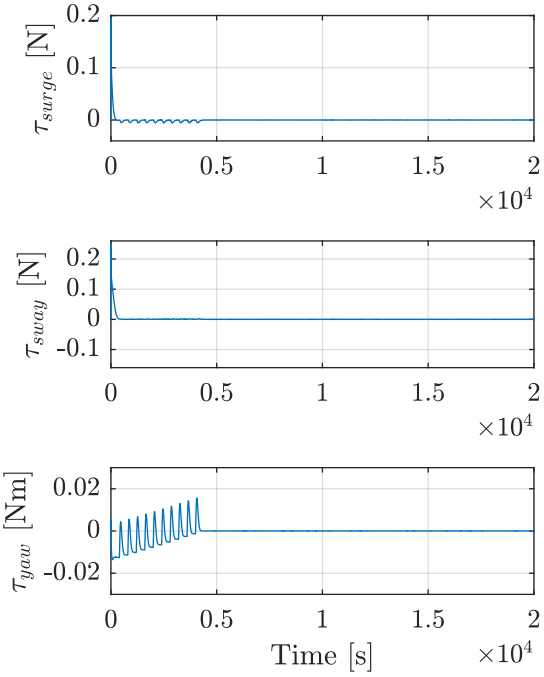

(b) Thrust used over time.

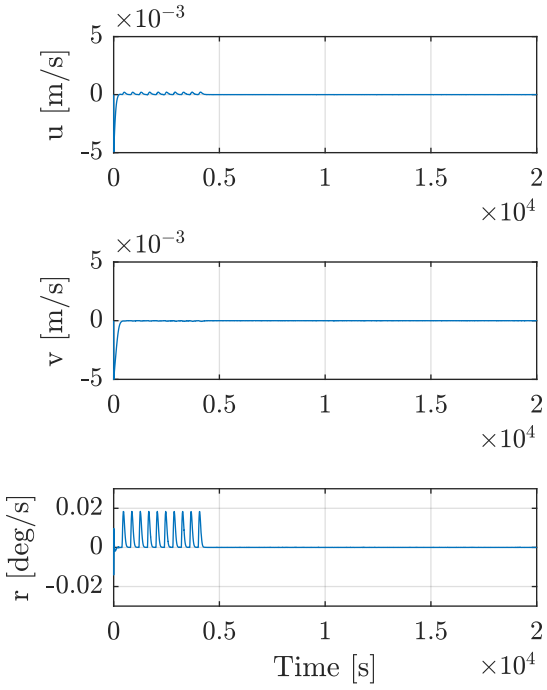

(c) Velocity over time.

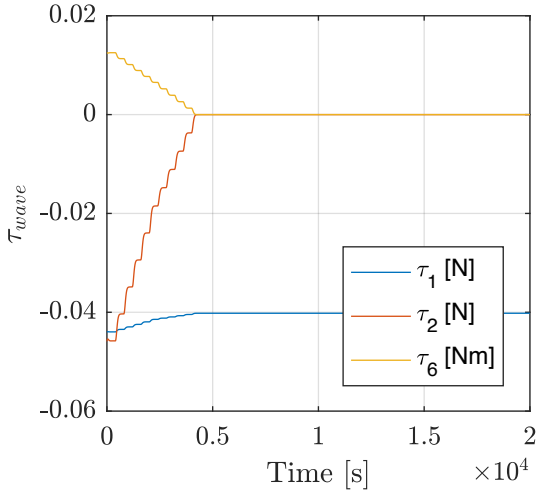

(d) Wave loads over time.

Figure 7.3: Guidance system number 3: Numerical optimization based ES autonomous guidance system for heading for scenario 1.

Figure 7.1 shows the simulation results using guidance system number 1, a user specified guidance system for heading in a combination with setpoint chasing for the North and East position. ψ_d was manually defined to be 20 degrees, and as seen in Figure 7.1a, the vessel heading converges to ψ_d after approximately 300 s. The setpoint chasing algorithm finds the optimal position of the vessel to be $(X_E, Y_E) = (-0.05m, -0.6m)$, right after the heading has reached its steady-state value. When both the position and heading are steady-state, the vessel uses zero thrust as seen in Figure 7.1b. This indicates that the vessel is in its optimal position and that the optimal heading for this scenario is 20 degrees. From Figure 7.1c, it can be seen that the vessel is stationary, meaning that the velocities and the rotational rate are zero. From the definition of the optimal heading, it is known that when the vessel reaches its optimal heading, there are zero moment and zero force working on the vessel in yaw and sway respectively. Based on this, it can also be verified from Figure 7.1d showing the wave loads, that 20 degrees is the optimal heading.

Figure 7.2 shows the simulation results using guidance system number 2, an autonomous guidance system for heading based on sinusoidal perturbation based ES in a combination with setpoint chasing for the North and East position. As seen in Figure 7.2a, the ES controller is seeking for an ψ^* equal 20 degrees, and finds this value after approximately 45000 s. Because of the perturbation signal this method operates with, ψ_d will oscillate around ψ^*, which again will cause oscillations in the vessels heading. The oscillations that appears in ψ_d, have a deviation of ± 5 degrees around ψ^* over a period of 1600 s, which is not a rapid change. Because of these oscillations, the yaw moment and the rotational rate will oscillate around zero, as seen in Figure 7.2b and Figure 7.2c, respectively. It will also have impact on the position, which will have small oscillations in order to obtain zero thrust and zero velocity in surge and sway. The optimal position of the vessel using the simplified model is $(X_E, Y_E) = (-0.4m, -0.9m)$, see Figure 7.2a. Figure 7.2d shows oscillations in the wave loads as a result of the oscillations in heading.

Figure 7.3 shows the simulation results using guidance system number 3, an autonomous guidance system for heading based on numerical optimization based ES in a combination with setpoint chasing for the North and East position. As seen in Figure 7.3a the numerical optimization based ES guidance system finds the optimal heading value to be $\psi^* = 20$ degrees after approximately 4000 s. From the same figure, it can be seen that the optimal position of the vessel depends on the value of the vessels heading. When the vessel has reached its optimal heading, the optimal position of the vessel is $(X_E, Y_E) = (-0.05m, -0.6m)$. When the vessel stands in its optimal position with its optimal heading, the vessel uses zero thrust in each of its DOFs, as seen in Figure 7.3b. When the vessel uses zero thrust, the velocities are also zero, see Figure 7.3c. From Figure 7.3d it can be seen that the wave loads are zero for sway and yaw when $\psi_d = \psi^*$.

7.1.3 Scenario 2: simulation results

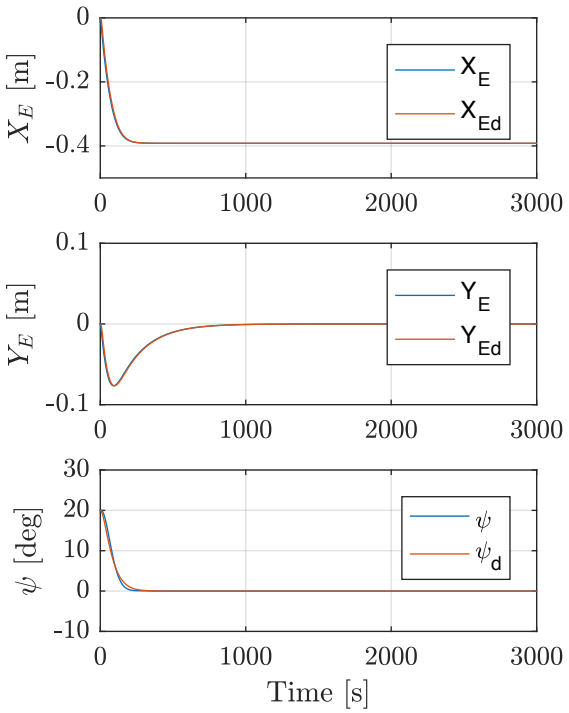

(a) Position over time.

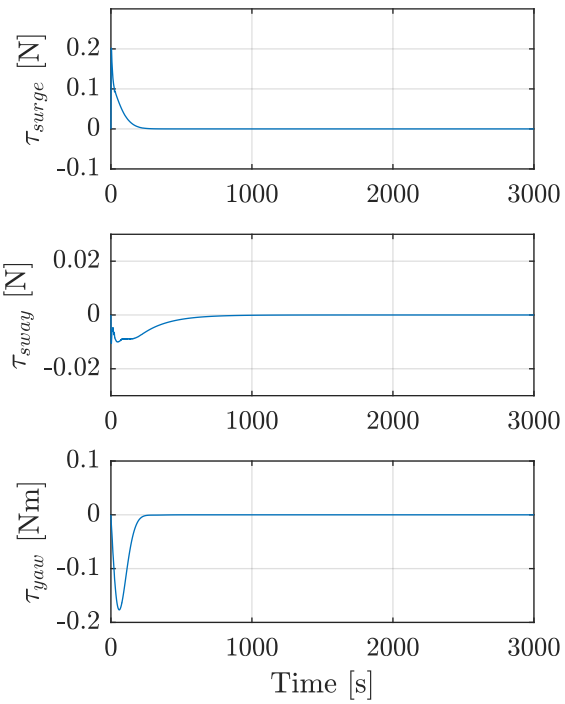

(b) Thrust used over time.

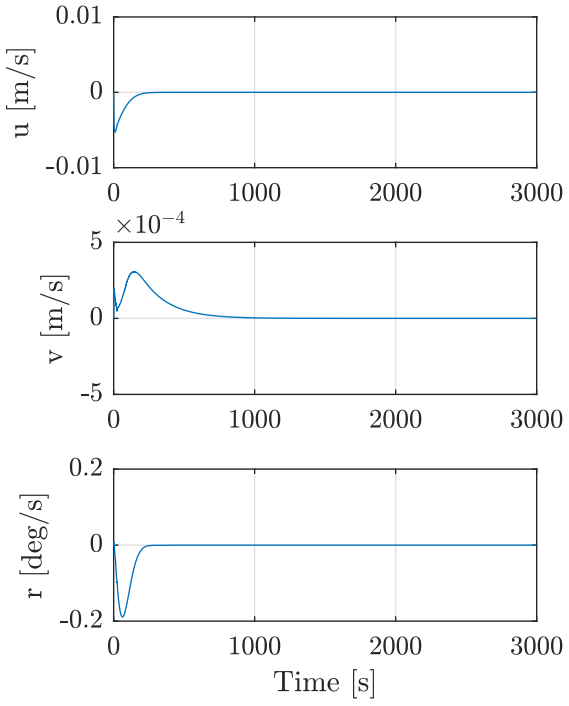

(c) Velocity over time.

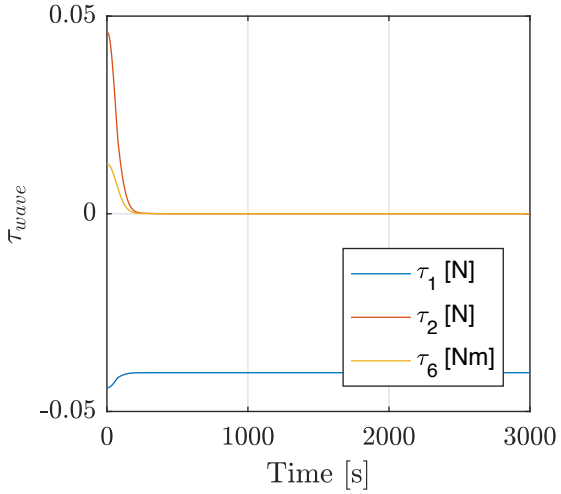

(d) Wave loads over time.

Figure 7.4: Guidance system number 1: User specified guidance system for heading for scenario 2.

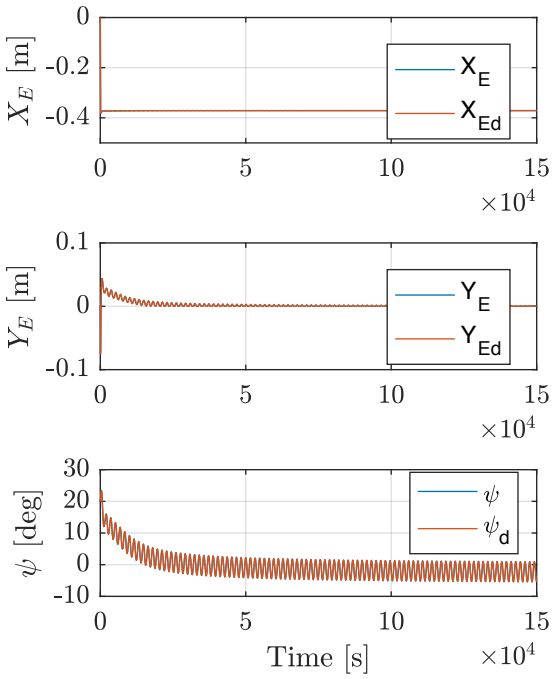

(a) Position over time.

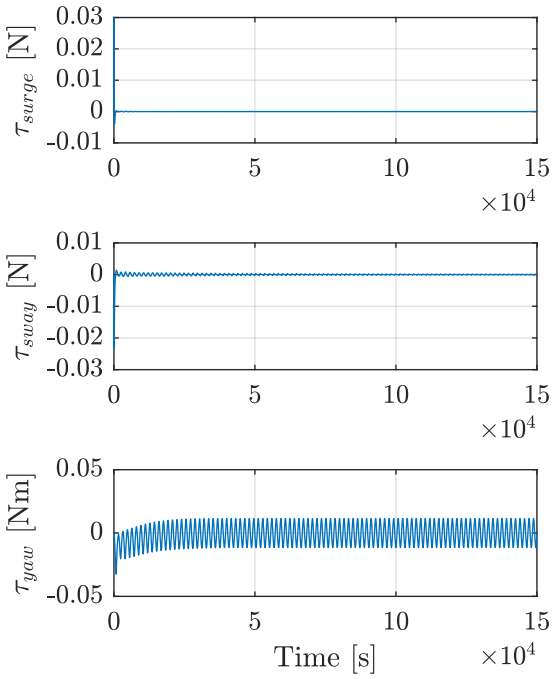

(b) Thrust used over time.

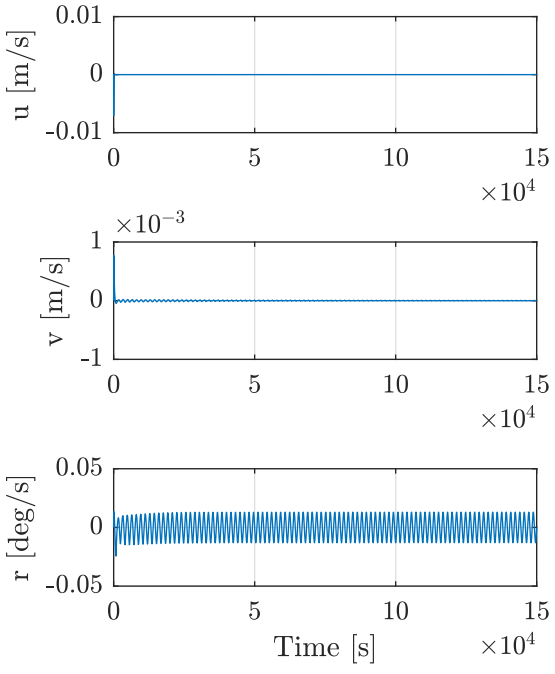

(c) Velocity over time.

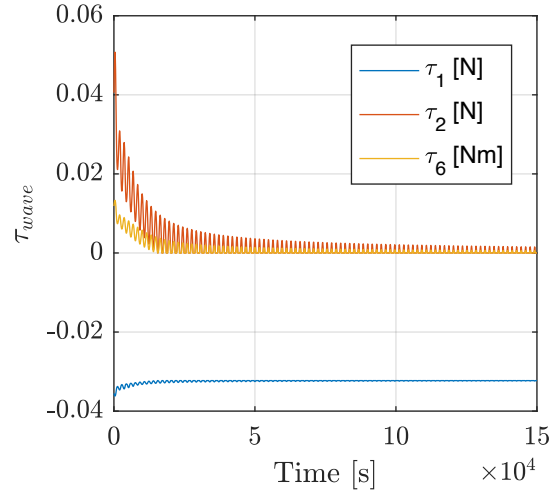

(d) Wave loads over time.

Figure 7.5: Guidance system number 2: Sinusoidal perturbation based ES guidance system for heading for scenario 2.

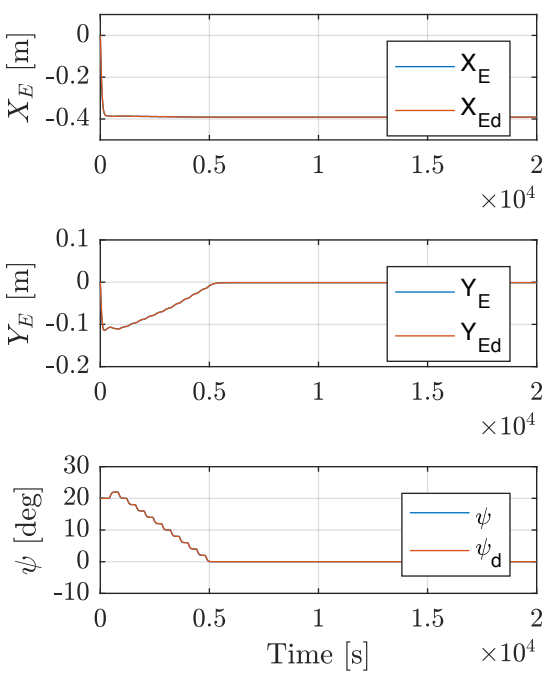

(a) Position over time.

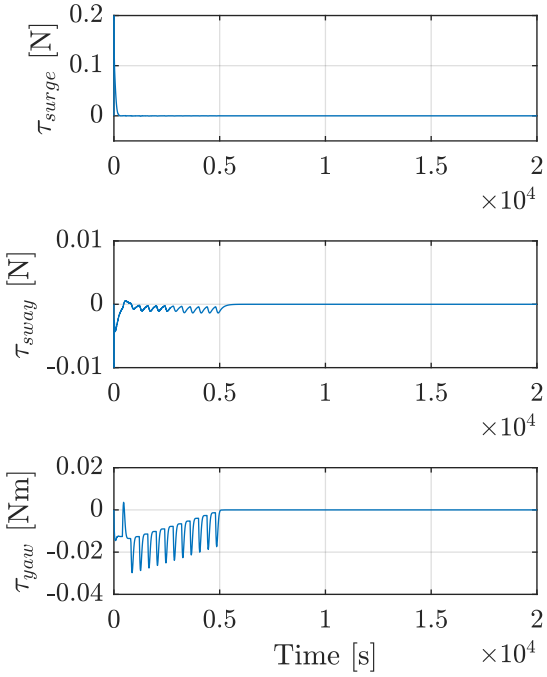

(b) Thrust used over time.

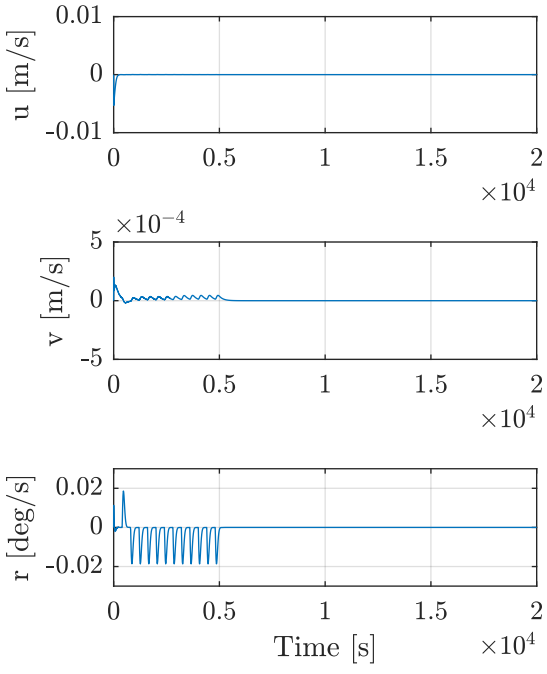

(c) Velocity over time.

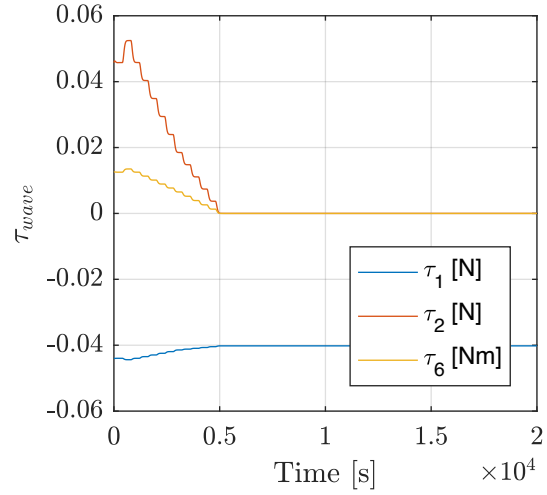

(d) Wave loads over time.

Figure 7.6: Guidance system number 3: Numerical optimization based ES autonomous guidance system for heading for scenario 2.

Figure 7.4 shows the simulation results using guidance system number 1, a user specified guidance system for heading in a combination with setpoint chasing for the North and East position. ψ_d was manually defined to be 0 degrees, and as seen in Figure 7.4a, the vessel heading converges to ψ_d after approximately 300 s. The setpoint chasing algorithm finds the optimal position of the vessel to be $(X_E, Y_E) = (-0.4m, 0m)$, right after the heading has reached its steady-state value. When both the position and heading are steady-state, the vessel uses zero thrust, and has zero velocities and rotational rate as seen in Figure 7.4b and Figure 7.4c, respectively. This indicates that the vessel is in its optimal position and that the optimal heading for this scenario is 0 degrees. From Figure 7.4d it can be seen that the wave loads are zero for sway and yaw when $\psi = \psi^*$.

Figure 7.5 shows the simulation results using guidance system number 2, an autonomous guidance system for heading based on sinusoidal perturbation based ES in a combination with setpoint chasing for the North and East position. As seen in Figure 7.5a, the ES controller is seeking for an ψ^* equal 0 degrees, and approaches this value after approximately 45000 s. Because of the perturbation signal used in this method, ψ_d will oscillate close to ψ^*, which again will cause oscillations in the vessels heading. The oscillations that appear in ψ_d, have a deviation of ± 5 degrees around ψ^* over a period of 1600 s, which is not a rapid change. Because of these oscillations, the yaw moment and the rotational rate will oscillate around zero, as seen in Figure 7.5b and Figure 7.5c, respectively. It will also have an impact the position, which will have small oscillations in order to obtain zero thrust and zero velocity in surge and sway. The optimal position of the vessel using the simplified model is $(X_E, Y_E) = (-0.38m, 0m)$, see Figure 7.5a. Figure 7.5d shows oscillations in the wave loads as a result of the oscillations in heading.

Figure 7.6 shows the simulation results using guidance system number 3, an autonomous guidance system for heading based on numerical optimization based ES in a combination with setpoint chasing for the North and East position. As seen in Figure 7.6a, the numerical optimization based ES guidance system finds the optimal heading value to be $\psi^* = 0$ degrees after approximately 5000 s. From the same figure, it can be seen that when the the vessel has reached its optimal heading, the optimal position of the vessel is $(X_E, Y_E) = (-0.4m, 0m)$. When the vessel stands in its optimal position with its optimal heading, the vessel uses zero thrust in each of its DOFs, as seen in Figure 7.6b. When the vessel uses zero thrust the velocities are also zero, see Figure 7.6c. From Figure 7.6d, it can be seen that the wave loads are zero for sway and yaw when $\psi = \psi^*$.

7.2 Experiment

In addition to the simulation described in Chapter 7.1, the optimistic plan was to test the same three guidance systems for heading during experiments in the MC Lab. However, due to limited access to the laboratory, and challenges discovered with the equipment during the experimental period, only the following guidance system was tested:

1. A user specified guidance system for heading in a combination with setpoint chasing for the North and East position.

This guidance system was tested for two scenarios inside the moderate wave condition, first with $H_s = 1.25\ m$ and then with $H_s = 2\ m$, which in model scale are $H_s = 0.0139\ m$ and $H_s = 0.0222\ m$, respectively.

The main challenge during the experiments was that the model ship early started to take in water, and because of that, the testing became more difficult. After a while, the leakage became more severe, which reduced the ability to test.

Some remarks are made regarding the experimental work.

The first remark is that all measurements from the experimental work in the MC Lab will contain noise because of wave frequency motions. This will require a good observer for the experiments, and the nonlinear passive observer described in Chapter 4.2 had to be used during all experiments.

The second remark concerns the plotting of the results. As described in Chapter 6, the vessel is moved during plotting such that the origin of the basin-fixed reference frame is located in the COT when no environmental loads act on the vessel.

The third remark is regarding all gains in the system. The gains used in the control system during the simulations, will not work during the experiments. Because of that, all gains used in the experiment were re-tuned manually using the method of trail and error. It is more challenging to find good gains for real life experiments than for simulations, and because of that, the results will not be equally smooth as for the simulations.

The last remark concerns the thrust allocation implemented in the model. It was noticed that it did not work optimal, and that the control force and the commanded thrust force did not follow each other at all time. A thrust allocation including 6 azimuth thrusters, is a hard optimization problem. In addition, it may also occur uncertainties in the mapping between the thrust output and the hardware on the model.

An observation was made during the tuning. When using a PID-controller for yaw to-

gether with a PD-controller in surge and sway, the results for all 3 DOF, and especially yaw, became poorer than for the results using only a P-controller for yaw. A reason for this can be the fact that the velocity is not estimated good enough due to time lag, which will give the damping part a destabilizing effect on the system. Because of this, only a P-controller was used for controlling the heading.

In the MC Lab, only waves can be included in the experiments. The waves will have a direction of $\beta_w = 180$ degrees, and by this it can be assumed that that $\psi_d = 0$. Because of that, the desired heading used in the user specified guidance system for yaw, was set equal to zero.

The results using a user specified guidance system for heading in a combination with setpoint chasing for the North and East position, can be seen in Figure 7.7 for $H_s = 0.0139m$ and in Figure 7.8 for $H_s = 0.0222m$.

When the vessel is exposed to waves with $H_s = 0.0139m$, it can be seen from Figure 7.7a and Figure 7.7b, that the controller follows the setpoints for North and East with an error of approximately $\pm 5mm$, while the heading is oscillating around zero with an error of approximately ± 2.5 degrees. From Figure 7.7c, it can be seen that the thrust in surge and sway, and the moment in yaw, are oscillating around zero.

When the vessel is exposed to waves with $H_s = 0.0222m$, it can be seen from Figure 7.8a and Figure 7.8b, that the controller follows the setpoints for North and East with an error of approximately ± 1.5 cm, while the heading is oscillating around zero with an error of approximately ± 6 degrees. From Figure 7.8c it can be seen that the controller forces in sway and surge are approximately zero, but that the commanded thrust does not follow this and gives some thrust both in surge and sway. The commanded thrust in yaw, on the other hand, is approximately zero, while the control moment is oscillating around zero with an amplitude of ± 0.1 Nm. This shows that the heading controller tries to compensate for the error in the heading, and that the commanded thrust struggles in order to be optimized in all directions at the same time.

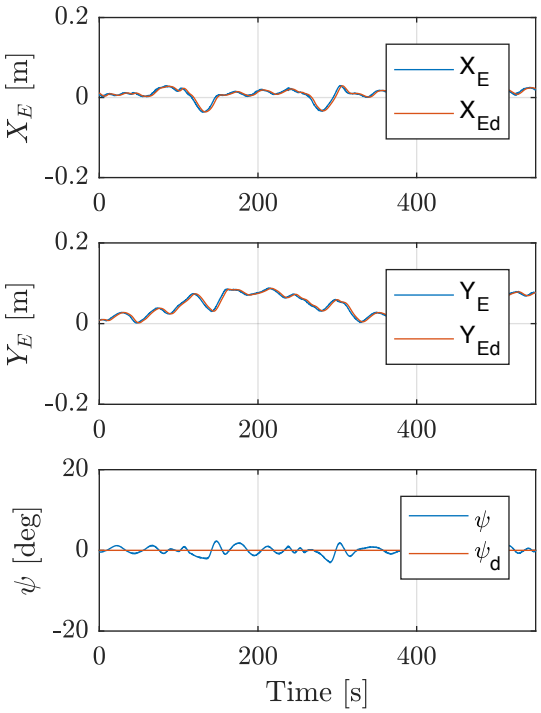

(a) Position and heading over time.

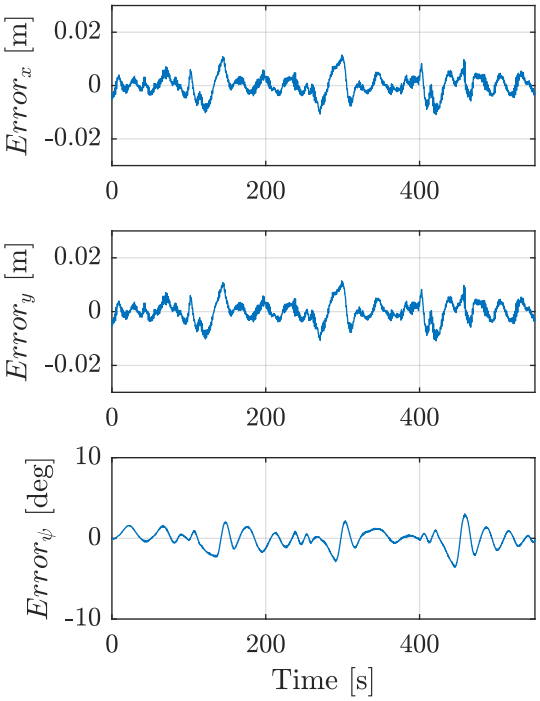

(b) Error in position and heading over time.

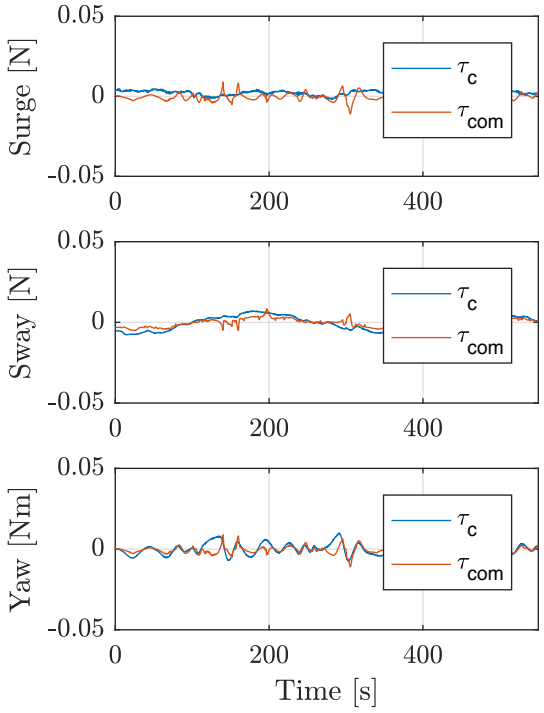

(c) Control force and commanded thrust over time.

Figure 7.7: Experiment, $H_s = 0.0139m$: User specified guidance system in heading and setpoint chasing for the North and East position.

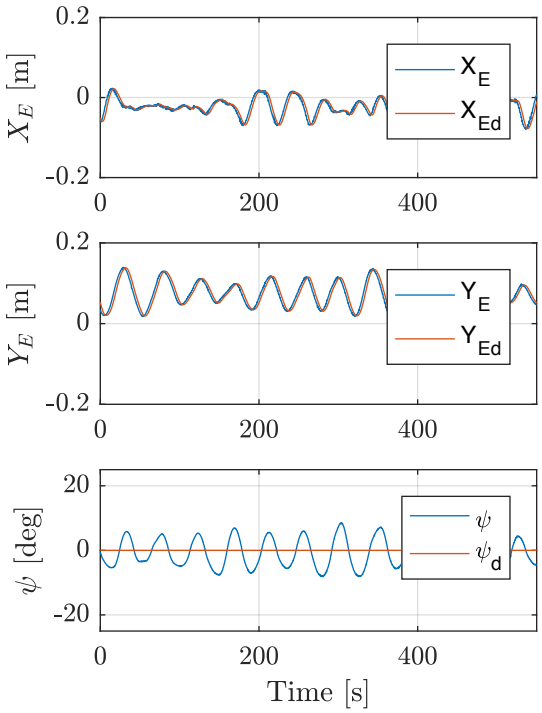

(a) Position and heading over time.

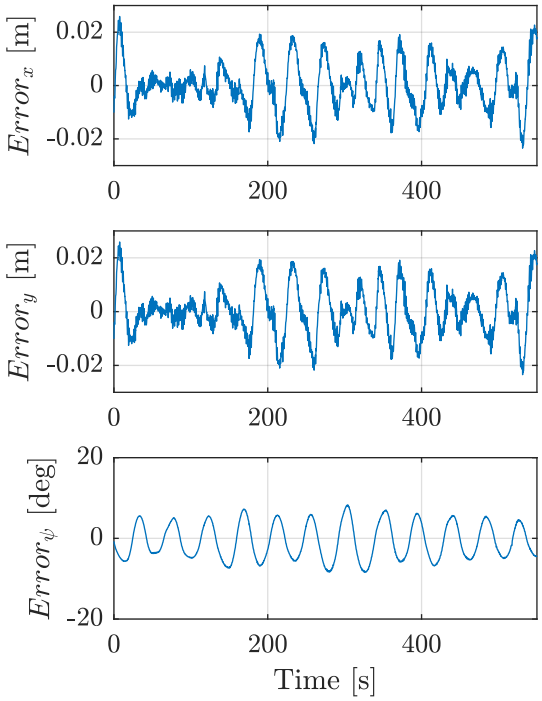

(b) Error in position and heading over time.

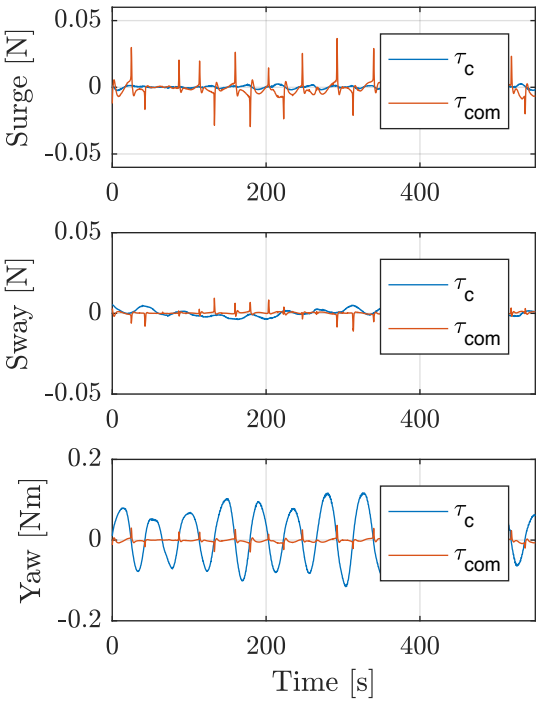

(c) Control force and commanded thrust over time.

Figure 7.8: Experiment, $H_s = 0.0222m$: User specified guidance system in heading and setpoint chasing for the North and East position.

In addition, the controller that rotates the basin frame described in Chapter 6.2, where tested with $H_s = 0.0139m$ waves. It was decided to turn the basin frame to an angle of -20 degrees from its original orientation. At this orientation, the vessel will experience that waves are arriving with an direction of 200 degrees. Because of that, the desired heading is set equal to 20 degrees in the user specified guidance system.

Figure 7.9 shows an experiment where the basin controller is switched off after 200 s, and replaced by a P-controller only for heading. At this time, there are not included any controllers for surge and sway. From this, it can be seen that the vessel keeps its heading at a steady-state value of 20 degrees, and that the thruster allocation works optimal when concerning only one DOF.

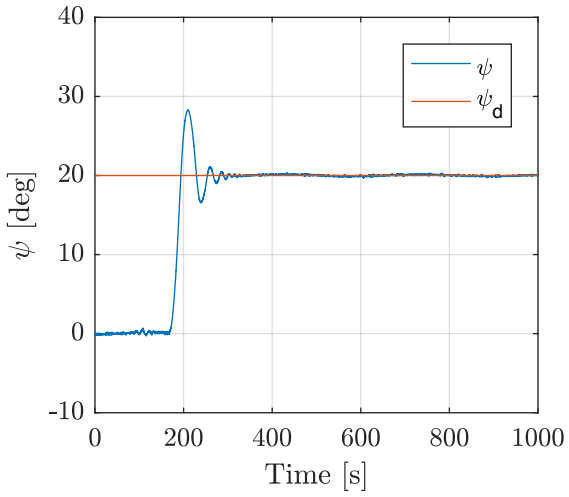

Figure 7.9: Experiment, $H_s = 0.0139m$: Rotation of basin frame.

Chapter 8

Discussion

During the simulations presented in Chapter 7.1, the following three different guidance systems for heading were tested:

1. A user specified guidance system for heading.
2. An autonomous guidance system for heading based on sinusoidal perturbation based ES.
3. An autonomous guidance system for heading based on numerical optimization based ES.

All of these heading guidance systems were combined with a guidance system based on setpoint chasing for the North and East position.

Before any further discussion of the results, a minor flashback with some reflections on why a guidance system is important for a control system, is discussed. As remarked earlier in this thesis, it is important that a vessel used during offshore operations contains a positioning system, like for instance an TAPM system. All positioning systems contain a controller where the intention is to control and maintain a vessel desired position and desired heading. Since a vessel in such environments is located in the same position over a long time, the choice regarding the positioning system is extremely important. Using a positioning system optimal due to the environment of the vessel, will minimize the amount of thrust required, leading to a reduced fuel consumption, which in turn will reduce both the operational cost and emission.

The optimal position of a TAPM vessel, is the position where the mean environmental loads acting on the vessel, are balanced by the mooring lines. This position will again depend on the vessels heading. The optimal heading of a vessel is depending on the

direction of the mean environmental loads, and is defined as the angle between true north and the vessels direction when the mean environmental loads act through its centre line.

Today, there are no system available in order to measure or compute the direction of the mean environmental loads. Because of that, it will be impossible to manually decide an optimal value for ψ_d. Based on this, two new autonomous guidance systems for heading are derived with the intention of automatically optimizing the desired heading in order to obtain the optimal value, online during an operation.

When using an autonomous guidance system for heading in a combination with setpoint chasing for the North and East position, the result will be a complete autonomous control system, with the intention of obtaining optimal control. A positive feature of such a system, is that the guidance system will be able to adjust its desired optimal values even when the direction of the mean environmental loads are changing.

During the simulation performed in Chapter 7.1, the focus were to check the validity of the three different guidance systems described in the beginning of this chapter, in order to determine how fast and how accurate they manage to find ψ^*.

As it appears from the results in scenario 1, see Chapter 7.1.2, and scenario 2, see Chapter 7.1.3, all three guidance systems have the possibility to seek the optimal heading form both directions. A deeper discussion regarding each of the guidance system, with both positive and negative remarks, will be described in the following.

Guidance system number 1
The simulations regarding the user specified guidance system for heading, were mainly performed in order to obtain a basis for testing and comparison. The results using this guidance system in a combination with setpoint chasing, can be seen in Figure 7.1 and Figure 7.4. When knowing the optimal heading, this system will obtain both fast response and accurate results. However, during offshore operations, it will as described earlier, be impossible to decide an accurate optimal heading manually. Even a small deviation from the optimal heading will result in an increased use of thrust, because the thruster will counteract for the environmental load and possibly fight against the mooring system.

Guidance system number 2
The results using an autonomous guidance system based on sinusoidal perturbation based ES for heading, in a combination with setpoint chasing, can be seen in Figure 7.2 and Figure 7.5. As proved during these simulations, it is possible to use this method in order to seek for an optimal value of the heading. The main drawback of this method is that the time used before the desired heading converges to an optimal heading, is too long in this context. Another drawback is that the desired heading calculated by the guidance

system contains oscillations, due to sinusoidal perturbation, which will cause oscillations also in the system. Even though the oscillation period is long, approximately 1600 s, fuel consumption will not be zero due to the thrust oscillation, and the system will therefore not be optimal.

The ES controller based on the method of sinusoidal perturbation is difficult to tune. That is mainly because it contains several parameters: ω, a, k, ω_l and ω_h, that have to be tuned in order to obtain good results. By further tuning, the response time and the oscillations in the system can be improved. In the following a discussion of the impact of each of the parameters will be described.

- By decreasing the value of the frequency of the perturbation signal, ω, the estimate of ψ_d will converge faster, but at the same time will it also oscillate faster.
- By increasing the amplitude of the perturbation signal, a, the desired heading will oscillate with a higher amplitude about ψ^*, which is not a desired behaviour. On the other hand, it will converge faster.
- The gain k is used to increase the convergence, and at the same time decrease the amplitude of the oscillations in the desired heading. By choosing a too large value, ψ_d will overshoot and can even lead to an unstable system.
- By choosing ω_l and ω_h too large, the seek will give wrong results.

Tuning is also required for the constant c in the performance function. Increasing the constant ensures that ψ_d converges to ψ^* faster. By choosing a too large value, ψ_d will overshoot and can even lead to an unstable system.

Further, the value of the environmental loads will have an impact on the choice of the parameters. Anyway, since the method uses the steady-state behavior of a system in its calculations, the convergence will be a bit slow. By inserting a controller with higher thrust capability, the convergence time may be reduced.

Based on the remarks mentioned above, the results using an autonomous guidance system based on sinusoidal perturbation based ES for heading indicates that this method can work, but should be further investigated.

Guidance system number 3

The last simulations concern the method of numerical optimization based ES. The result of an autonomous guidance system based on this method for heading, in a combination with setpoint chasing, can be seen in Figure 7.3 and Figure 7.6. As proved during these simulations, it is possible to use this method to seek for an optimal value for heading.

The main drawback using this method is that it is time consuming. This is mainly due to the fact that the calculation regarding this guidance system is based on the output of the controller after the heading has reached a steady-state value. In order to reduce the time a controller with higher thrust capability may be used.

However, this method shows better results, both in terms of efficiency and accuracy, than using the method of sinusoidal perturbation based ES. The numerical optimization based ES converges to the optimal value during 4000 s, which is much faster compared to the time of the sinusoidal perturbation based ES. In addition, the numerical optimization based ES does not introduce any oscillations as the perturbation does. Using this combination of autonomous guidance systems, the vessel will show optimal behaviour in surge, sway and yaw.

Experiments
Due to the limited time and challenges in the MC Lab, only the user specified guidance system for heading was tested, in a combination with setpoint chasing for the North and East position. The tests showed better results with $H_s = 0.0139m$ than with $H_s = 0.0222m$, see Figure 7.7 and Figure 7.8, respectively.

As described in Chapter 7.2, the thruster allocation used in the model is not optimal in all 3 DOF at the same time. One reason can be that the model uses the pseudo inverse matrix in the optimization problem. Using 6 azimuth thrusters lead to singularity of the pseudo inverse matrix and the results will not be optimal, especially for yaw. In order to improve the results for the heading, it was tried to give fixed thrust in two of the side thrusters in the bow, one fixed in -90 degrees and the other in 90 degrees. However, this did not improve the results.

According to Figure 7.9, the thrusters operate optimal when controlling only 1 DOF. Based on this it can be concluded that in order to be able to test the autonomous heading guidance systems also in the MC Lab, the controllers in surge and sway need to be switched off.

A comparison between the simulation results and the experimental results is challenging, due to several factors. The mooring configuration of the two system differs. The mooring model used in the simulations are taken from a full scale model and scaled down using Froude scaling, and may not fit the model correctly. It is difficult to make a mooring system which will generate the exact same forces as in the simulation model. There can also be uncertainties in the system parameters between the simulation model and the physical model.

Chapter 9

Conclusion

This thesis concerns the topic of Thruster-Assisted Position Mooring (TAPM), where a vessel with such system is operating in normal conditions. The model vessel C/S Inocean Cat I Drillship, in short C/S Arctic Drillship (CSAD), is used as the study object.

This thesis has focused on developing autonomous guidance systems for heading, in order to automatically find and control the vessels heading to an optimal value. A vessel with port/starboard symmetry, will obtain optimal heading when the mean environmental loads act through its centerline, such that the fuel consumption is minimized. Since an TAPM vessel is located at the same position over time, both optimal heading and optimal position will be important in order to reduce fuel consumption, which in turn will reduce the operational cost and emissions.

The theory of Extremum Seeking (ES) has been investigated as a possible method for automatically finding the optimal heading during an operation. Two autonomous guidance systems for heading are derived based on two approaches of the ES theory, the sinusoidal perturbation based theory and the numerical optimization based theory. These methods of ES are known from other industries, but have until now not been tested for an TAPM application.

In order to obtain a complete optimal control system, the autonomous heading guidance systems have been combined with a guidance system based on setpoint chasing for the North and East position.

From the results, it can be concluded that both methods of ES seek towards a value of the optimal heading. Even though the method of numerical optimization based ES performs faster than the the method of sinusoidal perturbation based ES, they are both time consuming. In order to reduce the computing time in both autonomous guidance

systems, a controller with a higher thrust capability may be tested. Since the desired heading found in the numerical optimization based ES scheme is a constant value equal to the optimal heading, the result will give optimal control. On the other hand, the desired heading found in the sinusoidal perturbation based ES scheme, is oscillating around the value of the optimal heading. Even if these oscillations are slow, it will impact the use of thrust. A method in order to filter out these oscillations should be further investigated.

In conclusion, it may appear that both methods can be used in order to seek towards an optimal heading. However, the methods will need to be further investigated and optimized in order to be used efficiently for this application. The findings of this thesis can be used for further research in the field of TAPM.

9.1 Further work

Based on the conclusion, there are still parts in the control system that need to be improved in order to work optimal.

- Both of the autonomous guidance systems derived, work depending on the steady-state behavior of the controlled system. By making the controller faster, the guidance systems will be able to improve the performance.
- Both of the ES schemes described, use a performance function in its optimization problem. In order to make a faster response in the guidance system, improvements regarding the performance functions can also be made.
- The signal given by the guidance system based on sinusoidal perturbation based ES, gives an oscillating signal. This will not be acceptable in real life, and improved methods to filter the signal should be investigated further.
- It can also be interesting to expand the guidance system based on sinusoidal perturbation based ES, to see if this method also can be used for surge and sway at the same time.

In addition, some improvements for CSAD are described, both regarding the model vessel and the simulation model.

- In order to be able to compare the simulation results with the experimental results, it is required that the mooring models are similar. The parameters used in the simulation model are scaled according to Froude scaling. Even after the scaling, these parameters will be to large to fit in the MC Lab. Due to this, new parameters fitting the MC Lab should be defined and implemented in the FEM model. In addition, a method to make more accurate mooring lines for the experiments, should be investigated.
- The thrust allocation algorithm should be further investigated in order to perform optimal in 3 DOF.
- According to Bjørnø (2016), the 6 DOF model is based on simplified work drawings, and can contain some deviations from the model vessel.

Bibliography

Aamo, O. M. and Fossen, T. I. (1999). Controlling line tension in thruster assisted mooring systems, *Proceedings of the 1999 IEEE, International Conference on Control Applications* **2**: 1104–1109.

Aamo, O. M. and Fossen, T. I. (2001). Finite element modelling of moored vessels, *Mathematical and Computer Modelling of Dynamical Systems* **7**(1): 47–75.

Ariyur, K. B. and Krstić, M. (2003). *Real-time optimization by extremum-seeking control*, Wiley-Interscience, Hoboken, N.J.

Berntsen, P. I. B., Aamo, O. M. and Leira, B. J. (2006). Dynamic positioning of moored vessels based on structural reliability, *Proceedings of the 45th IEEE Conference on Decision & Control* pp. 5906–5911.

Bjørnø, J. (2016). *Thruster-assisted position mooring of c/s inocean cat i drillship*, Master thesis, Norwegian University of Science and Technology.

Bjørnø, J., Heyn, H., Skjetne, R., Dahl, A. and Frederich, P. (2017). Modeling, parameter identification and thruster-assisted position mooring of c/s inocean cat i drillship, *Proceedings of ASME 2017, The 36th International Conference on Ocean, Offshore and Arctic Engineering, OMAE 2017* **36**.

Breu, D. and Fossen, T. I. (2010). Extremum seeking speed and heading control applied to parametric roll resonance, *IFAC Proceedings Volumes* **43**(20): 28–33.

DNVGL (2013). Position mooring, `https://rules.dnvgl.com/docs/pdf/DNV/codes/docs/2013-10/OS-E301.pdf`.

Faltinsen, O. M. (1990). *Sea loads on ships and offshore structures*, Cambridge ocean technology series, Cambridge University Press, Cambridge.

Fang, S., Leira, B. J. and Blanke, M. (2013). Position mooring control based on a structural reliability criterion, *Structural Safety* **41**: 97–106.

Fossen, T. I. (2011). *Handbook of Marine Craft Hydrodynamics and Motion Control*, Wiley, New York.

Fossen, T. I. and Strand, J. P. (1999). Passive nonlinear observer design for ships using lyapunov methods: full-scale experiments with a supply vessel, *Automatica* **35**(1): 3–16.

Fossen, T. I. and Strand, J. P. (2001). Nonlinear passive weather optimal positioning control (wopc) system for ships and rigs: experimental results, *Automatica* **37**(5): 701–715.

Frederich, P. (2016). *Constrained optimal thrust allocation for c/s inocean cat i drillship*, Master thesis, Norwegian University of Science and Technology.

Gjessing, I. A. (2015). *Control and simulation of a thruster-assisted moored offshore vessel in sea-ice*, Master thesis, Norwegian University of Science and Technology.

IMO (1994). Guidelines for vessels with dynamic positioning system, `http://www.uscg.mil/hq/cg5/ocsncoe/docs/DP%20Guidance/IMO%20MSC%20Circ.645.pdf`.

Inocean (2013). Cat i arctic drillship ncs, `http://www.inocean.no/cat-i-arctic-drillship-ncs`. [Online; accessed 19-March-2017].

Jorde, J. (2014). Design & engineering innovation of statoil's cat i arctic drillship, Presented at the IBC 3rd Annual Drillships, Singapore.

Killingsworth, N. and Krstic, M. (2006). Pid tuning using extremum seeking: Online, model-free performance optimization, *IEEE Control Systems Magazine* **26**(1): 70–79.

Leira, B. J., Berntsen, P. I. B. and Aamo, O. M. (2008). Station-keeping of moored vessels by reliability-based optimization, *Probabilistic Engineering Mechanics* **23**(2): 246–253.

Nesic, D. (2011). Analysis and design of extremum seeking controllers, `http://www.ieeecss-oll.org/lectures/2011/analysis-and-design-extremum-seeking-controllers`. Video lecture form CSS Webinar Series.

Nguyen, D. T. and Sørensen, A. J. (2007). Setpoint chasing for thruster-assisted position mooring, *Proceedings of OMAE 2007, The 26th International Conference on Offshore Mechanics and Arctic Engineering* **26**: 553–560.

Nguyen, D. T. and Sørensen, A. J. (2009). Setpoint chasing for thruster-assisted position mooring, *Oceanic Engineering, IEEE Journal of* **34**(4): 548–558.

NTNU (2017a). Marine cybernetics laboratory (mc-lab), https://www.ntnu.edu/imt/lab/cybernetics. [Online; accessed 27-March-2017].

NTNU (2017b). Ntnu marine cybernetics laboratory handbook, https://github.com/NTNU-MCS/MC_Lab_Handbook/blob/master/Version%202.0/MCLab%20Handbook/MCLab_Handbook.pdf. [Online; accessed 04-September-2017].

OSCAR (2014). Ocean surface currents (oscar), http://oceanmotion.org/html/resources/oscar.htm. [Online; accessed 22-March-2017].

Pinkster, J. A. and Nienhuis, U. (1986). Dynamic positioning of large tankers at sea, *Proceedings of the Offshore Technology Conference (OCT'86)*, Houston, TX.

Price, W. G. and Bishop, R. E. D. (1974). *Probabilistic theory of ship dynamics*, Chapman and Hall, London.

Ren, Z. (2015). *Fault-tolerant control of thruster-assisted position mooring system*, Master thesis, Norwegian University of Science and Technology.

Skjetne, R. (2014). Report: Literature survey on position mooring control systems. Unpublished work, Norwegian University of Science and Technology, Trondheim, Norway.

Steen, S. (2011). *Motstand og propulsjon, propell- og foilteori*, Kompendium, Marinteknisk senter, Institutt for marin teknikk, Trondheim.

Strand, J. P., Sørensen, A. J. and Fossen, T. I. (1997). Modelling and control of thruster assisted position mooring systems for ships, *Proceedings IFAC Conf. Manoeuvering and Cont. of Marine Crafts,* **4**: 160–165.

Strand, J. P., Sørensen, A. J. and Fossen, T. I. (1998). Design of automatic thruster assisted mooring systems for ships, *Modeling, Identification and Control* **19**(2): 61–75.

Sørensen, A. J. (2013). *Marine control systems : propulsion and motion control of ships and ocean structures*, Kompendium, Department of Marine Technology. Norwegian University of Science and Technology, Trondheim.

Sørensen, A. J., Leira, B., Peter Strand, J. and Larsen, C. M. (2001). Optimal setpoint chasing in dynamic positioning of deep-water drilling and intervention vessels, *International Journal of Robust and Nonlinear Control* **11**(13): 1187–1205.

Sørensen, A. J. and Peter Strand, J. (2000). Positioning of small-waterplane-area marine constructions with roll and pitch damping, *Control Engineering Practice* **8**(2): 205–213.

Sørensen, A. J., Strand, J. P. and Fossen, T. I. (1999). Thruster assisted position mooring system for turret-anchored fpsos, *Proceedings of the 1999 IEEE International Conference on Control Applications,* **2**: 1110–1117.

Triantafyllou, M. (1990). *Cable mechanics with marine applications*, Department of Ocean Engineering, Massachussetts Institute of Technology, Cambridge, MA 02139, USA.

Zhang, C. and Ordóñez, R. (2012). *Extremum-Seeking Control and Applications: A Numerical Optimization-Based Approach*, Springer, London.

Appendix A

Attached zip-file

A.1 Content

The following files are included in the attached zip-file:

- A digital version of the thesis.
- A digital version of the poster.
- A folder called **Experiment**, giving the results from the experimental work. The content of this folder is further described below.
- A folder called **Simulation**, giving all the MATLAB-files and Simulink models. The folder contain a sub-folder for each combination of guidance systems used in this thesis, including their results. The content of this folder is further described below.

A.2 Content of the folder: Experiment

- ***Basin rotation***
  Results from experiments.
- ***Setpoint chasing user heading***
  Results from experiments with user specified guidance system. Two different wave conditions.

A.3 Content of the folder: Simulation

- ***User specified guidance system***

  This folder contains the files needed to run the program of a user specified guidance system for 3 DOF. The file *run_ CSAD_ UserSpecifiedGuide.m* runs the the Simulink model *CSAD_ UserSecifiedGuide.slx*. The folder does also contain a folder with the results used in the report.

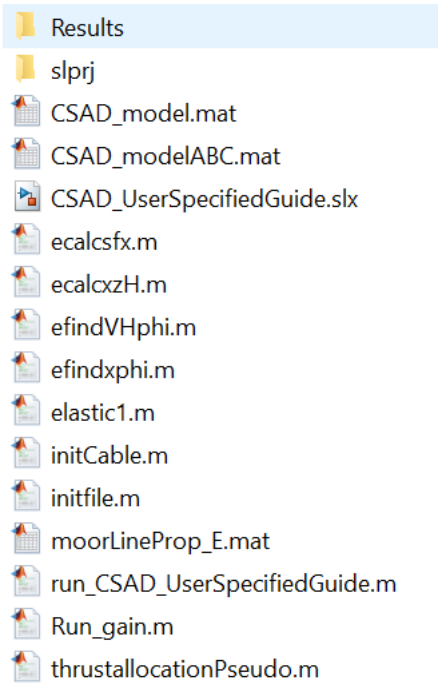

Figure A.1: Content of the folder User specified guidance system.

- ***SPES and SP***

  This folder contains the files needed to run the program of an autonomous guidance system for heading based on sinusoidal perturbation based ES and setpoint chaisng for surge and sway. The file *run_CSAD_SPES_SP.m* runs the the Simulink model *CSAD_SPES_SP.slx*. The folder does also contain a folder with the results used in the report.

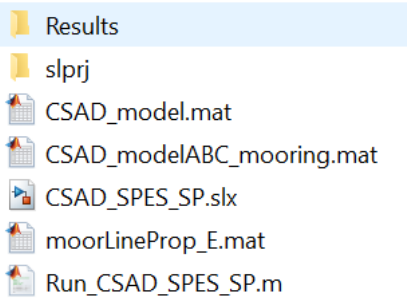

Figure A.2: Content of the folder SPES and SP.

- ***Simplified yaw ES***

  This folder contains the files needed to run the program of an autonomous guidance system for heading based on sinusoidal perturbation based ES for a simplified 1 DOF system. The file *run_ES_simplified.m* runs the the Simulink model *ES_simplified.slx*. The folder does also contain a folder with the results used in the report.

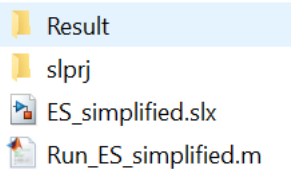

Figure A.3: Content of the folder Simplified yaw ES.

- ***Setpoint chasing user***

  This folder contains the files needed to run the program of a user specified guidance system for heading and setpoint chasing for surge and sway.
  The file *run_CSAD_setpointchasing_user.m* runs the the Simulink model *CSAD_setpointchasing_user.slx*. The folder does also contain a folder with the results used in the report.

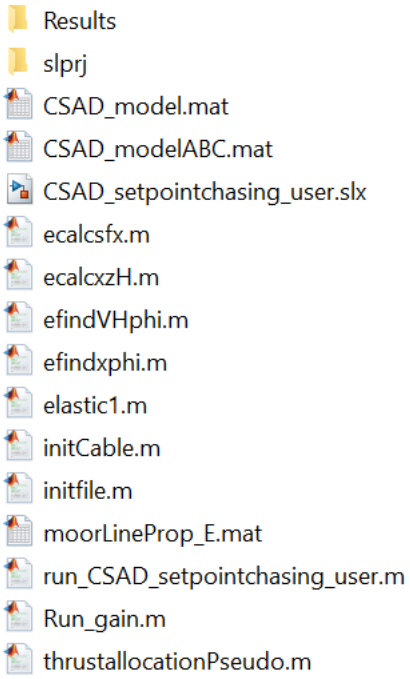

Figure A.4: Content of the folder Setpoint chasing user.

- ***Setpoint chasing***

  This folder contains the files needed to run the program of setpoint chasing for surge and sway. The file *run_CSAD_setpointchasing.m* runs the the Simulink model *CSAD_setpointchasing.slx*. The folder does also contain a folder with the results used in the report.

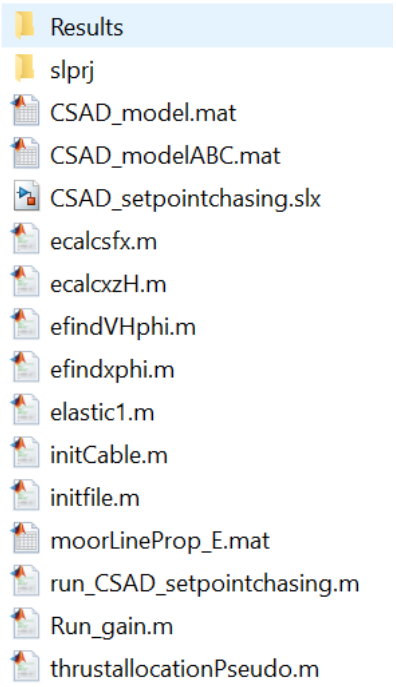

Figure A.5: Content of the folder Setpoint chasing.

- ***Open loop CSAD***

  This folder contains the files needed to run the verification of the open loop system. The file *run_CSAD_verificatin_openloop.m* runs the the Simulink model *CSAD_verificatin_openloop.slx*. The folder does also contain a folder with the results used in the report.

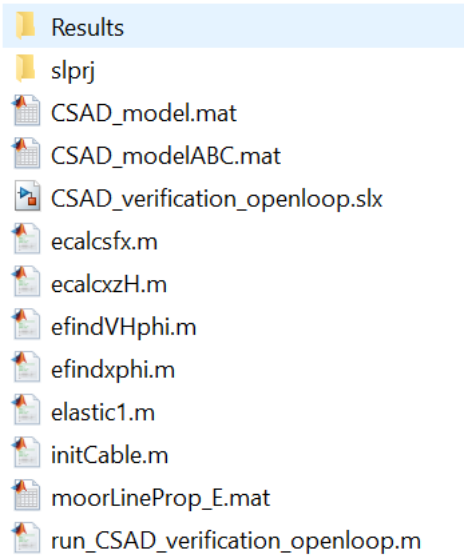

Figure A.6: Content of the folder Open loop CSAD.

- ***Numerical optimization guidance system***

  This folder contains the files needed to run the program of an autonomous guidance system based on numerical optimization based ES. The file *run_CSAD_NOES.m* runs the the Simulink model *CSAD_NOES.slx*. The folder does also contain a folder with the results used in the report.

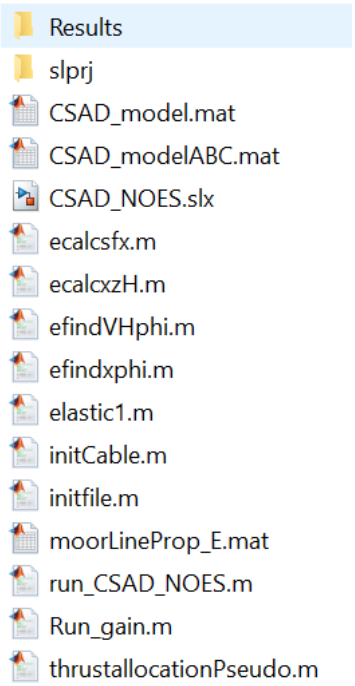

Figure A.7: Content of the folder Numerical optimization guidance system.

- ***NOES and SP***

  This folder contains the files needed to run the program of an autonomous guidance system based on numerical optimization based ES and setpoint chasing for surge and sway. The file *run_CSAD_NOES_SP.m* runs the the Simulink model *CSAD_NOES_SP.slx*. The folder does also contain a folder with the results used in the report.

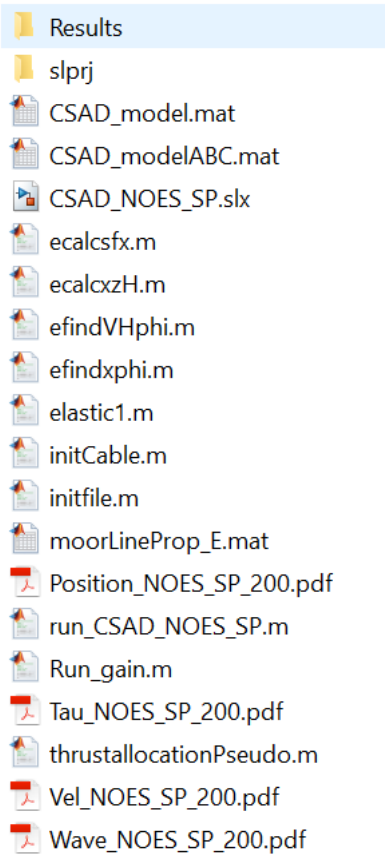

Figure A.8: Content of the folder NOES and SP.

A.4 Remarks regarding the programs

- Each simulation scenario have its own folder, which contains a run-file to run the system.
- Each simulation scenario have its own subfolder containing the results.
- Each simulation models in the zip-file has a initial position of zero and with environmental loads of 200 degrees.
- In order to start the vessel in another initial position, the start position of the reference filter and the ES guidance systems have to be changed manually inside the Simulink model.
- The start position of the vessel is defined inside the Simulink model, and can be changed by a double-click on the block "Virtual CS Inocean Cat I Drillship 6 DOF". The environmental loads can also be changed from here.
- In addition, if it is desirable to change the direction of the environmental loads, it should be noted that the direction of the current along the mooing lines are changed from the run-file.